PROTEOLYTIC REWIRING OF THE MITOCHONDRIA IN HYPOXIA

Inaugural-Dissertation

zur

Erlangung des Doktorgrades

der Mathematisch-Naturwissenschaftlichen Fakultät der Universität zu

Köln

vorgelegt von

Chandragiri Srikanth

aus Telangana, India

Köln, 2022

Berichterstatter:

Prof. Dr. Thomas Langer

Prof. Dr. Thorsten Hoppe

ॐ पूर्णमदः पूर्णमिदं पूर्णात्पुर्णमुदच्यते
पूर्णश्य पूर्णमादाय पूर्णमेवावशिष्यते ॥
ॐ शान्तिः शान्तिः शान्तिः ॥

- ईशोपनिषद्

Table of the contents

1.Abstract:

Molecular oxygen sustains intracellular bioenergetics and is consumed by more than 400 biochemical reactions, making it essential for most species on Earth. Reduced oxygen concentration (hypoxia) is a major stressor that generally subverts life of aerobic species and is a prominent feature of pathological states encountered in inflammation, bacterial infection, cardiovascular defects, wounds, and cancer. Despite the fundamental importance of oxygen in human physiology and disease, we currently lack a complete understanding of how the mitochondrial proteome adapts fluctuations in oxygen tensions. We recently identify a mTORC1-LIPIN1-lipid signaling cascade that activates the *i*-AAA protease YME1L in hypoxia to ensure pyrimidine synthesis. Here, we determined protein turnover rates of mitochondrial proteins in hypoxia. The mitochondrial m-AAA protease AFG3L2 was found to reshape the mitochondrial matrix and inner mitochondrial membrane (IMM) proteome in hypoxia. This proteolytic rewiring affects various biological pathways, such as lipid metabolism, protein import, OXPHOS and metabolism. Hypoxia is one of the main stressors of the mTORC1, we investigated the role of mTORC1 in AFG3L2 dependent proteolytic rewiring. In nutrient starvation mTORC1 is inhibited and activates AFG3L2-dependent proteolytic rewiring, whereas active mTORC1 inhibits AFG3L2 activity. NCLX is a Na+/Ca2+ exchanger, which effluxes Ca2+ from the matrix in exchange for Na+ from the intermembrane space and loss of NCLX activates AFG3L2 -dependent proteolysis. We show that in hypoxia changes protein turnover, the mitochondrial m-AAA protease AFG3L2 reshapes the mitochondrial proteome to adapt to hypoxia.

2. Introduction

Molecular oxygen (O2) is essential for sustaining life on the earth and is the one of the most abundant elements in the universe. The homeostasis of oxygen is very important for the survival of most prokaryotic and eukaryotic species. Molecular oxygen is key for mitochondrial ATP generation, the cellular energy currency. A normal adult male consumes approximately 380 liters of oxygen every day and around 90% oxygen is used in the electron transport chain (ETC) for the synthesis of ATP (1). The analysis of various metabolites' effect on the total number of reactions in the metabolic network revealed oxygen is among the most utilized compounds, even superseding adenosine triphosphate (ATP) and nicotinamide adenine dinucleotide (NAD+) (2). Many biochemical reactions use oxygen as a substrate. Although Oxygen is kinetically stable, it readily interacts with metals and cofactors (2, 206).

Humans are constantly exposed to different levels of oxygen tension, ranging from sea level (21%- 11%) to Mount Everest (5%). Humans can adapt to fluctuations in oxygen tension, however, if the fluctuations exceed the body's adaptive capacity leads to organ damage and disease. Excessive oxygen, hyperoxia increases hyperoxic risks by inducing oxygen toxicity, various oxygen toxicities associated with the lungs, central nervous system and ocular toxicity. These symptoms can be relieved as long as the hyperoxic inhalation is terminated and returned to normal. Low oxygen, hypoxia causes several pathological conditions such as cerebral stroke, myocardial infraction, tumor development, delayed wound healing, and pulmonary arterial hypertension. No oxygen, prolonged anoxia causes death (58, 35, 205, 206)

2.1.1 Mechanism of oxygen sensing

The deficiency of oxygen is called hypoxia. How cells sense changes in oxygen tension was a central question in biology. The major breakthrough in the understanding of oxygen sensing mechanism was the discovery of hypoxia-inducible factors (HIFs), prolyl hydroxylases (PHD1, PHD2 &PHD3), and von Hippel Lindau (VHL). These findings provided a detailed understanding of how cells sense oxygen and mount a robust transcriptional response. The HIF- VHL- PHD axis is well studied in hypoxia research (3).

HIF1 and HIF2 are major transcription factors involved in the hypoxia-mediated transcriptional response, they bind to hypoxia response elements (HRE) in the promoters of a large number of targets, including glycolysis, angiogenesis, and metastasis (Fig1). The initial discovery of HIF1 was studying the erythropoietin (EPO) gene (4, 5). In hypoxia, HIF1 binds HIF2 translocate to the nucleus and initiates a transcriptional program (6, 7). In normoxia, HIF1 is rapidly degraded by E3 ubiquitin-proteome pathways. Availability of oxygen is sensed by dioxygenase enzymes prolyl hydroxylase domain proteins (PHD) which hydroxylate HIF1α subunit at two proline residues (8,9). This reaction requires iron (Fe2+), oxygen and coupled with oxidative decarboxylation of α - ketoglutarate to succinate (10,11). This hydroxylated HIFα undergoes polyubiquitylation by VHL E3 ubiquitin ligase (VHL complex) and becomes a target for the proteasome. Hypoxia prevents the hydroxylation of HIF1α and oxygen-dependent degradation (ODD) by the proteasome (12). The stable HIF1α dimerizes with HIF1ß and translocate to the nucleus and initiates a transcriptional program by interacting with other transcription co-activators p300 and CBP (Fig1) (13).

The interaction between the transcriptional co-activators and HIF is regulated by another member of the α–ketoglutarate and Fe2+ dependent dioxygenase family protein FIH1 (Factor Inhibiting HIF). In low oxygen, FIH1 hydroxylates at asparagine (Asn803 in human HIF1α; Asn851 in human HIF2α) of HIF1α's C-TAD domain and this can be abrogated by the addition of iron chelators or competitive inhibitors of 2-oxoglutarate (14). This asparaginyl hydroxylation of HIF1α enzyme FIH1 is also a member of the dioxygenase family but differs in sequence with PHDs (15,16). Hydroxylation of HIF1α and HIF2α by FIH1 creates a steric clash that prevents the recruitment of the coactivators p300 and CBP and ultimately inhibits the hypoxia transcriptional program. FIH1 is more active in low levels of oxygen than PHDs, this helps to suppress the activity of HIFα proteins that escape degradation in moderate hypoxia (17,18). Therefore, FIH1-mediated asparaginyl hydroxylation of HIF1α provides a second level of oxygen-regulated mechanism (fig1).
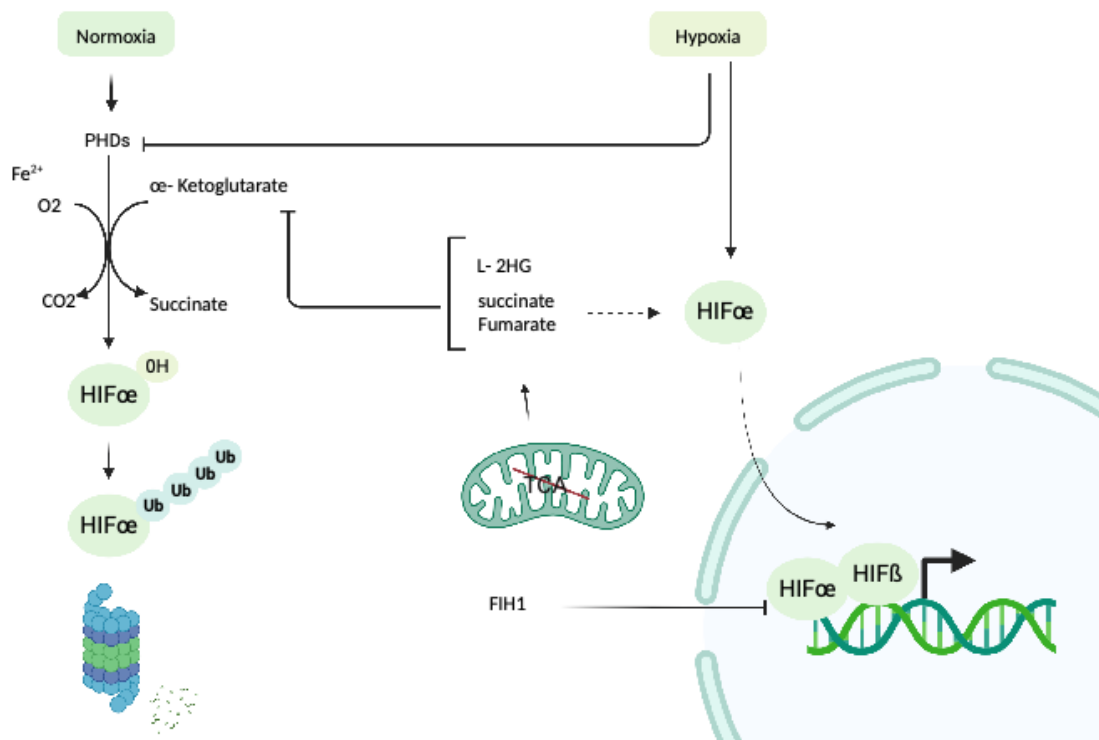
Figure 1. HIFa stabilization in hypoxia

HIF α hydroxylated under normoxia and targeted to ubiquitin- proteosome mediated degradation. In hypoxia PHD are inhibited, stabilizes HIF1 α and translocated to nucleus, initiates hypoxic transcriptional program.

There are nearly 60 dioxygenases in the cell, one of these dioxygenases is the important chromatin-modifying Jumonji C domain histone lysine demethylases (KDMs). It has been observed for a long-time that hypoxia induces histone lysine hypermethylation (19), but how oxygen sensors modify chromatin was largely unknown until recent discovery of two dioxygenases KDM5A and KDM6A (20, 21). These lysine-specific demethylases (KDMs) are sensitive to oxygen levels and have low oxygen affinities (KM values) compared to PHDs. KDM6A is a direct sensor of oxygen and modifies chromatin independent of HIF, hypermethylation of lysine 27 of histone H3 (H3K27) leads to gene repression (20). While KDM5A is responsible for hypermethylation of H3K4 leads to activating gene expression. This KDMs-mediated chromatin modification plays an important role in modulating genes responsible for embryogenesis, stem cell homeostasis, cancer and cardiovascular diseases (fig 2) (20, 21).
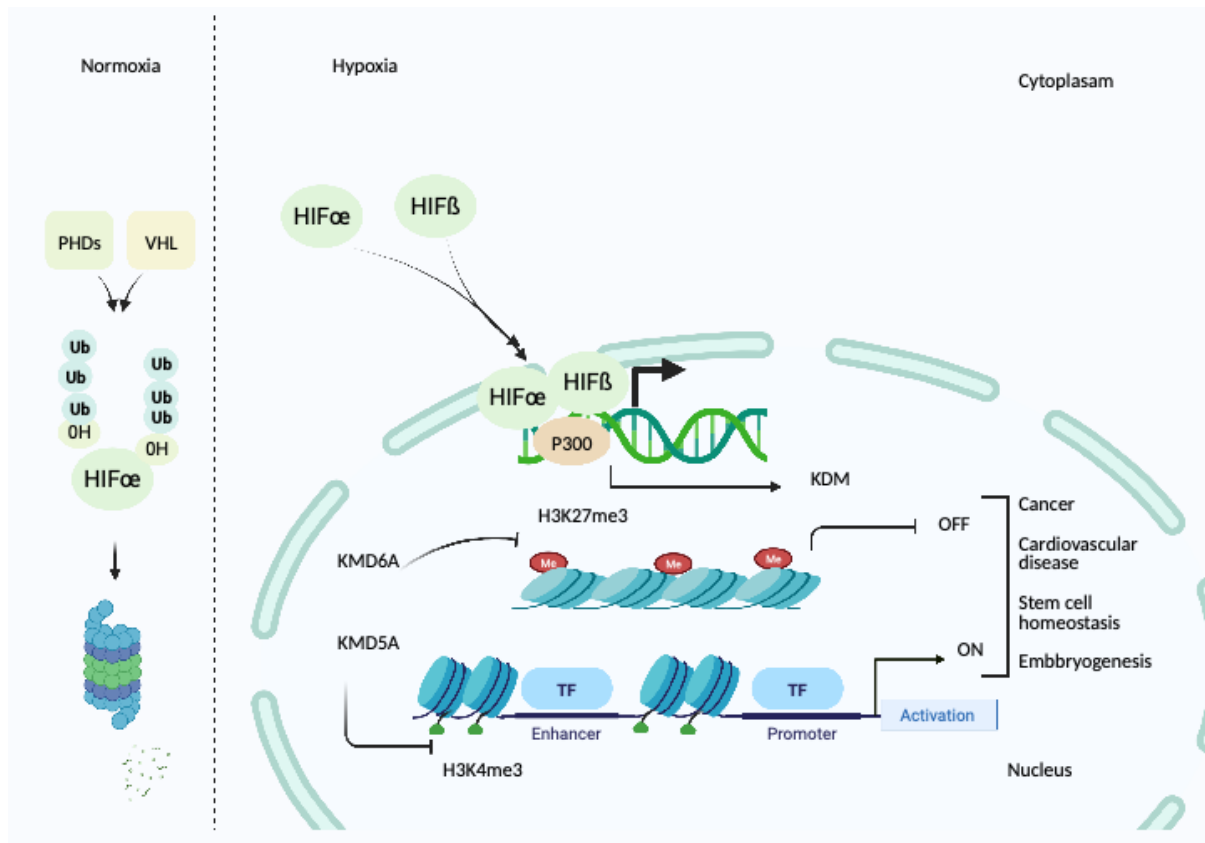
Figure 2: Hypoxia mediated chromatin modification

KDM6A and KDM5A are dioxygenases senses oxygen levels and modifies chromatin

2.1.2 Role of hypoxia on mitochondrial functions

Mitochondria are the essential organelle and is a hub for various metabolic reactions. Mitochondria regulate hypoxia response by maintaining the availability of TCA metabolites α–ketoglutarate and succinate. As we know oxygen is the ultimate electron acceptor of mitochondrial respiration. The high-energy electrons derived from the catabolism of food are passed through electron transport chain, generating a proton gradient across the mitochondrial inner membrane (1). Complex IV, cytochrome oxidase transfers electrons to oxygen. Cytochrome oxidase is located in the inner mitochondrial membrane and consists of 13 subunits, the ten regulatory subunits are nuclear-encoded and the 3 catalytic subunits are mitochondrial-encoded (22). In hypoxia, HIF1α enhances the gene expression of complex IV subunit COX4I-2 and mitochondrial protease LONP1. The nuclear-encoded COX4I-2 has a higher affinity for oxygen and higher efficiency to transfer electrons to oxygen during hypoxia. This enhanced expression of the mitochondrial protease LONP1 degrades less efficient electron transfer complex IV subunit COX4I-1, this proteolysis helps to swap highly efficient COX4I-2 in hypoxia. This enables COXIV to allow for a more efficient transfer of electrons to oxygen

in hypoxia (23). Another hypoxia-mediated complex IV regulation is through the hypoxia inducible domain family, member 1A (Higd1a), it is reported as a positive regulator of complex IV but the molecular mechanism is not yet understood (24). By contrast, hypoxia inhibits the activity of other electron transport chain complexes (Complex I, II, III). In hypoxia, HIF1α induces the expression of the mitochondrial NDUFA4L2 (NADH dehydrogenase [ubiquinone] 1 alpha subcomplex, 4-like 2). Silencing of NDUFA4L2 increase oxygen consumption rate in hypoxia and affects mitochondrial complex I activity in an unknown manner (fig3) (25). The mechanism of NDUFA4L2 mediated complex I function is yet to be investigated. Hypoxia induces several microRNAs, including mir-210, which repress iron-sulfur cluster assembly proteins ISCU1 & ISCU2 (26). These ISCU1/2 facilitate the assembly of [4Fe-4S] and [2Fe-2S] iron-sulfur clusters, prosthetic groups that promote oxidation-reduction reactions and electron transport, integral to numerous cellular processes, including heme biosynthesis, ribosome biogenesis, DNA repair, purine catabolism, and iron metabolism, among others (27). Importantly iron-sulfur clusters are incorporated into enzymes involved in mitochondrial respiration complexes (complex I, II, III) and energy production. In hypoxia HIF1α induced expression of mir-210 represses the expression of ISCU1/2, which distrupts the correct assembly of iron-sulfur clusters within ETC complexes I, II and III. mir-210 also represses the expression of complex I subunit NDUFA4, complex IV assembly protein COX 10, and complex II subunit succinate dehydrogenase subunit D (SDHD) (fig3) (28, 29).
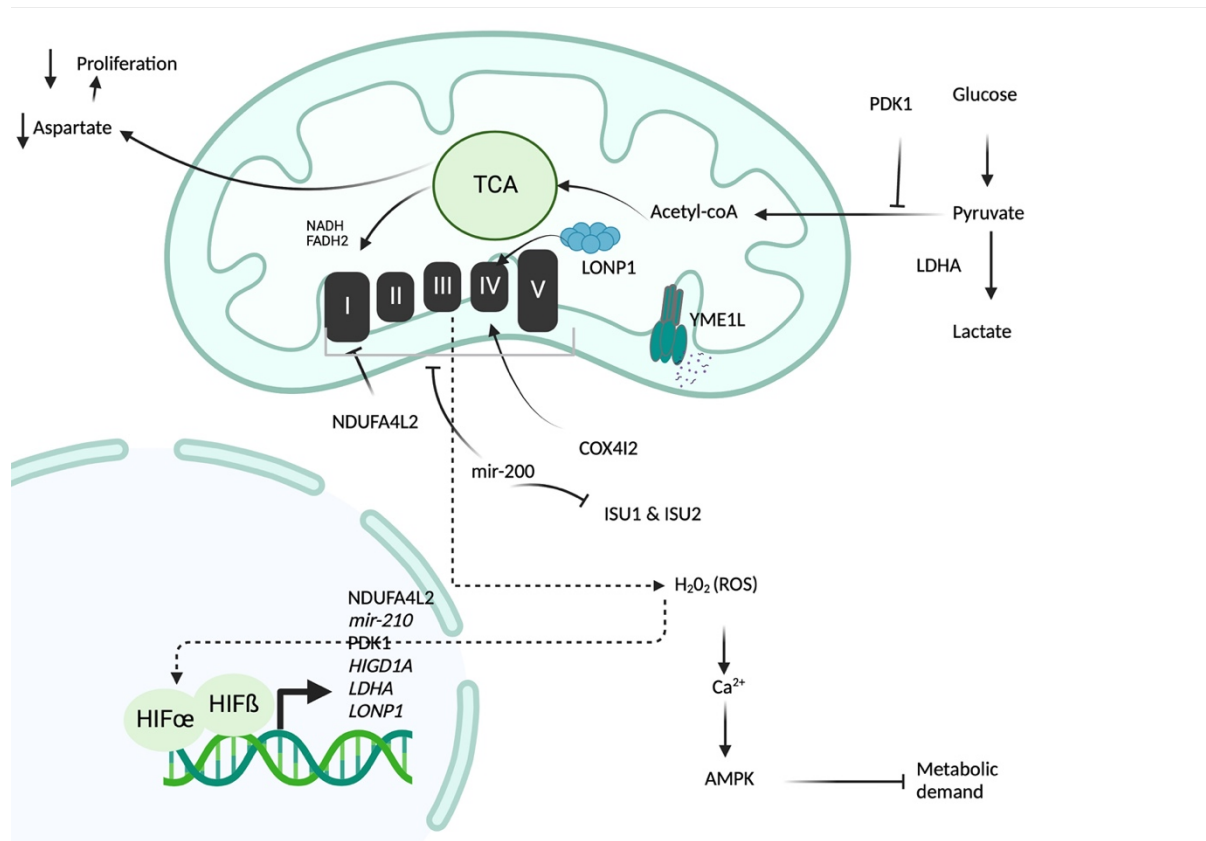
Figure 3: Role of hypoxia on mitochondrial function

Hypoxia regulates mitochondrial functions: OXPHOS, TCA cycle, ion homeostasis

In a genome-wide CRISPR screen in mitochondrial complex III inhibition, one of the most enriched sgRNA was VHL (Von Hippel-Lindau) (30). VHL is an E3 ubiquitin ligase, that plays an important role in hypoxia signaling by targeting HIF1α for proteasomal degradation (12). Since oxygen is a key substrate for the electron transport chain (ETC), inhibition or dysfunctional ETC may activate a hypoxic response as an adaptive mechanism. This test was carried out in a Leigh syndrome mouse model, an early-onset fatal neurodegenerative disease. To date, over 75 different genes are known to be involved in this syndrome. Complex I deficiency is the most frequent biochemical cause of the disease. Inactivation of complex I subunit NDUFS4 (NADH: ubiquinone oxidoreductase subunit S4) mouse model able to recapitulate many features of Leigh syndrome (32). NDUFS4 KO exposed to 21% oxygen (ambient/ breathing oxygen) displayed retard growth rates, impaired visual acuity, locomotor deficits and a delayed startle response. When NDUFS4 KO mice were exposed to high altitude atmospheric oxygen levels 11% prevented many disease symptoms and extended lifespan. This hypoxia-mediated reversal of disease symptoms and extension of lifespan is independent of the HIFα activation program (33). Hypoxia not only prevented the disease but also reversed brain

lesions in mice with advanced neuropathology. While hyperoxia 55% oxygen reduced lifespan and increased disease severity (34). The genome-wide CRISPR growth screen for essential genes in low oxygen concentration (21%, 5%, 1%), showed genes related to mitochondrial complex I, iron-sulfur cluster biogenesis, and lipid metabolism essential in hypoxia (35). These findings indicate the importance of mitochondrial genes in adaption to low oxygen concentration.

Reshaping intracellular metabolism is a common feature of hypoxia. Beyond electron transport chain (ETC) modulation, hypoxia controls the entry of pyruvate into TCA cycle by induction of pyruvate dehydrogenase kinase 1(PDK1) and lactate dehydrogenase (LDHA). Pyruvate dehydrogenase kinases phosphorylate the pyruvate dehydrogenase complex (PDH) and inactivate the catalytic activity of PDH. The pyruvate dehydrogenase complex consists of three enzymes that converts pyruvate to acetyl-CoA. HIFα dependent expression of PDK1 inhibits the activity of PDH, limits the entry of acetyl-CoA into the TCA cycle, and reduces oxygen consumption (36, 37). Similar to PDK1, lactate dehydrogenase also regulates acetyl-CoA entry into the TCA cycle by catalyzing pyruvate to lactate (38). Lactate is exported from the cell through monocarboxylic transporter 4 (MCT4). Extracellular lactate can be taken up by other cancer cells and used as a carbon source for the TCA cycle. Non-small-cell lung cancers incorporate more lactate-derived carbons into TCA cycle intermediates than those from glucose (51). This reduced entry of acetyl-CoA into the TCA cycle limits the generation of mitochondrial-reducing equivalents NADH and FADH2 and leads to a reduction in electron flux through the electron transport chain (ETC). Another important consequence of reduced TCA cycle flux in hypoxia diminishes the production of oxaloacetate (OAA), which is required for the synthesis of aspartate. Aspartate is required for the biosynthesis of nucleotides and proliferation (39, 40). Hypoxia reduces aspartate levels; this leads to impair cell proliferation and tumor growth and acts as a key limiting metabolite in hypoxia. Aspartate levels negatively correlate with the markers of hypoxia in primary human tumors (41, 42).

In hypoxia glucose-derived citrate reduces and glutamine becomes a major source of citrate. Mitochondrial isocitrate dehydrogenase (IDH2) reductively carboxylates glutamine-derived α-ketoglutarate to citrate. This reductive TCA cycle-generated citrate provides both the acetyl-coenzyme A for lipid synthesis and the four-carbon intermediates needed to produce the remaining TCA cycle metabolites and related macromolecular precursors. Hypoxia and ETC

dysfunction operate a reductive TCA cycle, glutamine anaplerosis can therefore maintain lipid homeostasis (43, 44, 45). It has long been known that succinate accumulated in ischemia and anoxia in vivo (46, 47). Either complex I or complex II, each of which deposits electrons into the ETC, can reverse the directionality of the SDH activity and accept electrons from ubiquinol during conditions of low oxygen, and ETC inhibition (48, 50). In hypoxia DHODH can still deposit electrons into the ETC, which leads to the accumulation of ubiquinol, driving the succinate dehydrogenase complex in reverse to enable denovo pyrimidine biosynthesis and NADH reoxidation. Mitochondria use fumarate as a terminal electron acceptor (TEA) in oxygen limitation (fig 4) (48, 49).
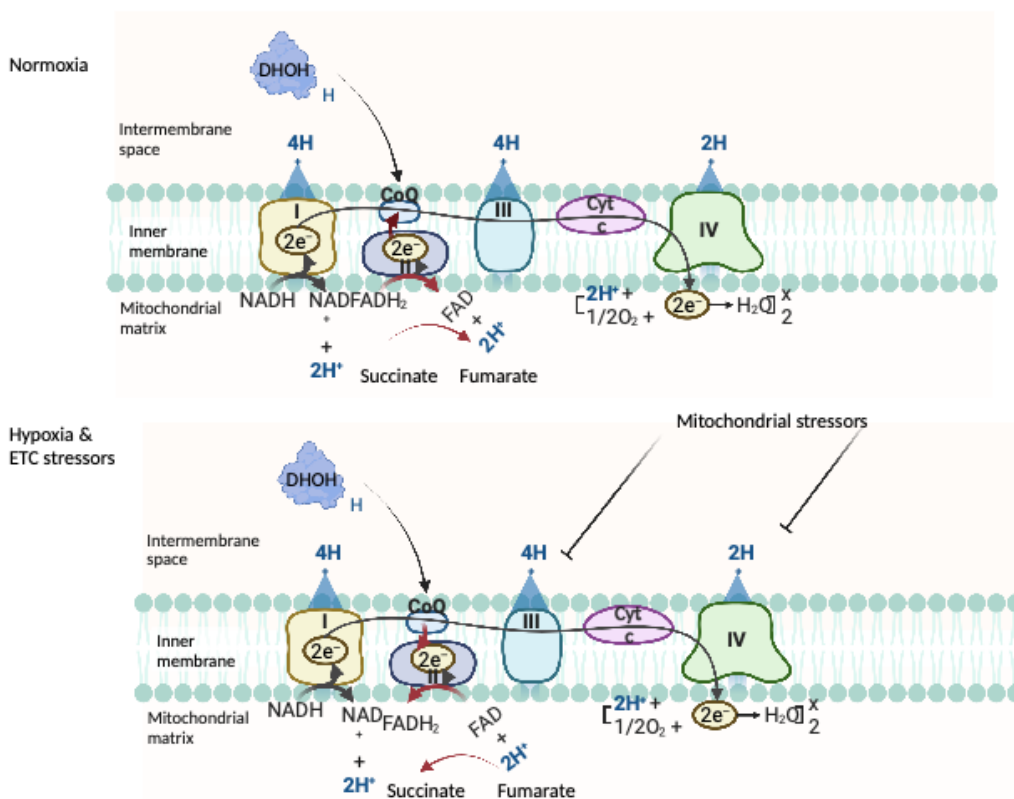
Figure 4: Fumarate act as terminal electron acceptor in hypoxia

Beyond its effects on ETC function and metabolism, hypoxia also controls mitochondrial morphology. In normoxia, mitochondria form a tubular network but undergo fragmentation in hypoxia (52, 53, 54). Hypoxia induces E3 ubiquitin ligase SIAH2 activity and promotes AKAP121 (scaffolding protein A-kinase anchoring protein 121) protein degradation. In hypoxia AKAP121 undergoes ubiquitin-mediated degradation and is no longer able to phosphorylate DRP1, this allows the interaction of DRP1 and FIS1 at the mitochondrial outer membrane, resulting in mitochondrial fission (55). Hypoxia may promote mitochondrial fission

to induce mitophagy, keep ROS production at a physiological low level, and maintain the integrity by a decrease in respiratory activity. Hypoxia can also activate mitophagy by expressing BNIP3L and dephosphorylating FUNC1. These proteins are localized to the mitochondrial outer membrane and serve as a receptor for the mitophagy machinery (56, 57). Currently, the mechanism of how hypoxia is sensed to trigger mitochondrial fission and mitophagy is not well understood.

2.2 mTORC1 signaling & nutrient stress

Oxygen availability is one of the main stressors of mTORC1 (mechanistic Target of Rapamycin complex 1) signaling (58). mTOR is a serine/threonine protein kinase in the PI3K-related protein kinases (PIKK) family (59). In mammals, it constitutes the catalytic subunit of two distinct complexes, mTORC1 and mTORC2, these are distinguished by their accessory proteins and sensitivity to rapamycin. The mTORC1 acts as a master nutrient sensor of the cell. mTORC1 coordinates eukaryotic cell growth and metabolism by integrating diverse environmental and nutritional cues. When nutrients are abundant, active mTORC1 promotes anabolism such as protein, lipid, nucleotide biosynthesis and inhibits catabolism like protein and organelle turnover, autophagy and lysosomal biogenesis (60). mTORC1 readily inactivates upon nutrient stress, growth factors withdrawal and oxygen. Given its central role in maintaining cellular and physiological homeostasis, dysregulation of mTORC1 signaling has been implicated in various metabolic disorders, cancer, neurodegeneration and ageing (60).

2.2.1Architecture of mTORC1

mTORC1 is nucleated by three core components: mTOR, mammalian lethal with SEC13 protein 8 (mLST8, also known as GβL) and its unique defining subunit, the scaffold protein RAPTOR (regulatory-associated protein of mTOR) (61,62,63). RAPTOR acts as a scaffold that is necessary for the integrity of the complex, and facilitates substrate recognition. mTOR binds mLST8 (mammalian lethal with SEC13 protein 8), a core component of the complex, structural data suggests that mLST8 stabilizes the kinase domain of mTORC1 (64), but ablation of mLST8 does not have any effect on mTORC1 known substrates phosphorylation in vivo (65). Raptor forms a scaffold platform for mTORC1 accessory factor PRAS40 (proline-rich AKT substrate 40 kDa; also known as AKT1S1), which acts as an endogenous inhibitor of mTORC1 activity (66,67). Another endogenous negative regulator of the mTORC1 component

is DEPTOR (DEP-domain-containing mTOR-interacting protein) which interacts with the FAT domain of mTOR (68). Most cancers express low levels of DEPTOR (fig 5).
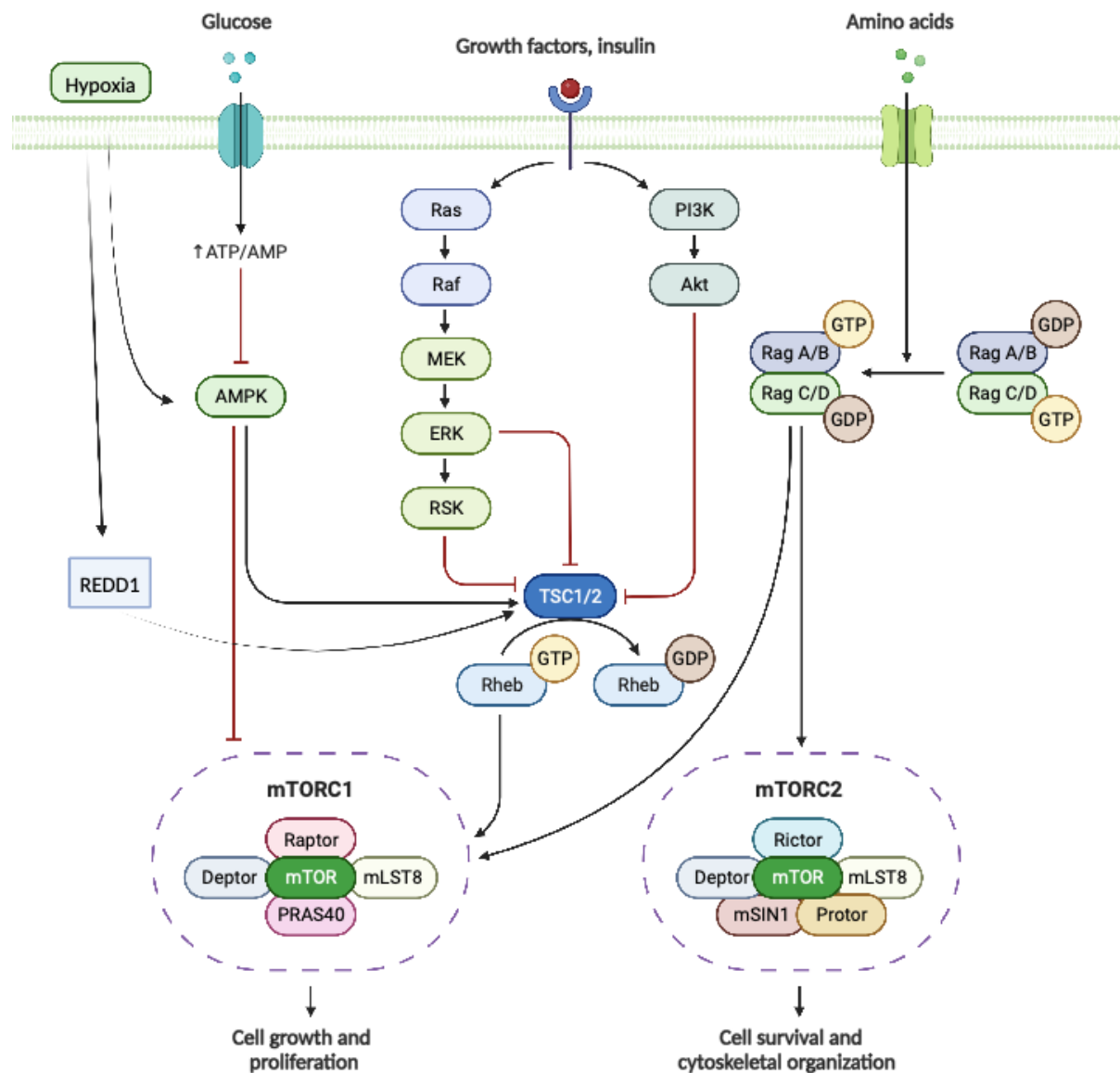
Figure 5: mTORC1 signaling pathway
Oxygen, growth factors and nutrients regulate mTOR function. There are two mTOR complexes mTORC1 and mTORC2, regulates cell growth and proliferation.

1.2.2 Role of mTORC1 in protein synthesis

One of the best characterized mTORC1 downstream processes is protein synthesis, it is the most energy-intensive and resource-intensive cellular process (69). When cells have sufficient building blocks mTORC1 promotes protein synthesis in many different ways. mTORC1

phosphorylates 4E-BP (eukaryotic initiation factor 4E binding proteins), in its unphosphorylated states binds to eukaryotic translation initiation factor 4E (eIF4E), an essential component of the eIF4F cap-binding complex (fig6). mTORC1 mediated phosphorylation of 4E-BP dissociates from eIF4E and enhances 5′ cap-dependent translation of mRNAs (70, 71, 72). The recent finding showed that mTORC1 directly phosphorylates and inactivates LARP1, it's another important repressor of TOP (terminal oligopyrimidine tract) mRNA translation (76). mTORC1 also regulates protein translation by phosphorylating S6K1 on its hydrophobic motif (T389) to stimulate kinase activity. S6K1 phosphorylates ribosomal protein S6, a component of the 40S subunit (73, 74). However, the function of S6 phosphorylation remains debatable: ablation of all five phosphorylation-serine residues on S6 does not affect organismal viability or translation efficiency (75). S6K also activates transcription of rRNA by directly phosphorylating the regulatory factors UBF (upstream binding factor), transcription initiation factor 1A (TIF-1A), and MAF1 ((repressor of RNA polymerase III transcription MAF1 homolog) (77, 78, 79). S6K1 also enhances protein synthesis by directly phosphorylating eIF4B (eukaryotic translation initiation factor 4B), a positive regulator of the 5′-cap-binding eIF4F (eukaryotic translation initiation factor 4F) complex, thus promoting the translation of mRNAs with complex 5′ untranslated regions (80). In addition, S6K1 is recruited to the newly synthesized mRNA by SKAR, which is deposited at the EJC (exon junction complex) during splicing, and SKAR and S6K1 boost the rate of the translation efficiency of spliced mRNA (81). Although 4E-BP1 and S6K1 both regulate global translation, recent evidence indicates that 4E-BP1 has a prominent role. Mice lacking S6K1 in mouse liver showed no reduced global translation (82, 83).

2.2.3 Role of mTORC1 in nucleotide biosynthesis & lipid biosynthesis

Proliferating cells require a constant supply of nucleotides for DNA replication, transcription and rRNA synthesis. mTORC1 regulates both pyrimidine and purine biosynthesis. mTORC1 increases the transcription factor ATF4 (cyclic AMP-dependent transcription factor ATF-4) dependent expression of the mitochondrial tetrahydrofolate cycle enzyme methylenetetrahydrofolate dehydrogenase 2 (MTHFD2), a key component of the mitochondrial tetrahydrofolate cycle needed for purines (84). S6K1 directly phosphorylates pyrimidine biosynthesis rate-limiting enzyme CAD (carbamoyl-phosphate synthetase 2, aspartate transcarbamoylase, dihydroorotase) (85). Finally, mTORC1 upregulates the oxidative

arm of the pentose phosphate pathway via SERBP, which provides a key components of nucleotide biosynthesis (86) (Fig 6).
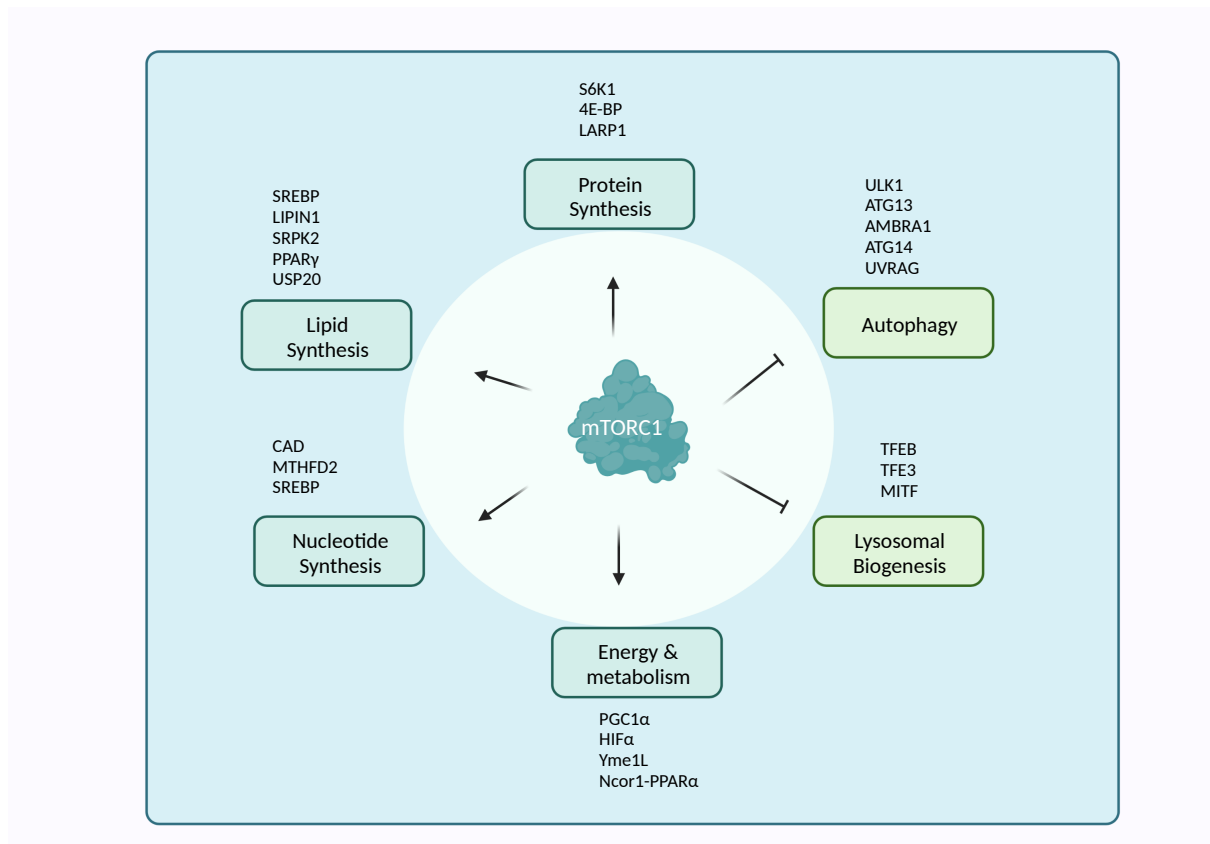
Figure 6: mTORC1 regulates various metabolic functions

mTORC1 promotes anabolism and inhibits catabolism. mTORC1 promotes growth and proliferation by synthesis of various macromolecules.

Cell growth requires sufficient lipids for new membrane formation and expansion. mTORC1 promotes de novo lipid biosynthesis through two axes centered on the transcription factors sterol regulatory element binding protein 1 & 2 (SREBP1/2) and peroxisome proliferator-activated receptor-γ (PPARγ). In low sterol levels, SREBP directly translocate from endoplasmic reticulum (ER) to the nucleus and upregulates genes for de novo lipid and cholesterol synthesis (87). The mTORC1 promotes SREBP transcriptional program by phosphorylating the SREBP inhibitor lipin1 to exclude it from the nucleus (88). mTORC1 also regulates the splicing of lipogenic-related transcripts by phosphorylating SRPK2 (SRSF protein kinase 2) but the mechanism is not yet understood (86). Additionally, the activity of PPARγ (peroxisome proliferator-activated receptor-γ), which promotes adipogenesis, is also tightly regulated by mTORC1 (89). Finally, a new additional level of regulation of lipid biosynthesis, mTORC1 phosphorylates UPS20 (deubiquitylase ubiquitin-specific peptidase

20) at S132 and S134, Phosphorylated USP20 is recruited to the cholesterol biosynthesis rate-limiting enzyme HMGCR complex (3-hydroxy-3-methylglutaryl-coenzyme A reductase) and antagonizes its degradation (90).

2.2.4 Role of mTORC1 in mitochondria and energy homeostasis

Proliferating cells demand a vast amount of energetic currency (ATP), and mTORC1 promotes mitochondrial biogenesis via PGC1α (PPARγ coactivator 1α) and 4E-BP. mTORC1 enhances the expression of mitochondrial genes by yin–yang 1 (YY1) –PPARγ coactivator 1α (PGC1α) transcriptional complex (91). mTORC1 selectively translates nucleus-encoded mitochondria-related mRNAs in a 4E-BP dependent manner (92). mTORC1 also regulates mitochondria post-translationally, inhibiting mitochondrial proteolytic rewiring by i-AAA protease YME1L through lipid signaling cascade (93). Collectively, mTORC1 promotes mitochondrial biogenesis (fig 6).

In parallel to promoting an increased mitochondrial energy production, mTORC1 also acts on metabolic pathways that support cell growth, either by providing energy in the form of ATP or by supplying precursors required for macromolecule biosynthesis. One of the best-studied mTORC1 -mediated metabolic regulations is the fate of glucose. mTORC1 upregulates transcription factor hypoxia-inducible factor 1α (HIF1α) both transcriptional (86, 93) and translationally (94, 95), Increased HIF1α in turn promotes several metabolic functions, including glycolysis, a main energy-producing metabolic pathway.

2.2.5 Role of mTORC1 in catabolism and autophagy

In addition to the various anabolic processes outlined above, mTORC1 also represses catabolic cellular functions, thus preventing the degradation of cellular components and macromolecules that are necessary for cell growth. One such process is autophagy, via which damaged proteins, cytoplasmic parts and organelles are directed to lysosomes for degradation, facilitating the recycling of cellular components. mTORC1 controls autophagy at several stages via the phosphorylation of key components of the autophagic machinery. mTORC1 inhibits autophagy at the stage of initiation by phosphorylating ULK1 and ATG13 (97, 98). Another target of mTORC1 involved in autophagy biogenesis is AMBRA1 (activating molecule in BECN1-regulated autophagy protein 1), which is crucial for ULK1 protein stability (99). mTORC1 inhibits the PtdIns 3-kinase activity of ATG14-containing PIK3C3 by phosphorylating ATG14, which is involved in the early steps of autophagy (100). In starvation, mTORC1 also

phosphorylates UVRAG (UV radiation resistance-associated gene product), which normally associates with the HOPS complex to assist in trafficking and fusion, as well as Rab7(Ras-related protein 7) activation. By disrupting this interaction, mTORC1 inhibits autophagosome maturation and the conversion of endosomes into lysosomes. (Fig 6) (101).

mTORC1 also regulates autophagy in part by phosphorylating and inhibiting the nuclear translocation of the transcription factor TFEB, which drives the expression of genes for lysosomal biogenesis and the autophagy machinery, as well as the related factors MITF (microphthalmia-associated transcription factor) and TFE3 (transcription factor E3) (102,103,104). Newly formed lysosomes then break down proteins and macromolecules and release constituent monomers back to the cytoplasm to regenerate the pool of cellular amino acids, enabling reactivation of the mTORC1 pathway after prolonged starvation (105). In starvation, mTORC1 targets ribosomes to autophagic degradation by recruiting nuclear fragile X mental retardation-interacting protein 1 (NUFIP1) (106).

2.2.6 Regulation of mTORC1 function

To mediate between cellular behavior and the cellular environment, mTORC1 integrates upstream signals, including oxygen, growth factors, nutrient levels, energy and stress. mTORC1 activity oscillates depending on the nutrient availability and other environmental changes stimulated by feeding or fasting. Because mTORC1 initiates a resource-intensive anabolic program, it should only turn 'on' when energy, growth factors, and macromolecular building blocks are all plentiful.

2.2.6.1 Growth factors

mTORC1 acts as a downstream effector for growth factors and other mitogens, largely mediated by the tuberous sclerosis complex (TSC complex) (107). It is a heterotrimeric complex consisting of TSC1, TSC2 and TBC1D7, which acts upstream of Rheb (108). Functions as a GTPase activating protein (GAP) for Rheb, catalyzing the conversion from the active Rheb-GTP state to the inactive GDP-bound state (109, 110). This step is a key brake for mTORC1 activation. TSC activity is regulated at various levels, insulin, insulin/insulin-like growth factor 1 (IGF-1) activates Akt, which phosphorylates TSC2 at multiple sites to dissociate TSC from the lysosomal surface and releases inhibition of Rheb and mTORC1(111, 112, 113, 114). To sustain mTORC1 activity and restore TSC at lysosomes, the mTORC1

substrate S6K1 then directly phosphorylates insulin receptor substrate 1 (IRS-1) as part of a negative feedback loop, blocking further insulin-mediated activation of the PI3K–Akt pathway (115, 116). mTORC2 also phosphorylates Akt at multiple residues, thus establishing crosstalk between the two mTOR complexes (117). Growth factors also modulate mTORC1 activity independent of TSC and Rheb, by Akt phosphorylates PRAS40, leading to its sequestration by a cellular 14–3–3 scaffold protein and restoring mTORC1 activity (67). The additional branch of growth factor signaling pathway receptor tyrosine kinase-dependent Ras signaling pathway activates mTORC1 via the MAP Kinase Erk and its effector p90RSK, both of which also phosphorylate and inhibit TSC2 (118). Wnt signaling pathway component GSK3β (glycogen synthase kinase-3 beta) directly phosphorylates TSC2 and regulates the activity of mTORC1(119). Unlike most phosphorylation events that take place on TSC2, the inflammatory cytokine TNFα stimulation downstream target IKKβ (inhibitor of nuclear factor kappa-B kinase subunit beta) directly phosphorylates the TSC1 component (120). Precisely how the TSC complex integrates these various signals and their relative impact on mTORC1 activity in various contexts remains an active area of study.

2.2.6.2 Nucleotides and Lipids

mTORC1 stimulates nucleotide biosynthesis, in turn, purine levels regulate mTORC1 activity by either influencing RHEB farnesylation and membrane association (121) or by inhibiting TSC activity (122). The availability of lipids also regulates mTORC1 activity, and Phosphatidic acid (PA) regulates the localization and stability of mTORC1 (123). Additionally, in recent years, an increasing body of evidence showed that cholesterol signals directly activate mTORC1 at the lysosomal surface, via a mechanism that involves SLC38A9 (sodium-coupled neutral amino acid transporter 9) and the NPC1 (Niemann-Pick disease, type C1) cholesterol transporter (124, 125, 126).

2.2.6.3 Oxygen, energy and glucose

mTORC1 also responds to extracellular and intracellular stresses that are incompatible with growth such as hypoxia, low levels of ATP and DNA damage. Reduced intracellular ATP or glucose and oxygen activate master metabolic stress regulator AMPK (5′-AMP-activated protein kinase; also known as PRKAA1), Active AMPK directly phosphorylates TSC2 and RAPTOR within mTORC1 complex to reduce its activity (127,128). A recent study showed that glycolysis intermediate DHAP (dihydroxyacetone phosphate) as a metabolite that activates

mTORC1 independently from AMPK, through an unknown mechanism (129). Hypoxia regulates mTORC1 activity by upregulating REDD1 (regulated in development and DNA damage responses 1) levels. In normoxic conditions, TSC2 is inactivated by binding to 14-3-3 proteins. REDD1 binding to 14-3-3 proteins releases TSC2, which in turn inhibits mTORC1 activity (130,131).

2.2.6.4 Amino acids

Amino acids are essential building blocks of protein synthesis but also sources of energy and carbon for many other metabolic pathways. The availability of amino acids plays a dominant role in regulating mTORC1 activity. A breakthrough in the understanding of amino acid sensing by mTORC1 came with the discovery of the Rag-GTPases, key players in amino acid sensing and mTORC1 regulation (132, 133). The Rags are heterodimers, consisting of RagA or RagB is bound to RagC or RagD, they can be found in one of two stable conformations: an 'on' state, in which RagA/B is bound to GTP and RagC/D to GDP; and an 'off' state, Rag GTPases adopt the opposite nucleotide loading state (134). In amino acid sufficiency converts the Rags to their active nucleotide-bound state, allowing them to bind Raptor and recruit mTORC1 to the lysosomal surface, where Rheb is also located. The availability of amino acids and nutrients modulates its GTP states by upstream GEF proteins. The first identified GEF pentameric LAMTOR complex (comprising p18, p14, MP1, C7orf59 and HBXIP) for RagA/B and their interaction dependent on amino acids and the v-ATPase activity. Later another GEF was identified for Rag A, SLC38A9 (sodium-coupled neutral amino acid transporter 9), an AA transporter that resides on the lysosomal surface (139). In similar to GEFs they are two GAPs have been discovered GATOR1 and FLCN-FNIP2 (Folliculin, FLCN-interacting proteins 1 and 2) (137, 138). GATOR1 has three stably interacting subunits: DEPDC5, NPRL2 and NPRL3, with GAP activity residing in the NPRL2 subunit. When cytosolic amino acid levels are reduced GATOR1 hydrolyses the GTP bound to RagA/B and inhibits the mTORC1 pathway, but the mechanism is poorly understood (135). GATOR1 interacts with the pentameric complex GATOR2 (WDR59, WDR24, MIOS, SEH1L and SEC13), through an unknown molecular mechanism GATOR2 inhibits GATOR1 activity. The relationship between GATOR1 and GATOR2 activity remains one of the most intriguing challenges in the field of mTOR biology (136) (fig 7).

Under acute leucine starvation, SESTRIN2 is a direct leucine sensor upstream of mTORC1 that directly binds to GATOR2 and inactivates. Leucine binding SESTRIN2 relieves GATOR2 inhibition and activates mTORC1 via Rags in the presence of abundant leucine levels (141, 142). Additionally, leucine can also be sensed by LARS (leucyl-tRNA Synthetase 1) can activate in a Rag GTPase-dependent manner (143). Another leucine sensing mechanism described recently, a downstream leucine catabolic product acetyl-CoA, which acetylates RAPTOR and activates mTORC1 (144). Recently, SAR1B found as a leucine sensor, in leucine deprivation SAR1B directly binds to GATOR2 and inhibits mTORC1 activity. In leucine abundance, SAR1B binds to leucine, undergoes a conformational change and dissociate from GATOR2, which leads to mTORC1 activation. (169) (fig 7).
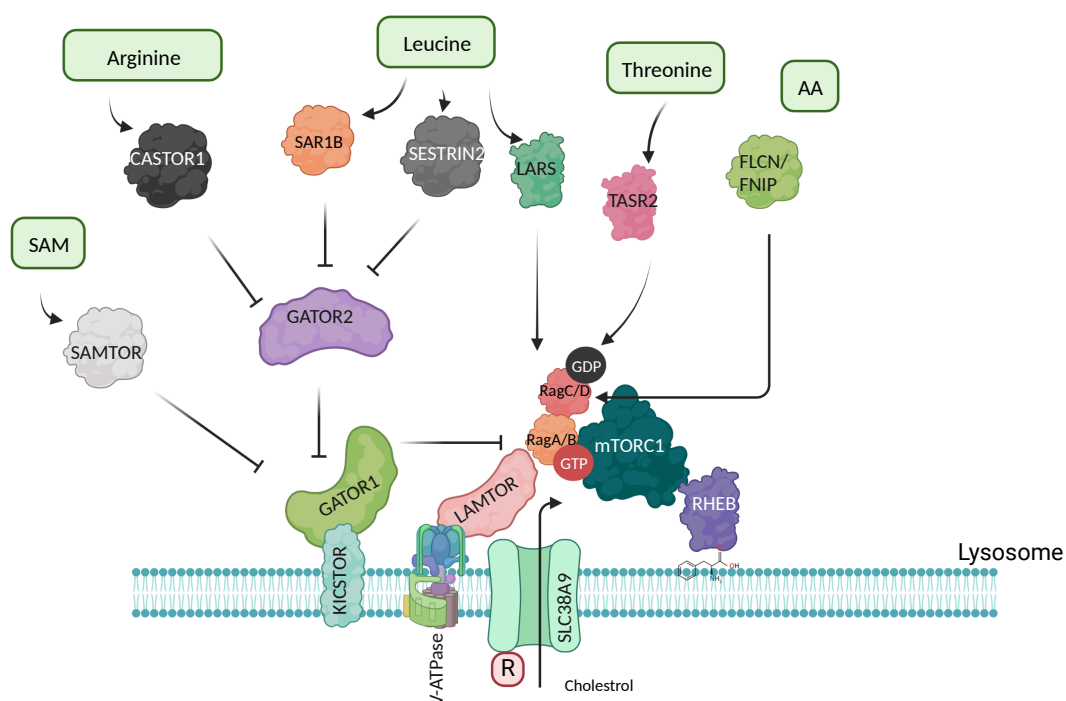
Figure 7: The mechanism of amino acids sensing

mTORC1 is master regulator of nutrient sensing. mTORC1 senses different amino acids availability.

Similar to leucine, the amino acid Arginine is also regulating mTORC1 activity through arginine sensor CASTOR1/2 (cytosolic arginine sensor for mTORC1) binds and inactivates GATOR2 when arginine levels dropped, thus inactivating mTORC1 activity. When abundant arginine availability, arginine binds to CASTOR1 and dissociates from GATOR2 to activates

mTORC1 signaling (145, 146). Additionally, there is another arginine sensor on lysosomes, SLC38A9 is a neutral amino acid transporter that acts as a lysosomal arginine sensor. Upon binding to arginine, SLC38A9 activates mTORC1 in a v-ATPase- and LAMTOR-dependent manner (147, 148).

Similar to leucine catabolic product, methionine downstream metabolite S-adenosylmethionine (SAM) also regulates mTORC1 activity through SAM sensor SAMTOR. Unlike Sestrin2 and CASTOR1, SAM does not signal via GATOR2, instead, SAMTOR negatively regulates mTORC1 by binding GATOR1 and KICSTOR under methionine or SAM deprivation (149). Threonine also activates mTORC1 by TARS2 (mitochondrial threonyl-tRNA synthetase 2), which directly binds GTP-bound RagC. TARS2 does not have a GEF domain, so the mechanism of GEF activity via TARS2 on Rags is unknown, there could be additional protein may involve (fig 7) (150).

At present, we do not know how other amino acids impact mTORC1 activation, more research is required to fully understand the differential activation of mTORC1 by distinct amino acids, and additional direct amino acid sensors are likely to emerge soon.

1.2.7 mTORC1 in physiology and pathophysiology

The fluctuations in the availability of nutrient sources following feeding or fasting require alterations in whole-body metabolism to maintain homeostasis. Under starvation, levels of nutrients and growth factors are reduced, inducing catabolism in which energy stores are mobilized to maintain essential functions. Alternatively, the fed-state trigger a switch towards anabolic growth and energy storage. Since mTORC1 plays an important role in energy homeostasis, physiological studies in mice have revealed that mTOR signaling is essential for proper metabolic regulation at the organismal level. Modulation of proper mTORC1 signaling is crucial in response to nutrient status, therefore, discrepancies in mTORC1 signaling lead to various metabolic diseases, cancer and aging-associated diseases (151).

mTORC1 plays an important role in glucose homeostasis and type 2 diabetes. Liver from 24 hours fasted mice showed decreased 25% body weight, which was explained by changes in cell size but not from changes in cell number (152). Strikingly, this fasting-induced reduced cell size was abolished in mice with liver-specific knockouts of TSC1, Raptor, or the autophagy gene Atg7, suggesting that the switch from anabolism to catabolism is primarily regulated by mTORC1 (152,153). β-cell-specific TSC2 knock out (β-TSC2KO) mice have a biphasic effect

on β-cell function, with young β-TSC2KO mice showing increased β-cell mass, higher insulin levels, and improved glucose tolerance. This effect was reversed when mice grow older. Thus, active mTORC1 in the pancreas is beneficial initially for glucose tolerance, but later it leads rapid decline in β-cell function over time (154,155). Ablation of S6K1 can protect against diet-induced obesity and enhances insulin sensitivity (156) but long-term treatment of mTORC1 inhibitors in ageing studies showed mice developed insulin resistance and immunosuppression. This is partly due to disruption in mTORC2- Akt-dependent insulin response. (157)

WAT (white adipose tissue) is the largest reservoir of energy in the body. Active mTORC1 increases the synthesis and deposition of triglycerides in white adipose tissue. Given the importance of mTORC1 role in lipogenesis and differentiation of pre-adipocytes, adipocyte-specific Raptor knockout reduces WAT tissue mass and enhances lipolysis in mouse models, resistant diet-induced obesity. These defects in adipocyte expansion can drive fat deposits to accumulate in the liver instead, leading ultimately to hepatic steatosis and insulin resistance (158, 159).

Surprisingly, mTORC1 kinase is rarely mutated in cancers but its upstream oncogenic nodes are highly mutated especially the PI3K–Akt pathway and the Ras-driven MAPK pathway. As a result, mTOR signaling is hyperactive in a majority of human cancers to sustain cancer cell growth and survival (160). The tumor microenvironment is often poorly vascularized, hence loss of nutrient sensing mechanism by mTORC1 may help cancer cells evade metabolic checks on anabolism and proliferation. However, mTORC1 inhibitors have not met success in cancer treatment so far, which may be largely due to the cytostatic nature of the inhibitors (161).

Ageing is characterized by a progressive decline in multiple cellular and organismal functions, collectively described as "the hallmarks of ageing. Nutrient sensing is one of the hallmarks of ageing (162). Genetic inhibition of the mTORC1 signaling pathway through deletion of mTOR or Raptor has been shown to extend lifespan in organisms from single cellular organism yeast to mammals (163,164,165). In a similar line, chemical inhibition of mTORC1 with rapamycin also promotes longevity. In middle-aged mice, transient rapamycin treatment not only increased lifespan but also promoted an improvement of healthy span (reversing age-associated phenotypes) (166). One of the longevity interventions is a dietary restriction or caloric restriction (CR), shown to extend lifespan in a wide range of organisms (162). Given the

critical role of mTORC1 in sensing nutrients and insulin, this has led many to speculate that the extension of lifespan in CR is due to reduced mTORC1 signaling. Indeed, CR on top of genetic or chemical inhibition of mTORC1 fails to confer any additional longevity benefit in flies, worms and yeast. This indicates an overlapping mechanism (163,165,168).

In conclusion, mTORC1 is a master sensor for nutrient availability and regulates cell growth and homeostasis. Dysregulation of mTORC1 signaling or nutrient sensing is associated with various metabolic diseases and cancer.

## 2.3 Cellular Proteolytic quality control

In cells, proteins are continuously synthesized and degraded, a process referred to as protein turnover. This process is tightly regulated and helps to maintain protein homeostasis, also known as proteostasis. Proteostatic mechanisms are one of the cell's most essential processes, as they ensure that functional proteins are maintained at their proper concentrations and in the right locations needed for different cellular activities (170). The continuous protein turnover is necessary for cells to adapt their proteomes to internal and external perturbations and eliminates damaged, aged and misfolded proteins. This is important for preserving cellular function relevant to health and disease. Disruption of proteostasis leads to various diseases such as neurodegeneration, inflammation, infection, cancer and ageing (172). There are two major intracellular quality control and recycling mechanisms that are responsible for cellular homeostasis, the ubiquitin-proteasome system (UPS; ubiquitin-proteasome pathway, UPP) and autophagy (lysosomal proteolysis pathway). They regulate various cellular functions, including cell signaling, cell cycle, stress response, apoptosis and protein expression. Ubiquitin-proteasome pathway efficiently degrades short-lived proteins and soluble unfolded/misfolded proteins and polypeptides. Whereas autophagy eliminates large and potentially dangerous cellular components such as protein aggregates and dysfunctional or superfluous organelles. Although autophagy and proteasome pathways operate independently, recent growing literature showed UPS and autophagy are also interconnected (173).

2.3.1 Ubiquitin-proteosome pathway

The proteasome (26S) is a multicatalytic, ATP-dependent protease, composed of two subcomplexes- a catalytic core particle (CP or 20S) and a 19S regulatory particle (RP) (Fig 8). The catalytic CP composed of four heptameric rings ($\alpha7\beta7\beta7\alpha7$) from seven structurally

similar α and β subunits, forms a cylindrical structure with an entrance pore. The multicatalytic protease activity of the catalytic core particle (CP) is achieved by three distinct β - subunits, β1 (caspase-like), β2 (trypsin-like), and β5 (chymotrypsin-like), which cleaves peptides at their respective specificity and generates peptides of 2–24 amino acids, ensuring that no protein will remain intact after entry into the CP and providing an essential source for amino acids (174, 175, 176). The catalytic activity of these β subunits is dependent on threonine residues at their N termini, which classifies the proteasome as a threonine protease, it separates from other well-studied proteases (Cysteine, Serine and Carboxyl). The α- subunits of CP regulate the selectivity and entry of peptides and prevent non-selective degradation (177). The 19S regulatory particle (RP) associates with one or both ends of the 20S Core particle, serves to recognize ubiquitinated substrate proteins and prepares them for degradation in the CP. The regulatory particle (RP) is composed of base and lid sub-assemblies situated on both ends or one end of the 20S. The lid subcomplex is composed of nine subunits (Rpns 3, 5, 6, 7, 8, 9, 11, 12, 15) and regulates several crucial functions that unfold the substrates and deubiquitylation (175). The base subcomplex is composed of 10 subunits, six AAA+ (ATPases associated with various cellular activities) ATPases (Rpt1–6) and four non-ATPase regulatory subunits (Rpns 1, 2, 10, 13), plays an important role in ubiquitin recognition, substrate unfolding and translocation of the unfolded polypeptide into the catalytic chamber (175, 178, 179,180).
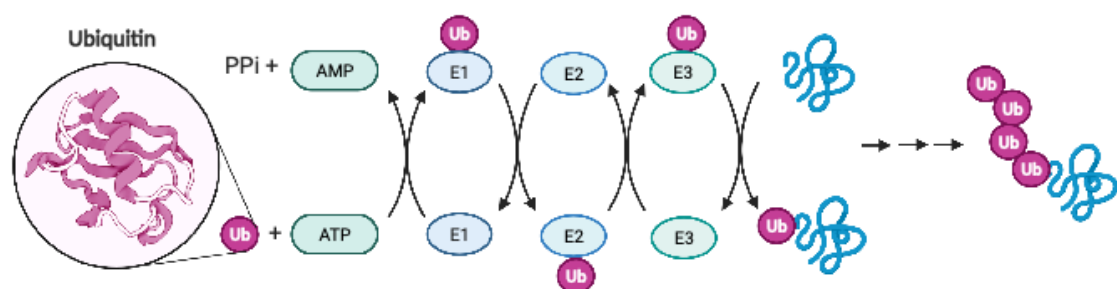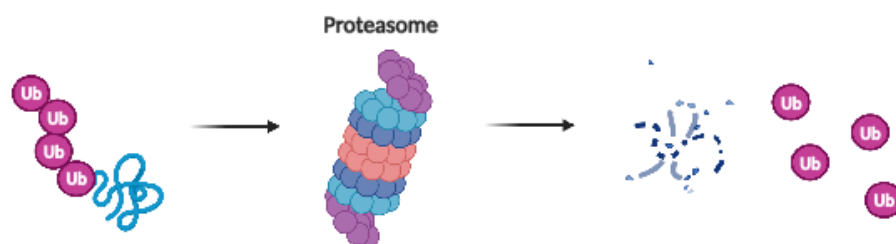
Figure 8: Ubiquitin proteasome pathway

Aged and misfolded proteins undergo ubiquitination and target to the proteasome mediated degradation.

The targeted protein degradation by proteosome is highly regulated and well-studied. UPS system selectively targets for degradation of proteins tagged with ubiquitin (Ub). The ubiquitylation of proteins is carried out by a hierarchically acting enzymatic cascade (E1, E2, E3), E1 (ubiquitin-activating enzyme), E2 (ubiquitin-conjugating) and E3 (ubiquitin ligase) (181,182). In the first step, E1 creates a thiol-ester linkage between the enzyme and the ubiquitin polypeptide in an ATP-dependent manner. Then transferred to E2 for conjugation, finally, the ubiquitin is transferred to a lysine residue of a target protein by ubiquitin ligase enzyme (E3). This ubiquitination is the signal for proteasome-mediated degradation (183). In humans, they are two known E1 enzymes, E2s are n > 50 and nearly 500 E3s, these latter enzymes are endowed with substrate specificity (184, 186). Specific ubiquitin linkage, length and structure determine the fate of the protein, K48-linked ubiquitin chain formation was introduced as the degradation signal for proteasomal degradation (185). Some mono-ubiquitination alters protein localization and some are targeted for degradation by the proteasome. ubiquitin conjugation is readily reversible owing to the existence of numerous deubiquitinating enzymes. Ubiquitination not only targets proteins to proteosome-mediated degradation but also regulates several regulatory functions (fig 8) (172).

2.3.2 Autophagy

Autophagy is a fundamental cellular catabolic process, that eliminates subcellular elements (nucleic acids, proteins, lipids) and organelles, via lysosome-mediated degradation. There are three types of major autophagic pathways, macroautophagy, microautophagy, and chaperon-mediated autophagy. Macroautophagy (hereafter autophagy), is a complex cellular process that promotes both bulk and selective degradation of damaged proteins and organelles or spare molecules to generate macromolecular building blocks and fuel metabolic pathways (Fig 9). There are 20 core autophagy proteins encoded by ATG genes, recruited to the site of phagophore assembly site (PAS). Nucleation and followed by expansion of the phagophore forms a cup-shaped structure, called a phagophore. Further expansion of phagophore by a series of ATG proteins engulfs cytosolic materials. The isolation membrane eventually seals into a double membraned vesicle, termed the autophagosome, then targeted to the lysosome, fuse

with the lysosome forms an autolysosome, which is followed by the degradation of the autophagic body together with its cargo by the autolysosomal hydrolytic enzymes (fig 9) (187,188,189).
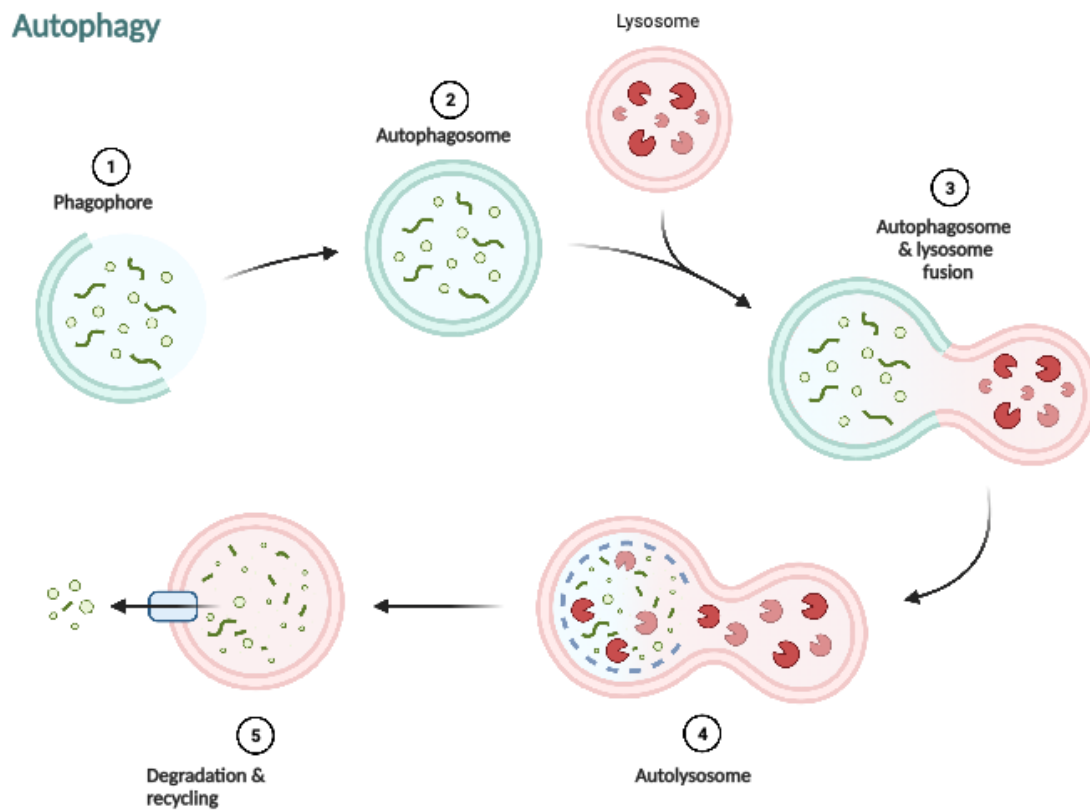
Figure 9: Autophagy

Initiation of autophagy and formation of Phagophore 2. Formation of autophagosome 3. Fusion of autophagosome and lysosome 4. Formation of autolysome 5. lysosomes mediated degradation of intracellular content and recycle macromolecule components.

Autophagy recycles the organelles and macromolecules, replenishes amino acids, nutrients, produce energy and promote protein synthesis. Autophagy regulates intracellular lipid levels, by lipophagy. The autophagy-mediated lipolysis selectively targets lipid droplets, and intracellular lipid stores that serve as an energy source through the hydrolysis of triglycerides (TG) into free fatty acids (FFA) (190). Chaperone-mediated autophagy also regulates intracellular lipid homeostasis by targeting LD to lysosomes. The blockage of either macrolipophagy or CMA-mediated lipophagy develops hepatic steatosis (191). Ribosomes also undergo autophagic degradation under nutrient starvation using NUFIP1 (Nuclear FMR1 Interacting Protein 1) as a receptor (106). Other sub-cellular organelles also undergo

autophagic degradation, such as mitochondria (mitophagy), the nucleus (nucleophagy), the ER (reticulophagy or ER-phagy) and lysosomes (lysophagy) (192).

Mitophagy is the selective autophagic elimination of dysfunctional or surplus mitochondria, which is induced by an array of cellular events hypoxia, differentiation and mitochondrial damage. Cells possess several mitophagy mechanisms, they are classified into ubiquitin-dependent and ubiquitin-independent (193). In functional mitochondria, PINK1 is transported into the inner mitochondrial membrane (IMM), and it gets cleaved by PARL protease. In depolarized mitochondria, membrane insertion of PINK1 is inhibited and stabilizes on the outer mitochondrial membrane (OMM) (194). PINK1 is activated by auto-phosphorylation leading to Parkin translocation to the mitochondrial surface and promoting ubiquitination at the mitochondrial outer membrane. This poly-ubiquitination signals and targets mitophagy (195). In addition to Parkin, they are several other ubiquitin E3 ligases, such as SMURF1, Gp78, MUL1 SIAH1, and ARIH1 play a role in mitophagy. In addition to ubiquitin-dependent mitophagy, there are mitochondrial proteins that serve as mitophagy receptors, targeting dysfunctional mitochondria directly to autophagosomes for degradation (196, 197, 198,199). In yeast, ATG32 act as a receptor for mitophagy (200). In humans, The OMM proteins and FUNDC1 (FUN14 domain-containing protein 1), NIX (NIP3-like protein X) and BNIP3 (BCL2 interacting protein 3) are mitophagy receptors that fine-tune mitochondrial populations in response to various stimuli (56, 57, 201). NIX has a critical role in programmed mitophagy during the maturation of erythroid cells (201). Recently, PHB2 (prohibitin) has been identified as a mitophagy receptor mediating parkin-dependent mitochondrial removal during energetic stress (202). Similar to PHB2, mitochondrial inner membrane phospholipid cardiolipin externalizes during mitochondrial damage and interacts with LC3 initiating a signaling cascade for the elimination of damaged mitochondria by autophagosomes (203). Impairment of mitophagy leads to various diseases, such as neurodegenerative diseases, metabolic disorders, myopathies, inflammation and cancer (204).

2.3.3 Mitochondrial proteolytic quality control

Mitochondria harbor an independent proteolytic system that allows for the complete degradation of proteins to amino acids in different mitochondrial compartments. Initially, many proteases were considered to be mainly quality control enzymes that remove damaged proteins and prevent their possible deleterious accumulation as the first line of defense against

mitochondrial damage, before mitophagy could act upon them. However, recent evidence indicates, mitoproteases regulate numerous mitochondrial functions by the proteolytic process of regulating proteins. Mitochondrial proteases were found to broadly affect mitochondrial functions, such as lipid homeostasis, protein import, mitochondrial gene expression, calcium signaling, and oxidative phosphorylation (OXPHOS) complex assembly to mitochondrial dynamics, mitophagy, and cell death. There are 23 peptidases exclusively localized within mitochondria, and others were found to shuttle between the cytosol and mitochondria. Among these proteases, 6 are pseudoproteases and the remaining 18 intrinsic proteases are dived into four functional categories processing peptidases, ATP-dependent peptidases, oligopeptidase, and other mitochondrial peptidases. The detailed functions of all intrinsic proteases are listed in table (207). Here onwards we are focusing on mainly AAA-proteases.

Category	Protease	Localization	Regulatory functions
ATP dependent proteases	AFG3L2 SPG7	Matrix/IM	Ribosome assembly MCU assembly
	CLPP	Matrix	Transcription/translation Riobosome assembly
	LONP1	Matrix	mtDNA maintainence mtDNA replication, hypoxia adaptation
	YME1L	IM/IMS	Protein import, Lipid trafficking Mitochondrial dynamics, Metabolism, innate immune response
Processing peptidase	ATP23	IMS	protein maturation ATP synthase assembly
	OMA1	IMS/IM	Mitochondrial dynamics, ISR signalling
	PARL	IM	Apoptosis, Mitophagy Lipid trafficking, CoQ biosynthesis complex III assembly
	IMMP	IM/IMS	Protein maturation Apoptosis/senesence
	METAP1D	Matrix	Protein maturation
	MIP	Matrix	Protein maturation, CoQ biosynthesis Complex III and IV activity
	XPNPEP3	Matrix	Protein maturation and stability
	PMPCB	Matrix	Protein maturation
Oligopeptidase	MEP	IMS	ND
	PITRM1	Matrix	ND
Other mitochondrial protease	HTRA2	IMS	Stress signalling, Apoptosis
	LACTB	IMS	PE metabolism

Abbreviations: IM, inner membrane; IMS, intermembbrane space; ND, no data adopted and modified from *Deshwal et al 2020*

Table1: List of mitochondrial proteases and its functions

ATP-dependent proteases localized in different compartments of mitochondria and represents core components of the mitochondrial proteolytic system and exhibit both quality control and regulatory functions. These are matrix-localized LONP1, CLPP and membrane-bound YME1L and AFG3L2 (Fig10). LONP1 maintains matrix protein control and regulates mitochondrial genome maintenance. Lonp1 degrades unbound TFAM (mitochondrial transcription factor A) to mtDNA, TFAM is a central player in mtDNA replication, transcription and inheritance (208). LONP1 is upregulated in hypoxia by HIF1 and regulates mitochondrial complex IV activity (23). Another, matrix AAA protease CLPP targets the N- module of complex I (209), and a LONP1–CLPP proteolytic axis degrades the peripheral arm of respiratory complex I to limit ROS production in depolarized mitochondria (210). CLPP also regulates mitochondrial ribosomal assembly and translation by degrading ERAL1 (figure 10) (211).

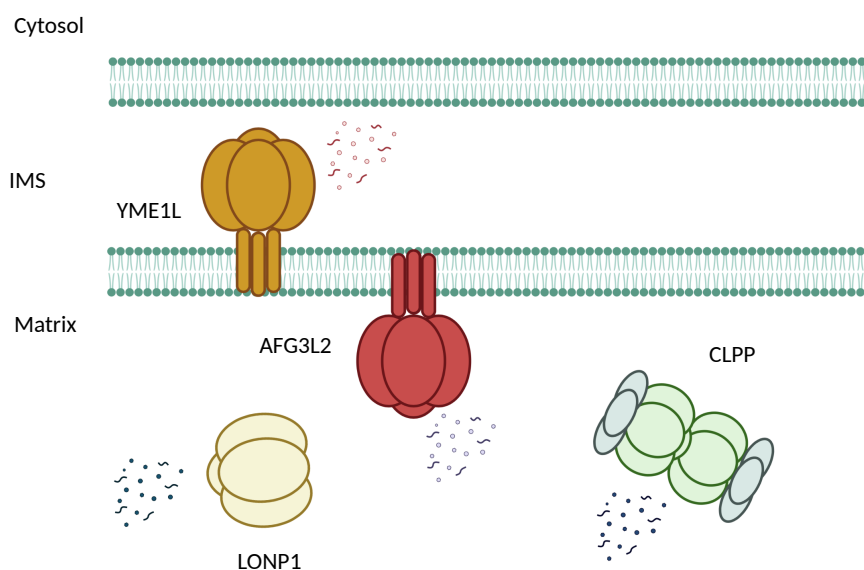**Figure 10: Mitochondrial AAA-proteases**

Mitochondrial AAA- protease maintains mitochondrial protein quality control in different compartments.

The i-AAA protease YME1L faces towards the inner membrane space (IMS), composed of six subunits and forms a homo-oligomeric structure. YME1L interacts with scaffold protein in inner mitochondrial membrane SLP2 and protease PARL, forming SPY complex (SLP2–

PARL–YME1L), which modulates membrane protein turnover (212). YME1L toghether with another inner mitochondrial protease OMA1 regulates mitochondrial dynamics by processing OPA1 (213). YME1L is essential for embryonic development and Cardiac-specific ablation of Yme1l in mice leads to dilated cardiomyopathy and heart failure and stabilization of OPA1 by deleting OMA1 restored cardiac function, suggesting the deleterious effect of mitochondrial fragmentation in the heart (214). Loss of YME1L in the mammalian nervous system impairs eye development and causes axonal degeneration. In contrast to the heart, deletion of OMA1 in the nervous system aggravated the disease phenotypes, this may indicate the tissue-specific role of YME1L (or OMA1) that may be related to the different metabolic demands of neurons and cardiomyocytes (215). In hypoxia and nutrient deprivation conditions, YME1L is activated by lipid cascade and rewires the inner mitochondrial membrane (IMM) and inner mitochondrial space (IMS) proteome. Upon nutrient starvation, mTORC1 is inactivated, and it no longer phosphorylates LIPIN1, this activated LIPIN1 decreases PS (phosphatidylserine) levels, which is required for the synthesis of mitochondrial PE (phosphatidylethanolamine). Reduced PE in the inner mitochondrial membrane activates YME1L activity and initiates proteolytic rewiring. This proteolytic rewiring limits mitochondrial biogenesis by modulating mitochondrial import, phospholipid biogenesis and metabolic homeostasis in hypoxia and nutrient starvation. YME1L-mediated proteolytic rewiring plays an important role in pancreatic ductal adenocarcinoma (PDAC) tumorigenesis. In addition, YME1L-mediated proteolytic rewiring mitochondria is critical for cellular adaptation to oxygen and nutrient starvation (93). YME1L influences pyrimidine biosynthesis and regulates innate immune response in a cGAS-STING dependent manner (216).

Another AAA protease AFG3L2 (m-AAA) localized in the inner mitochondrial membrane and its catalytic domain faces towards the matrix. AFG3L2 is composed of six subunits, either from homo-oligomeric structures or hetero-oligomeric structures with SPG7 (paraplegin) (217). Mutations in genes encoding m-AAA protease subunits have been associated with neurodegeneration and neuronal loss in humans. Recessive mutations in SPG7 (paraplegin) cause hereditary spastic paraplegia (HSP7), it's an autosomal recessive disorder that causes progressive bilateral lower limb weakness and urinary urgency due to degeneration of motor axons of the cortico-spinal tracts (218). Mutation in genes encoding the AFG3L2 protease subunit causes spinocerebellar ataxia type 28 (SCA28), which is accompanied by the loss of Purkinje cells. spinocerebellar ataxia type 28 is an autosomal dominant disorder, rare ataxia

with early onset, which is characterized by progressive gait and limb ataxia with eye movement abnormalities due to cerebellar abnormalities (219). Given the pleiotropic functions of m-AAA proteases in mitochondria, the pathogenic cascade in these diseases remains unclear.

AFG3L2 maintains protein quality control in the inner mitochondrial membrane and matrix, one of the best characterized substrates is MRPL32. Mitochondria lacking AFG3L2 affects mitochondrial assembly and mitochondrial protein synthesis (220). Loss of AFG3L2 activates OMA1 and promotes mitochondrial fragmentations, however, OMA1-mediated mitochondrial fragmentation apparently does not play a prominent role in axonal degeneration in AFG3L2-deficient neurons (221). AFG3L2 regulates mitochondrial calcium homeostasis by regulating the function of the mitochondrial Ca2+ uniporter (MCU) complex. m-AAA degrades non-assembled EMRE subunits and thereby ensures MCU assembly and mitochondrial Ca2+ homeostasis. In the absence of AFG3L2, accumulated EMRE assembles with MCU and forms a constitutively active MCU complex, leading to mitochondrial Ca2+ overload, the opening of the mitochondrial membrane permeability transition pore (mPTP), and inducing cell death (222, 223). Therefore, it is very important to have tight regulation of mitochondrial calcium homeostasis in neurons, Given the evidence, it has been proposed that neuronal cell death observed in the SCA28 mouse model may come from calcium-induced (overload). However, the deletion of MCU a Purkinje cell specific Afg3l2 mouse model did not rescue neuronal death (224). *MitoTag* mice cell type specific profiling of brain mitochondria revealed Purkinje cells express very lower levels of MCU, may be lower expression levels of MCU could be the reason not able to rescue neuronal death in AFG3L2 knockout (227). Recent findings suggests that Ca^{2+}/H$^+$ exchanger TMBIM5 binds and inhibits the AFG3L2 activity (230) However, it is also very important to understand AFG3L2-mediated proteolytic rewiring and find novel substrates.

3. Aim of the thesis

Molecular oxygen sustains intracellular bioenergetics and is consumed by more than 400 biochemical reactions, making it essential for most species on Earth. Reduced oxygen concentration (hypoxia) is a major stressor that generally subverts life of aerobic species and is a prominent feature of pathological states encountered in inflammation, bacterial infection, cardiovascular defects, wounds, and cancer. Despite the fundamental importance of oxygen in human physiology and disease, we currently lack a complete understanding of how the mitochondrial proteome adapts fluctuations in oxygen tensions.

1. In this study, first aim is to study protein turnover changes in hypoxia.
2. Mitochondrial protein quality control is mainly governed by mitochondrial proteases. Here we aimed to identify mitochondrial proteases responsible for reshaping the mitochondrial proteome in hypoxia.
3. How this proteolytic rewiring helps cells to adapt to hypoxia.

4. Materials and Methods

All the original data including metabolomics and proteomics are duly stored in the Maxplanck institute for biology of ageing servers and accessible to all lab members.

If not mentioned otherwise, all the chemicals were purchased from Sigma, Merck and Roth.

4.1 Cell biology

4.1.1 Cell culture

All cell lines were cultured in a humidified incubator at $37°C$ with 5% CO_2. Cells were grown with DMEM -GlutaMAX (4.5grams/Liter glucose) supplemented with 10% fetal bovine (Sigma; F7524) serum and 1mM sodium pyruvate. All reagents were purchased from Gibco otherwise mentioned.

Performing hypoxia experiments, cells were cultured in a hypoxia chamber (Don Whitley Scientific) at $37°C$ with 5% CO_2 and oxygen 0.5%. Culture media and supplements are similar to the above culture conditions.

Normoxia experiments, cells were grown at $37°C$ with 5% CO_2 and oxygen 21%.

All cells were cultured without antibiotics and routinely checked for mycoplasma contamination. The cell number was counted with trypan blue using Themo Countess automated cell counter.

Cell line	Source
Hela wildtype	ATCC
MEF wildtype	ATCC
HeLa AFG3L2$^{-/-}$	Yvonne Lasarzewski
MEF CLPP wildtype & Knockout	Trifunovic Lab
MEF 4E-BP wildtype & Knockout	K. Winklhofer Lab
MEF TSC2 wildtype & Knockout	Demetriades Lab
MEF ATG5 wildtype & Knockout	McBride Lab

4.1.2 Transfection of siRNA and esiRNA

Cells were transfected with Lipofectamine RNAiMAX (Thermo) and incubated for 72 hours (media change at 24 hours). All the esiRNA were purchased from Sigma, for negative control esiRNA targeted to GFP was used. Human Lonp1 esiRNA (EHU072201) and NCLX or SLC8B1(EHU154091).

4.2 Biochemistry

4.2.1 Isolation of crude mitochondria

Crude mitochondria were isolated from TSC2 wildtype and TSC2 $^{-/-}$, cells were harvested at 80% confluency and incubated with isotonic homogenization buffer (220 mM Mannitol, 70mM Sucrose, 20 mM HEPES-KOH (pH 7.4), 1x complete protease inhibitor (ROCHE) for 15 minutes at 4ºC. Cells were homogenized twice using homgen (Schuett Biotech), at 1000 RPM, 2 seconds pulse for 10 times. After first rounds of homogenization After the first rounds of homogenization intact cells and cell debris were isolated by centrifugation at 1,000 g for 10 min at 4°C. The pellet was resuspended with isotonic homogenization buffer and repeat homogenization. The pooled supernatants were centrifuged at 8,000 g for 10 min at 4 °C to obtain the crude mitochondrial fraction. Isolated crude mitochondria can be stored at -80°C.

4.2.2 SDS-PAGE and immunoblotting

Cells were suspended with RIPA buffer (50 mM Tris-HCl pH 7.4, 1% TX-100, 0.1% SDS, 0.5% Sodium Deoxycholate, 1 mM EDTA, 150 mM Sodium Chloride, 1x Complete protease inhibitor (Roche), 1x phosphatase inhibitor (PhosSTOP, Roche)) and incubated for 30 minutes on ice. After lysis cell were centrifuged at 15000 RPM for 10 min. Then, Collected supernatant and quantified protein concentration with Bradford assay. 50-100μg of total protein mixed with LDS Sample Buffer (Invitrogen) were separated using SDS-PAGE (Schägger & von Jagow, 1987). Depending on the desired protein of interest 8-12% Tris/ Tricine gels were used. SeeBlue Plus2 Pre-Stained Protein Standard (Thermo) was used as a size reference. After separation of proteins were transferred to nitrocellulose membrane (GE Amesham). Immunoblotting was performed using antibodies as listed in Table. All antibodies were diluted in 5% milk in TBS/T (TBS, 0.05% Tween-20, 0.02% NaAz). For chemiluminescent detection Western Bright ECL (Roth) or Super Signal West Femto Maximum Sensitivity substrate

(Thermo) was used and the signal was obtained using Chemostar Touch ECL & Fluorescene Imager (Intas).

Antibody	Supplier	dilution
SDHA	Abcam (ab14715)	1:20000
CLPP	Sigma (SAB4100123)	1:2000
ALDH4A1	Abcam (ab181256)	1:2000
ALDH18a1	Abcam (ab127829)	1:5000
NADK2	Abcam (181028)	1:2000
TIMMDC1	Abcam (ab171978)	1:5000
GAPDH	Santa Cruz (sc-32233)	1:10000
HIF1-a	Cayman Chemical (10006421)	1:2000
Vinculin	Cell signaling (#13901)	1:10000
S6	Cell signaling (mAb#2217)	1:5000
pS6 (Ser235/236)	Cell signaling (#2211)	1:5000
TIMM17A	Gene Tex (16468)	1:2000
DNAJC15	Proteintech (16063-1-AP)	1:1000
PRELID1	Fisher scientific (16867553)	1:2000
AFG3L2	Biogene	1:1000
LONP1	Sigma (HPA002192)	1:2000
TUBULIN	Santa Cruz (sc-5286)	1:10000

4.2.3 Measurement of oxygen consumption rate (OCR)

Mitochondrial respiration was measured by Seahorse analyser XFe96 with mito stress test kit (Agilent; 103015) according to the manufacturer's protocol. 40000 MEF cells were seeded per well on XFe96 plate, next day (24 hours) media was exchanged with fresh media containing torin (200nM) and glutamine starvation media. After 3 hours cells were washed with assay medium and add $180\mu l$ media with the above mentioned compounds and incubated for 1 hour at 37c in the non-CO2 chamber. OCR was measured with subsequent injections of the following compounds (Oligomycin 2 μM, FCCP or CCCP 0.5 μM, Rotenone+Antimycin A

0.5 µM each). After the assay, Diverse parameters of mitochondrial functions were calculated by the Seahorse XF report generator (Agilent WAVE).

4.3 Proteomics

SILAC measurement

MEF cells were grown for 5-7 doubling times in the presence of heavy amino acids (N15 Arginine and Lysine). Later switched to media containing light amino acids (N14 Arginine & Lysine), collected cells at different time points (0, 4, 8 &12 hours). Washed with PBS and snap freeze with liquid nitrogen.

Reagents used in SILAC labeling

DMEM without Arginine, Lysine & Glutamine (Silantes, # 280001300)

- 100x PSG (Penicillin-Streptomycin-Glutamine) (Gibco, # 10378016)

- dialyzed FBS (Gibco, # 26400044)

- Arginine (0, 6, 10) (labeled amino acids from Silantes)

- Lysine (0, 4, 8) (labeled amino acids from Silantes)

Protein digestion for proteomics

Cell pellet were lysed in 1% sodium laurate by sonication and heating to 70 °C for 20 min. Centrifuge at 12500 RPM/10 minutes and transfer samples to new low binding protein tube. 40μl sample is used for digestion, proteins were reduced with and alkylated using 10 mMTCEP (tris-(2-carboxethyl)-phosphine) and 55 mM CAA (2-chloroacetamide) (45 min, room temperature in the dark), respectively. Then add Lys C (Wako) (1μg/μL) as Pre-Digestion (not more than 1μl, Lys C:100 protein) shake for 2hours at 37°C. Add Trypsin (1μg/μL) (Sigma) (not more than 1μl, 1 trypsin:100 protein) shake overnight at 37°C 550rpm. stoped digestion with 10% TFA by adding 5 x digestion volume, SDC will precipitate. centrifuge (10min,12600 rpm, RT) and transfer supernatant (contains peptides) to new LoBind Protein Tube.

After digestion, estimated protein concentration with BCA method and desalted peptides with SDBRPS Stage Tip technique.

- SDBRPS resin
- Methanol
- Buffer A (80% Acetonitril, 0,1% Formaldehyd
- Buffer B (0,1% Formaldehyd)
- Buffer E (prepare fresh, 60% Acetonitrile, 1% Ammoniumhydroxid)

- Buffer R

Materials used in Stage Tip technique.

Peptides were desalted on a magnet using 2 x 200 μL acetonitrile. Peptides were eluted in 10 μL 5% DMSO in LC-MS water (Sigma Aldrich) in an ultrasonic bath for 10 min. Formic acid and acetonitrile were added to a final concentration of 2.5% and 2%, respectively. Samples were stored at -20°C before subjection to LC-MS/MS analysis.

Liquid Chromatography and Mass Spectrometry

LC-MS/MS instrumentation consisted of an Easy-LC 1200 (Thermo Fisher Scientific) coupled via a nano-electrospray ionization source to an Exploris 480 or QExactive HF-x mass spectrometer (Thermo Fisher Scientific, Bremen, Germany). An in-house packed column (inner diameter: 75 μm, length: 40 cm) was used for peptide separation. A binary buffer system (A: 0.1 % formic acid and B: 0.1 % formic acid in 80% acetonitrile) was applied as follows for a total gradient time of 90 minutes: Linear increase of buffer B from 4% to 27% within 70 min, followed by a linear increase to 45% within 5 min. The buffer B content was further ramped to 65 % within 5 minutes and then to 95 % within 5 minutes. 95 % buffer B was kept for a further 5 min to wash the column. Prior to each sample, the column was washed using 5 μL buffer A and the sample was loaded using 8 μL buffer A. The RF Lens amplitude was set to 55%, the capillary temperature was 275°C and the polarity was set to positive. MS1 profile spectra were acquired using a resolution of 120,000 (at 200 m/z) at a mass range of 320-1150 m/z and an AGC target of 1×10^6. For MS/MS independent spectra acquisition, 48 equally spaced windows were acquired at an isolation m/z range of 15 Th, and the isolation windows overlapped by 1 Th. The fixed first mass was 200 m/z. The isolation center range covered a mass range of 357–1060 m/z. Fragmentation spectra were acquired at a resolution of 15,000 at 200 m/z using a maximal injection time of 22 ms and stepped normalized collision energies (NCE) of 26, 28, and 30. The default charge state was set to 3. The AGC target was set to 3e6 (900% - Exploris 480, 1e6 for QExactive HF-x). MS2 spectra were acquired in centroid mode.

Analyze SILAC data:

To analyze pulse SILAC DIA data, a library was first created using the Spectronaut's Pulsar search engine using the direct DIA approach applying default settings. The reference Mus Musculus (21984 entries, downloaded September 2019). Data were exported on the precursor

level and the H/L ratios were calculated. Precursor information were aggregated to the protein level using the median of uniquely identified modified peptide sequences.

To calculate the incorporation rates, the remaining heavy fraction was determined by calculating the natural logarithm of H/L / (H/L + 1). Calculated model fit and determined protein turnover rate constant K. The filter applied on r (regression coefficient) values less than 0.85.

To determine cell doubling time, 5000 cells were seeded in 6 well plates and collected cells every 24 hours for five days. Then calculated cell doubling time with

$$\mu = (\,(\log_{10} N - \log_{10} N_0)\,2.303\,) / (t - t_0)$$

$$\mu = \text{Growth rate constant}$$

Cell doubling time for normoxia was 21.6 hours and hypoxia 27.6 hours.

Then we subtracted cell doubling time with protein turnover rate constant

K-LN (2)/ doubling time

After correcting protein turnover with cell doubling time, calculated protein half-lives.

$$T1/2 = ln(2)/K$$

The filtered applied to protein half- lives above 300 hours and calculated the difference in the protein half-lives percentage.

For TSC2 knockout SILAC proteomics experiment was similar to the above-mentioned protocol except for determining the protein turnover rate constant and cell doubling time. In the Tsc2 knockout SILAC experiment there was no difference in the incorporation of light amino acids and also no difference in the light-to-heavy ratios between wildtype and knock out. Hence protein degradation rates were determined by calculation of heavy intensities. First, we calculated Area Under Curve (AUC) for heavy intensities and performed a t-test.

4.4 Metabolomics

Extraction:

4×10^5 cells were seeded, after 24 hours cells were treated with a 1:1 ratio labeled glutamine and unlabeled glutamine for 10 hours. Washed cells with the wash buffer (75 mM ammonium carbonate, pH 7.4) and the plates were snap frozen in the liquid nitrogen. $400 \mu l$ of extraction buffer (acetonitrile:methanol:H2O=4:4:2, -20°C) was added to the wells, scraped and repeated three time extraction and centrifuged at 21000g for 10 minutes at 4ºC. The supernatants were dried by vacuum centrifugation (Labogene) for 6 hours at 20°C while the pellets were used for protein quantification after lysed in the buffer (50 mM Tris- KOH pH 8.0, 150 mM NaCl, 1% SDS) by BCA assay (Thermo; 23225). No internal standard was added for the isotopologue tracing experiments. Isotopologues used in the experiments are as follows: $^{13}C_5$ L- glutamine (Sigma; 605166).

Semi-targeted liquid chromatography-high-resolution mass spectrometry-based (LC-HRS-MS) analysis of amine-containing metabolites:

The LC-HRMS analysis of amine-containing compounds was performed as described previously (225)

In brief: 50 μL of the available 150 μL of the above mentioned (AEX-MS) polar phase was mixed with 25 μl of 100 mM sodium carbonate (Sigma), followed by the addition of 25 μl 2% [v/v] benzoylchloride (Sigma) in acetonitrile (UPC/MS-grade, Biosove, Valkenswaard, Netherlands). Derivatized samples were thoroughly mixed and kept at 20°C until analysis.

For the LC-HRMS analysis, 1 μl of the derivatized sample was injected onto a 100 x 2.1 mm HSS T3 UPLC column (Waters). The flow rate was set to 400 μl/min using a binary buffer system consisting of buffer A (10 mM ammonium formate (Sigma), 0.15% [v/v] formic acid (Sigma) in UPC-MS-grade water (Biosove, Valkenswaard, Netherlands). Buffer B consisted of acetonitrile (IPC-MS grade, Biosove, Valkenswaard, Netherlands). The column temperature was set to 40°C, while the LC gradient was: 0% B at 0 min, 0-15% B 0- 4.1min; 15-17% B 4.1 – 4.5 min; 17-55% B 4.5-11 min; 55-70% B 11 – 11.5 min, 70-100% B 11.5 - 13 min; B 100% 13 - 14 min; 100-0% B 14 -14.1 min; 0% B 14.1-19 min; 0% B. The mass spectrometer (Q-Exactive Plus, Thermo Fisher Scientific) was operating in positive ionization mode recording the mass range m/z 100-1000. The heated ESI source settings of the mass spectrometer were: Spray voltage 3.5 kV, capillary temperature 300°C, sheath gas flow 60 AU, aux gas flow 20 AU at 330°C and the sweep gas was set to 2 AU. The RF-lens was set to a value of 60.

Semi-targeted data analysis for the samples was performed using the TraceFinder software (Version 4.1, Thermo Fisher Scientific). The identity of each compound was validated by authentic reference compounds, which were run before and after every sequence. Peak areas of $[M + nBz + H]^+$ ions were extracted using a mass accuracy (<5 ppm) and a retention time tolerance of <0.05 min. Areas of the cellular pool sizes and the isotopologue enrichment values were calculated as described in the AEX-MS method.

Anion-Exchange Chromatography Mass Spectrometry (AEX-MS) for the analysis of anionic metabolites

Extracted metabolites were re-suspended in 150 μl of UPLC/MS grade water (Biosolve), of which 100 μl were transferred to polypropylene autosampler vials (Chromatography Accessories Trott, Germany) before AEX-MS analysis.

The samples were analysed using a Dionex ionchromatography system (Integrion Thermo Fisher Scientific) as described previously (226). In brief, 5 μL of polar metabolite extract were injected in push partial mode, using an overfill factor of 1, onto a Dionex IonPac AS11-HC column (2 mm × 250 mm, 4 μm particle size, Thermo Fisher Scientific) equipped with a Dionex IonPac AG11-HC guard column (2 mm × 50 mm, 4 μm, Thermo Fisher Scientific). The column temperature was held at 30°C, while the auto sampler was set to 6°C. A potassium hydroxide gradient was generated using a potassium hydroxide cartridge (Eluent Generator, Thermo Scientific), which was supplied with deionized water (Millipore). The metabolite separation was carried at a flow rate of 380 μL/min, applying the following gradient conditions: 0-3 min, 10 mM KOH; 3-12 min, 10–50 mM KOH; 12-19 min, 50-100 mM KOH; 19-22 min, 100 mM KOH, 22-23 min, 100-10 mM KOH. The column was re-equilibrated at 10 mM for 3 min.

For the analysis of metabolic pool sizes the eluting compounds were detected in negative ion mode using full scan measurements in the mass range m/z 77 – 770 on a Q-Exactive HF high resolution MS (Thermo Fisher Scientific). The heated electrospray ionization (ESI) source settings of the mass spectrometer were: Spray voltage 3.2 kV, capillary temperature was set to 300°C, sheath gas flow 50 AU, aux gas flow 20 AU at a temperature of 330°C and a sweep gas glow of 2 AU. The S-lens was set to a value of 60.

The semi-targeted LC-MS data analysis was performed using the TraceFinder software (Version 4.1, Thermo Fisher Scientific). The identity of each compound was validated by authentic reference compounds, which were measured at the beginning and the end of the sequence. For data analysis the area of the deprotonated $[M-H^+]^{-1}$ or doubly deprotonated [M-

2H]$^{-2}$ isotopologues mass peaks of every required compound were extracted and integrated using a mass accuracy <5 ppm and a retention time (RT) tolerance of <0.05 min as compared to the independently measured reference compounds. For the pool size determination, the areas of the cellular pool sizes were derived from the sum of all isotopologues. These areas were then normalized to the internal standards, which were added to the extraction buffer, followed by a normalization to the protein content of the analyzed sample. The relative monoisotope distribution was calculated from the proportion of the peak area of each isotopologue towards the sum of all isotopologues, while the ^{13}C enrichment, namely the summed area of ^{13}C molecules traced in the sum of all isotopologues was calculated by multiplying the peak area of each isotopologue with the proportion of the ^{13}C and the ^{12}C carbon number in its corresponding isotopologue. The obtained ^{13}C areas of each isotopologue are subsequently summed up, providing the absolute ^{13}C enrichment. Dividing this absolute ^{13}C area by the summed area of all isotopologues provides the relative ^{13}C enrichment factor.

5.Results

5.1 Hypoxia regulates protein turnover:

Hypoxia stimulates the transcriptional program by stabilizing HIF-α and helps to transcribe various genes involved in metabolism, angiogenesis, erythropoiesis and stem cell fate, etc. Though hypoxia-mediated transcriptional programs are well studied but post-translational program are less understood. To comprehensively analyze the post-translational regulation of hypoxia, we have employed a methodology that combines metabolic isotopic labeling i.e. dynamic pulse SILAC (Stable Isotope Labelling with Amino Acids in Cell Culture) approach. This enabled us to measure global endogenous protein turnover. Cells were cultured in heavy amino acids labeled with (Arginine & Lysine N15) for 5-7 doubling times and later shifted to light amino acids (Arginine & Lysine N14) and collected at different time intervals (0,4,8,12 hours) in both normoxia and hypoxia (Fig 5.1A). Later measured heavy and light intensities in Mass spectrometry. Using these measurements, we calculated model fit and protein turnover rate constant(K). The critical protein turnover parameter (K), corresponds to the time it takes for a cell's pre-existing pool of proteins to be reduced to half, this is certainly true for non-proliferating cells (non-dividing cells), but in proliferating cells, the pre-existing protein pool will be reduced to half with every cell division even without any active protein degradation. In proliferating cells, the cell division rate must be taken into account and should be included (171,229). We have determined the cell division rate of the cells in both normoxia and hypoxia and calculated protein turnover rates. From the protein turnover rate, we calculated protein half-lives (calculations and formulas are described well in materials & methods).

We have observed >10% of total proteome having faster protein turnover in hypoxia. The median protein half-lives of the cellular proteome are around 25 hours (Fig 5.1B) and HIF-α target genes have faster protein turnover e.g., glycolysis metabolic proteins, when we perform Reactome analysis for faster turnover proteins to understand the biological pathways affected, it shows metabolism, membrane trafficking, SUMOylation, Notch signaling & P53 mediated transcription being the top most affected pathway. Recently it has been shown that mitochondrial i- AAA protease YME1L rewires mitochondrial proteome under hypoxia (94). Here we could successfully identify YME1L substrates, indicates that robustness of the data.

A

B

C
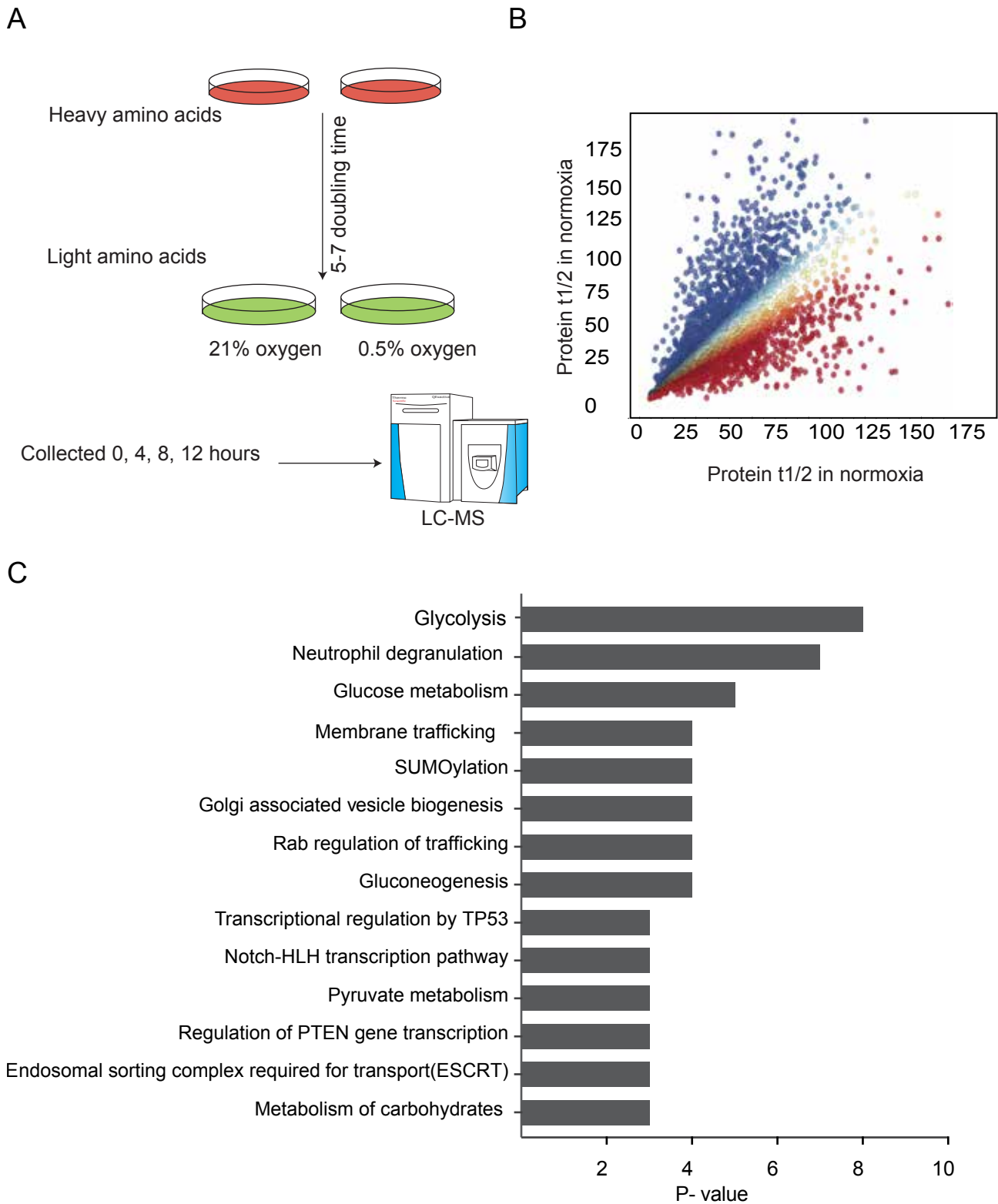
5.1. Hypoxia dependent protein turnover.
A.Schematic depiction of experiment flow for dynamic SILAC in hypoxia. B. Volcano plot representation
of protein half-lives determined by SILAC in the pressence of normoxia and hypoxia. C. Reactome analysis
for proteins having at least 20% of half-lives difference between normoxia and hypoxia.

As we know mitochondria are a hub for metabolism, we further investigated mitochondrial protein turnover in detail. When comparing total mitochondrial proteome >10% mitochondrial proteins have faster turnover in hypoxia. Mitochondrial faster turnover proteins are distributed to different sub-compartments of mitochondria. The majority of the faster turnover proteins are located in the matrix, inner mitochondrial membrane, and inner mitochondrial space (IMM &IMS). This is similar to mitochondrial protein distribution (Fig 5.2A). To identify biological pathways affected under hypoxia, we have used Reactome pathway analysis and found TCA cycle, ETC and metabolism are the most affected pathway under hypoxia(Fig 5.2B). When we carefully assessed the metabolism affected faster turnover proteins, we found proline metabolic proteins have faster turnover in hypoxia (Fig 5.2C). Indeed, we further confirmed with immunoblot, NADK2 levels were increased and ALDH4a1 levels were reduced in hypoxia. ALDH18a1 levels were not changed under hypoxia. (5.3A).

These results indicate hypoxia regulates protein turnover of proline metabolism. Hypoxia regulates mitochondrial protein turnover at different subcompartments of mitochondria. The only subset of mitochondrial proteins (>10%) has faster turnover, indicating it may not be a general protein turnover like autophagy or mitophagy. Mitochondria proteolytic quality control largely governed by mitochondrial proteases and plays an important role in hypoxia. Then we further investigated the role of mitochondrial proteases in faster protein turnover under hypoxia.
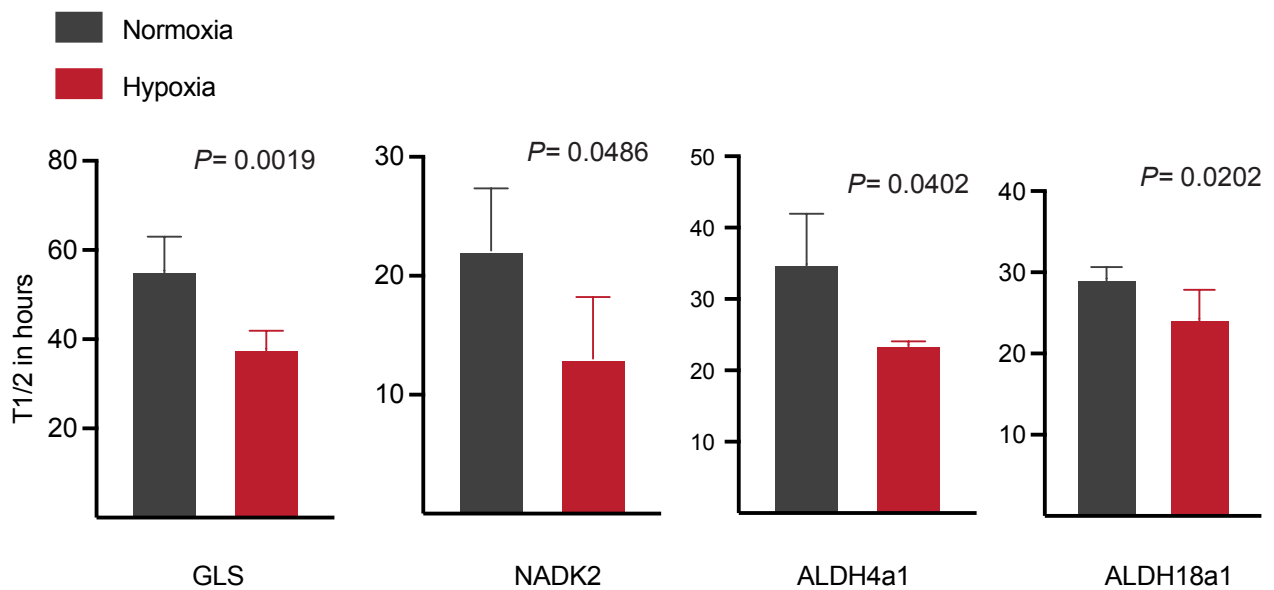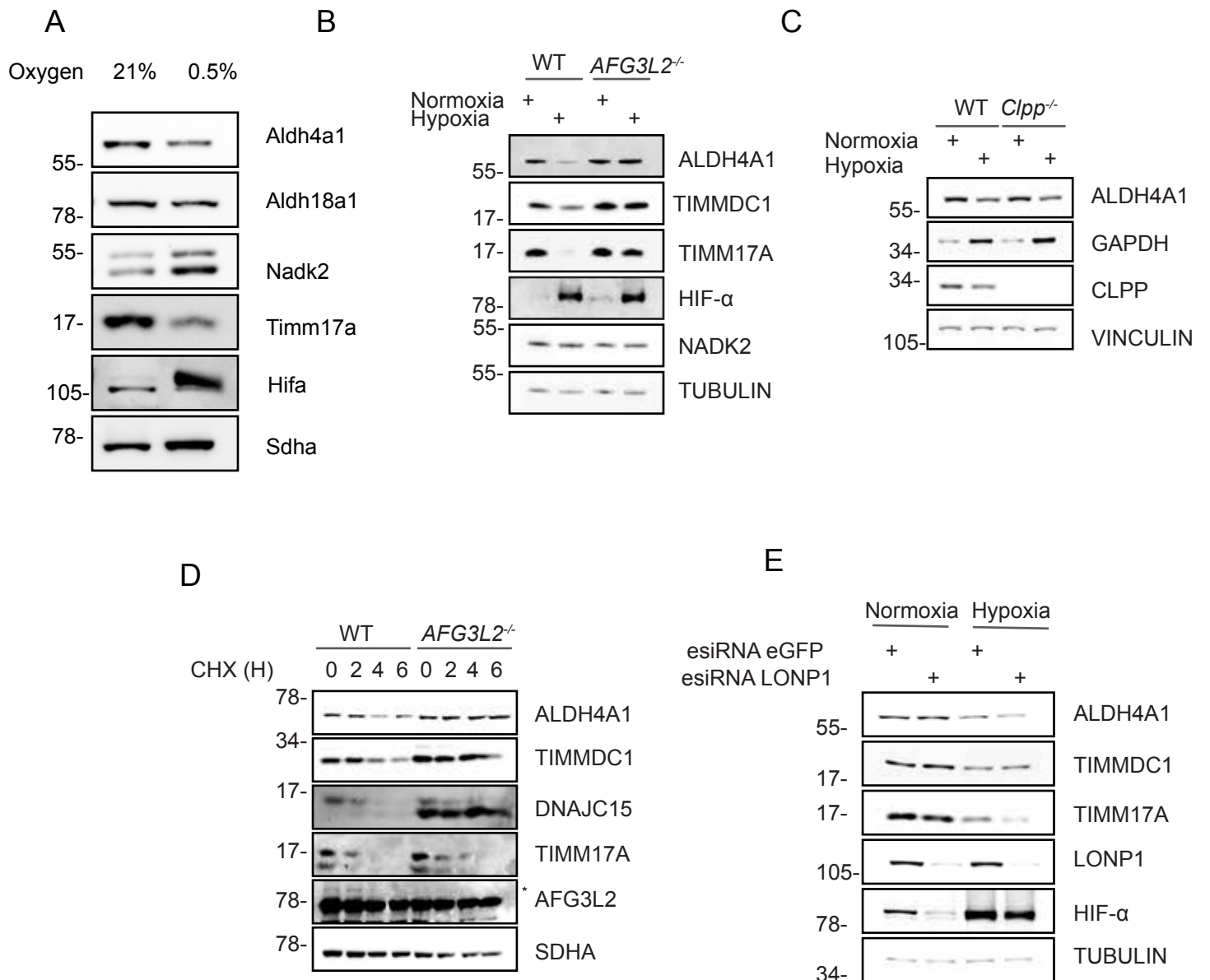
A
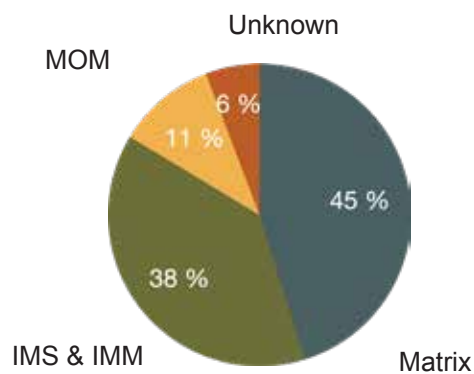
B
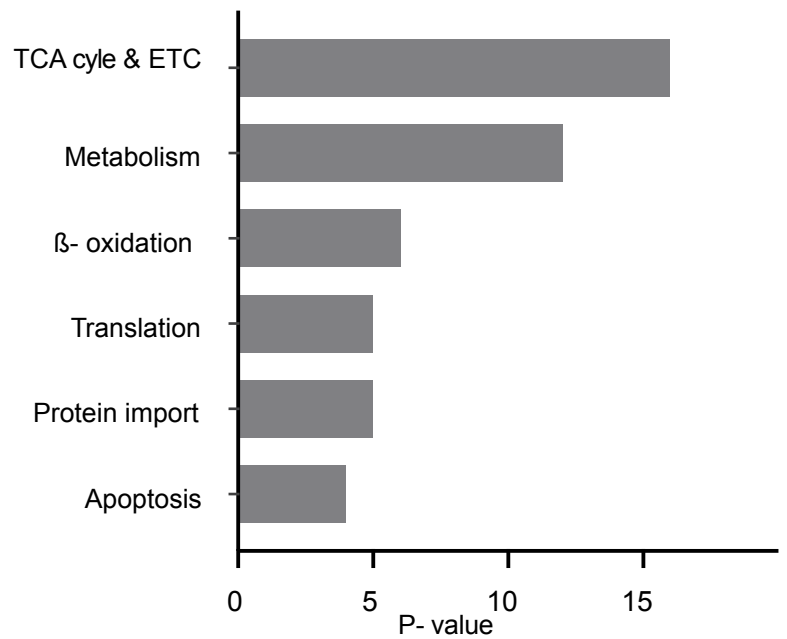
C

5.2. Mitochondrial protein turnover in hypoxia
A. Localization and distrubution of mitochondrial faster turnover proteins B.Reactome analysis for
mitochondrial faster turnover proteins. C. Representation of protein half-lives for proteins
 involved in proline metabolism.

5.2 Hypoxia activates AFG3L2 dependent proteolysis:

Since ALDH4a1 is a matrix protein we screened for matrix proteases responsible for its degradation. Three proteases regulate mitochondrial matrix protein quality control (207), CLPP, LONP1 and AFG3L2. To find protease active upon hypoxia and degrades ALDH4a1, we screened all three proteases under hypoxia. Wild type and CLPP KO were cultured in both normoxia and hypoxia and Aldh4a1 levels didn't affect in loss of CLPP (Fig 5.3C). We further explored to find possible protease, knockdown of lonp1 using small interfering RNA (esiRNA) didn't affect the levels of ALDH4a1 levels in hypoxia (Fig 5.3E). Since, previously showed that i-AAA protease YME1L activates upon hypoxia and rewires mitochondrial proteome (94), we tested the role of AFG3L2 is an m-AAA protease in ALDH4a1 degradation. The loss of AFG3L2 stabilizes ALDH4a1 levels in hypoxia but not in wildtype (Fig 5.3B). This result indicates that AFG3L2 is active under hypoxia. To confirm further confirm AFG3L2-mediated proteolysis upon hypoxia, cells were cultured in hypoxia in the presence of cycloheximide (CHX) and collected at different time intervals. In wild-type cells, AFG3L2 possible substrates were degraded with time but not in AFG3L2 KO cells (Fig 5.3D). This further confirmed that reduced levels of possible substrates of AFG3L2 due to proteolysis. These results suggest that AFG3L2 is activated in hypoxia and regulates the mitochondria proteolysis.

A. Oxygen 21% 0.5%

55-	Aldh4a1
78-	Aldh18a1
55-	Nadk2
17-	Timm17a
105-	Hifa
78-	Sdha

B. WT   *AFG3L2*⁻/⁻

Normoxia +   +
Hypoxia   +   +

55-	ALDH4A1
17-	TIMMDC1
17-	TIMM17A
78-	HIF-α
55-	NADK2
55-	TUBULIN

C. WT   *Clpp*⁻/⁻

Normoxia +   +
Hypoxia   +   +

55-	ALDH4A1
34-	GAPDH
34-	CLPP
105-	VINCULIN

D. WT   *AFG3L2*⁻/⁻

CHX (H) 0 2 4 6 0 2 4 6

78-	ALDH4A1
34-	TIMMDC1
17-	DNAJC15
17-	TIMM17A
78-	* AFG3L2
78-	SDHA

E. Normoxia Hypoxia

esiRNA eGFP +   +
esiRNA LONP1   +   +

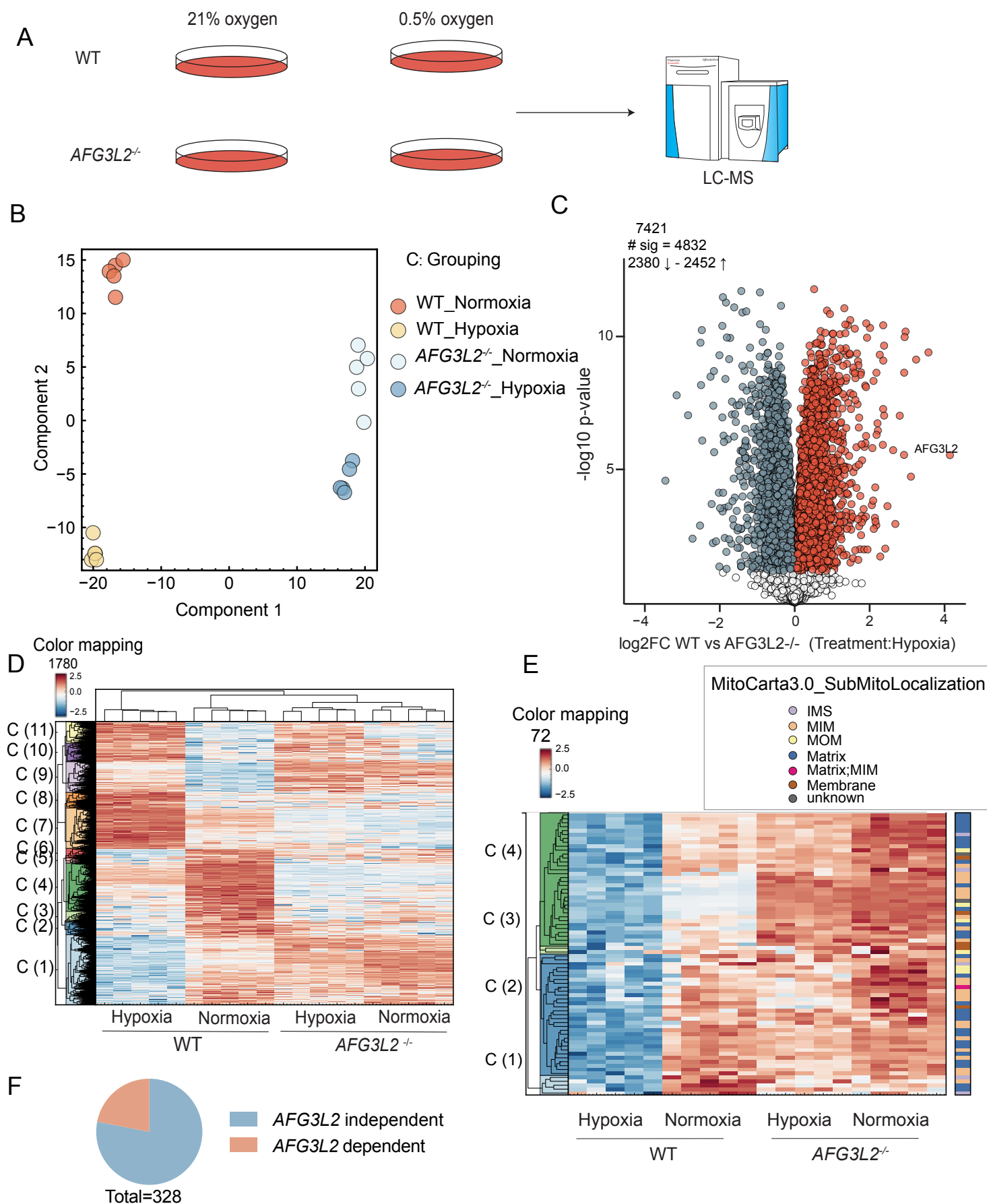| 55- | ALDH4A1 |
17-	TIMMDC1
17-	TIMM17A
105-	LONP1
78-	HIF-α
34-	TUBULIN

5.3. Hypoxia activates AFG3L2 dependent proteolysis

A. immuno blot analysis of proline metabolic proteins in hypoxia for 16 hours (MEF) (n=3). B. Immunoblot analysis of WT and AFG3L2⁻/⁻ HeLa cells in hypoxia for 16 hours (n=3). C. Immunoblot analysis of WT and CLPP⁻/⁻ MEF cells in hypoxia for 16 hours D. Immunoblot analysis of WT and YME1L−/− HeLa cells in the pressence of cyclohexamide (CHX) (n=3). E. Immunoblot analysis of HeLa cells transfected with eGFP and esiRNA Lonp1 in the pressence of hypoxia for 16 hours (n=3).

5.3 AFG3L2 rewires mitochondrial proteome in hypoxia:

To better understand the proteolytic rewiring of AFG3L2, cells were cultured in normoxia and hypoxia and quantitative proteomics was performed (Fig 5.4A). We performed a two-way ANOVA (ANOVA) analysis on the data to understand the genotypic and treatment interaction. Principal component analysis (PCA) of the combined data from wildtype and AFG3L2 knockout suggested marked differences in their response to hypoxia (component1) and there were also marked difference in genotype-dependent changes (component 2) (Fig 5.4B). There are 1780 proteins significantly changed in two-way ANOVA analysis and mapped into 11 clusters. Clusters from 1- 6 show proteins that were reduced upon hypoxia whereas clusters from 7-11 show proteins accumulated upon hypoxia (Fig 5.4 C, D). Cluster 1 proteins showed reduced levels in hypoxia in wild-type cells but were stable or unchanged in cells lacking AFG3L2. Among cluster 1 proteins there are 72 proteins were mitocarta 3.0 positive (Fig 5.4E). Proteins reduced in cluster 1 mitochondrial proteins could be AFG3L2 substrates. Then we mapped these 72 cluster 1 proteins to their sub-localization within the mitochondria. The majority of the proteins were localized either to the matrix or to the inner mitochondrial membrane (IMM) (Fig 5.4E). Since AFG3l2 is an m-AAA protease localized at the inner mitochondrial membrane (IMM) and faces towards matrix, sub-localization of cluster 1 mitochondrial proteins high likely AFG3L2 substrates. We also observed some of the YME1L substrates were stable in cells lacking AFG3L2 in hypoxia, this indicate that there is across-talk between AFG3L2 and YME1L activity. The number of total mitochondrial proteins decreased in hypoxia are 328, out of which 23% proteins are AFG3L2 dependent (Fig 5.4F). These putative substrates of AFG3L2 play several important roles in various cellular functions such as ETC, mitochondrial protein imports, ß- oxidation, glutathione metabolism, etc.

These results indicate that AFG3L2 rewires mitochondrial proteome in hypoxia and maintains homeostasis in normoxia. Mitochondrial proteases YME1L and AFG3L2 reshape the mitochondrial proteome in hypoxia, helping cells to adapt to low oxygen tension.

A. 21% oxygen / 0.5% oxygen — WT, *AFG3L2^−/−* → LC-MS

B. Component 2 vs Component 1

C: Grouping
- WT_Normoxia
- WT_Hypoxia
- *AFG3L2^−/−*_Normoxia
- *AFG3L2^−/−*_Hypoxia

C.
7421
sig = 4832
2380 ↓ - 2452 ↑

AFG3L2

-log10 p-value vs log2FC WT vs AFG3L2-/- (Treatment:Hypoxia)

D. Color mapping
1780
2.5
0.0
−2.5

C (11), C (10), C (9), C (8), C (7), C (6), C (5), C (4), C (3), C (2), C (1)

Hypoxia Normoxia — WT
Hypoxia Normoxia — *AFG3L2^−/−*

E. Color mapping
72
2.5
0.0
−2.5

MitoCarta3.0_SubMitoLocalization
- IMS
- MIM
- MOM
- Matrix
- Matrix;MIM
- Membrane
- unknown

C (4), C (3), C (2), C (1)

Hypoxia Normoxia — WT
Hypoxia Normoxia — *AFG3L2^−/−*

F.
AFG3L2 independent
AFG3L2 dependent
Total=328

5.4. AFG3L2 rewires mitochondrial proteome in hypoxia

A. Schematic depiction of experimental work flow for quantative proteomics in hypoxia. (n=5) B. Principal component analysis (PCA) of WT and AFG3L2 -/- HeLa quantitative proteomics. C. Volcano plot representing WT and AFG3L2 -/- in hypoxia. D. Heat map of Z-scores of log2-transformed LFQ intensities of significantly changed proteins in HeLa cells in hypoxia. E. Heat map of Z-scores of Clusture 1 mitochondrial proteins and its mitchondrial localization.

5.4 mTORC1 regulates the mitochondrial function

It has been known that oxygen availability regulates mTORC1 activity (58). Here we monitored mTROC1 role in mitochondrial function using various OXPHOS modulators. To test mitochondrial bioenergetics under mTORC1 inhibition, cells were treated with either torin or glutamine starvation (Fig 5.5 B). Under the inhibition of mTORC1, basal respiration and ATP production are reduced (Fig 5.5 C,D). In addition to this, spare respiratory capacity is decreased, caused by either a loss of ETC integrity or decreased substrate availability (Fig 5.5E). These results suggest that mTORC1 regulates mitochondrial biogenetics.
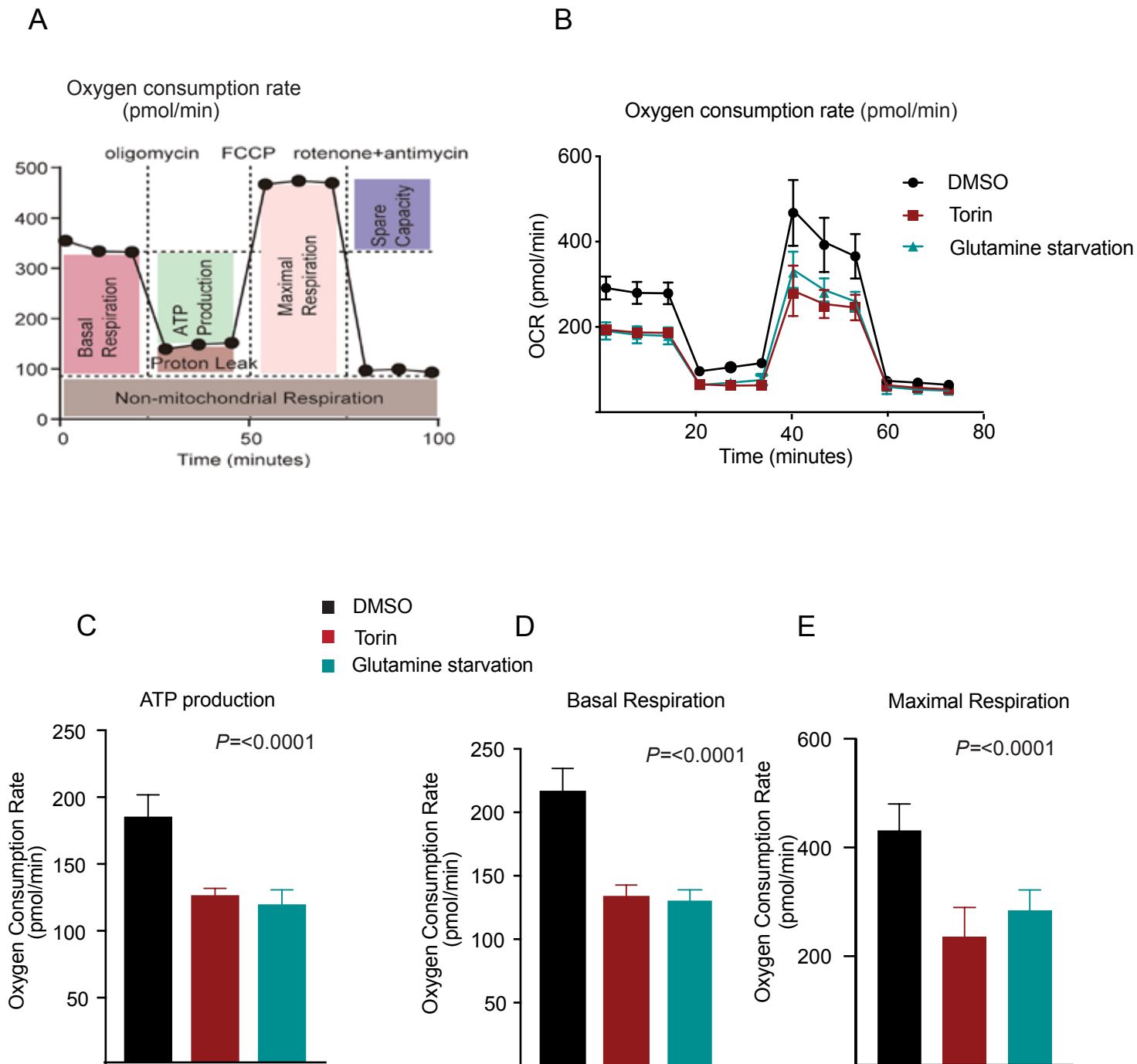
A. Illustration of XF cell mito stress test profile, showing the key parameters of mitochondrial function. **B**. Representive seahorse analysis of OCR in MEF cells in the pressence of torin (200nM) and glutamine starvation for 4 hours. **C, D, E.** Calculation of ATP production, basal respiration and maximal respiration based on seahorse OCR analysis (n=3, mean /SD).

5.5. mTORC1 regulates mitochondrial function

5.5 Inhibition of mTORC1 promotes AFG3L2-dependent proteolysis:

Hypoxia is the one of the main regulators of mTORC1 signaling (58) and mTORC1 regulates mitochondrial function, we tested whether hypoxia induced AFG3L2 dependent proteolysis is dependent on mTORC1. We tested mTORC1 role in AFG3L2 activation, cells were treated with mTORC1 inhibitors Rapamycin and Torin (active site inhibitor of mTORC1). Upon inhibition of mTORC1, AFG3L2 substrates levels were reduced in wildtype cells but not in cells lacking AFG3L2 (Fig 5.6A). Amino acid availability regulates mTORC1 activity (60), so to check the role of nutrient availability in AFG3L2 mediated proteolysis, the cells were starved with either glutamine or amino acids are showed enhanced AFG3L2 dependent proteolysis (Fig 5.6B, C). When the addition of amino acids to the starved cells showed inhibition of AFG3L2-dependent proteolysis (Fig 5.6C). These results collectively suggest that inhibition of mTORC1 promotes AFG3L2-dependent proteolysis.
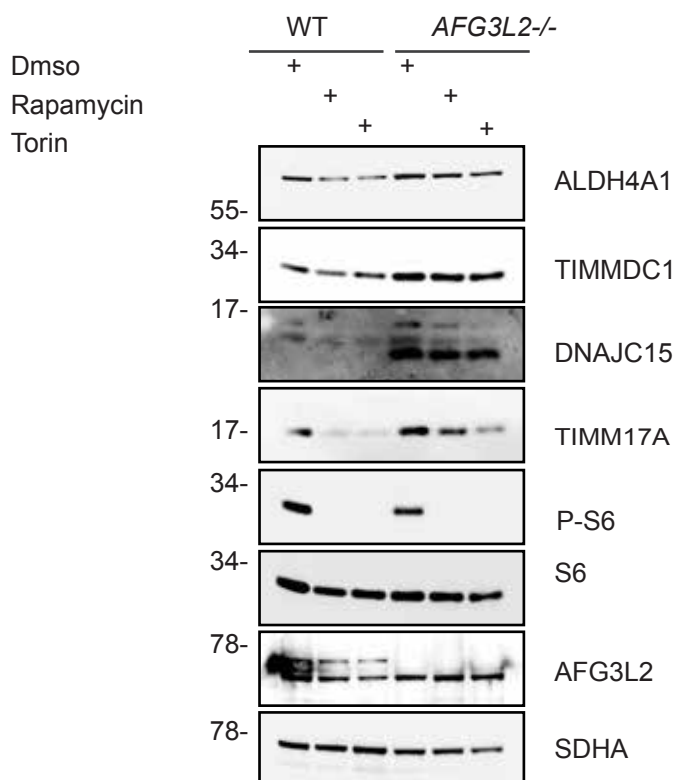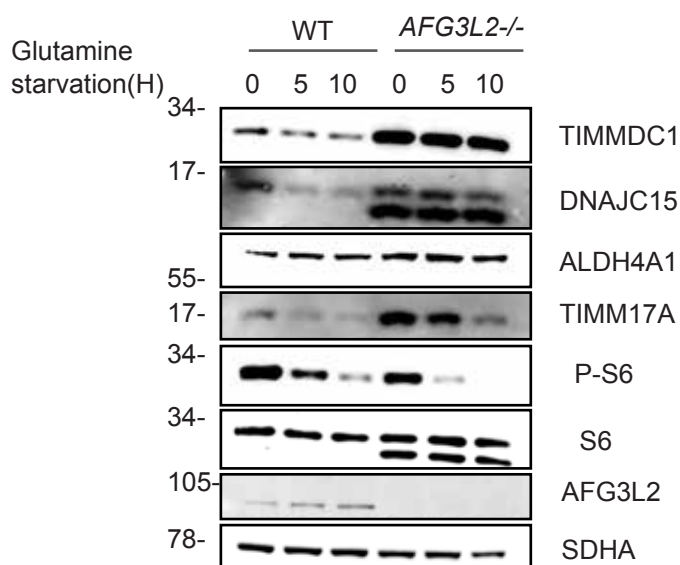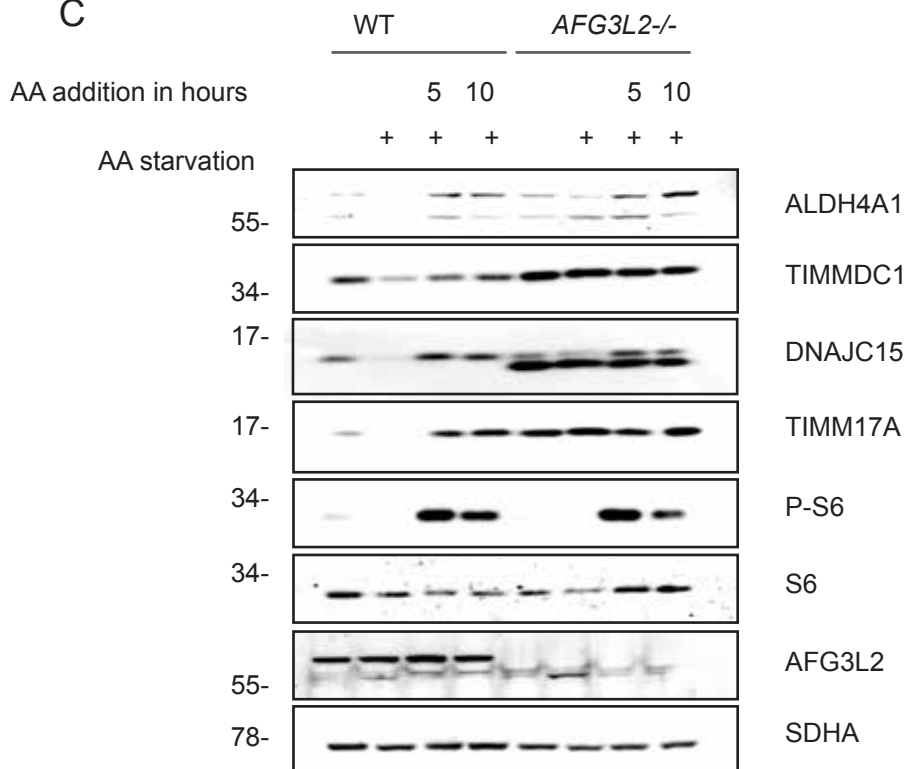
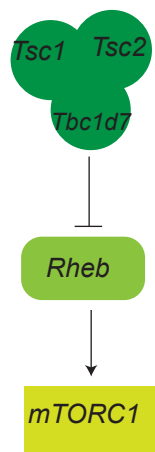**5.6. Inhibition of mTORC1 activates AFG3L2 depedent proteolysis**
A. Immunoblot analysis of WT and *AFG3L2-/-* Hela cells cultured in the pressence of Rapamycin and Torin for 12 hours (representive image of n=3). **B**.Immunoblot analysis of WT and *AFG3L2-/-* Hela cells cultured in the absence of glutamine for 12 hours (representive image of n=3). C. Immunoblot analysis of WT and *AFG3L2-/-* Hela cells cultured in the absence of amino acids for 12 hours, then amino acids are added at 0, 5, 10 hours (representive image of n=3).

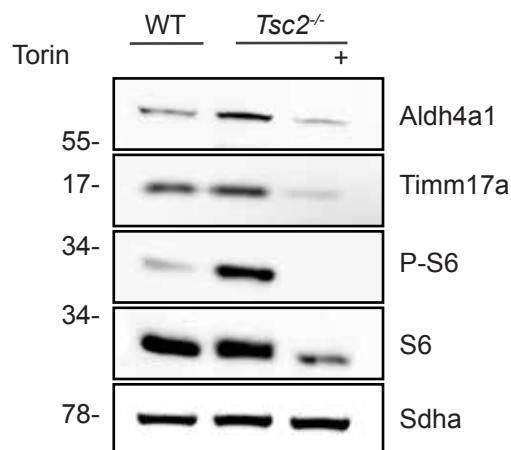**5.6 mTORC1 inhibits AFG3L2-dependent proteolysis**:

To further investigate the role of mTORC1 in the AFG3L2-dependent proteolysis, we have used TSC2 (Tuberous Sclerosis Complex 2) knock-out cells, which are constitutively active for mTORC1 (Fig 5.7A) (107). Lack of TSC2 showed an accumulation of AFG3L2 substrates and this can be reversed by the addition of torin(Fig5.7B). We further confirmed active mTORC1 inhibition of AFG3L2 dependent proteolysis using quantitative proteomics. We isolated crude mitochondria from wild-type and knock-out cells and performed label-free quantitative proteomics (Fig 5.7C). The TSC2 KO cells showed accumulation of AFG3L2 substrates when compared to the wild type and ALDH4a1 is one of the highly accumulated proteins in the cells lacking TSC2 (Fig 5.7D). These results indicate that mTORC1 activation inhibits AFG3L2-dependent proteolysis.

Since mTORC1 regulates mitochondrial proteome at various levels of transcription, translation, and post-translation (91, 92), to confirm that accumulated proteins of AFG3L2 substrates are not due to general regulation of mTORC1. We employed a dynamic pulse SILAC (Stable Isotope Labelling with Amino Acids in Cell Culture) approach to monitor protein degradation kinetics. Cells were cultured in heavy amino acids (Arginine N15 & Lysine N15) for 5-7 doubling times and later shifted to light amino acids (Arginine N14 & Lysine N14) and collected at different time intervals after which measured heavy and light intensities were measured by Mass spectrometry (Fig 5.8A). We calculated the incorporation rate and light-to-heavy ratio (L/H) and didn't see any difference in wild type and TSC2 knockout. This indicates that there is no dilution effect or proliferation difference influenced protein turnover between wild type and TSC2 KO (Fig 5.8 B, C). Then we calculated the area under the curve (AUC) for heavy intensities and monitored proteins stability. In total proteome among significantly changed proteins, its stability and degradation are equipoised but mitochondrial proteins are more stable in TSC2 KO compared to wildtype (Fig 5.8 D, E). This could be due to either inhibition of mitophagy and inhibition of mitochondrial proteases YME1L. We further investigated the stability of AFG3L2 substrates stability and found the majority of the AFG3L2
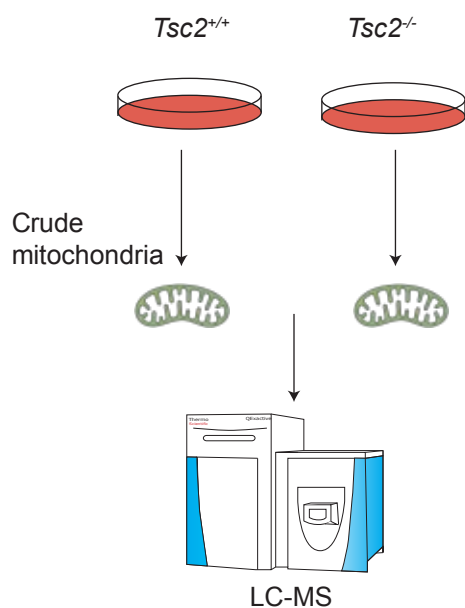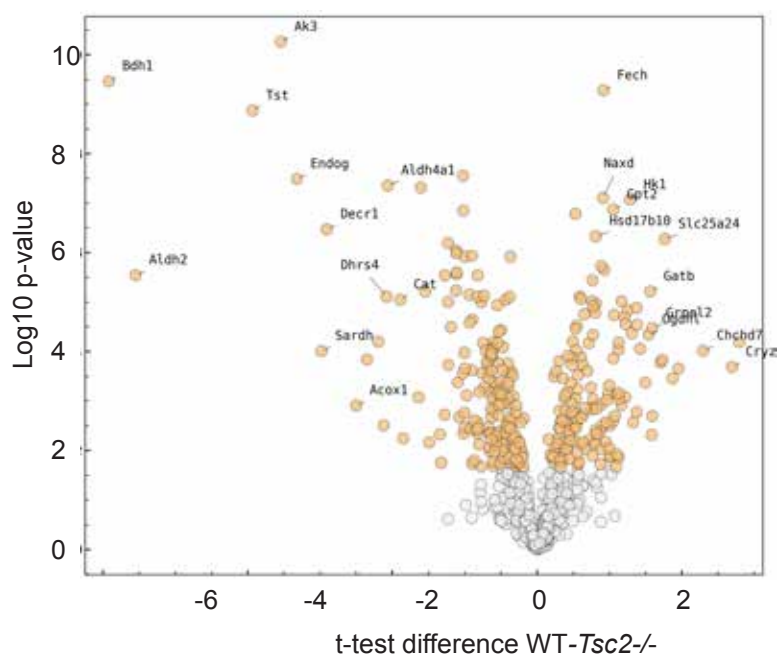
A

B

	WT	$Tsc2^{-/-}$	
Torin		+	

55-   Aldh4a1
17-   Timm17a
34-   P-S6
34-   S6
78-   Sdha

C

$Tsc2^{+/+}$ $Tsc2^{-/-}$

Crude mitochondria

LC-MS

D

Log10 p-value

t-test difference WT-$Tsc2-/-$

5.7. mTORC1 inhibits AFG3L2 dependent proteolysis
A. Schematic illustation of TSC2-mTORC1 signalling axis B. Immunoblot analysis of WT and
$Tsc2^{-/-}$ in the pressence of torin for 12 hours. (n=5) C. Schematic depiction of workflow for quantitative
proteomics for WT and Tsc2$^{-/-}$. D. Volcano plot representing Log2 fold changes of protein for both
WT and Tsc$^{-/-}$ (n=5).
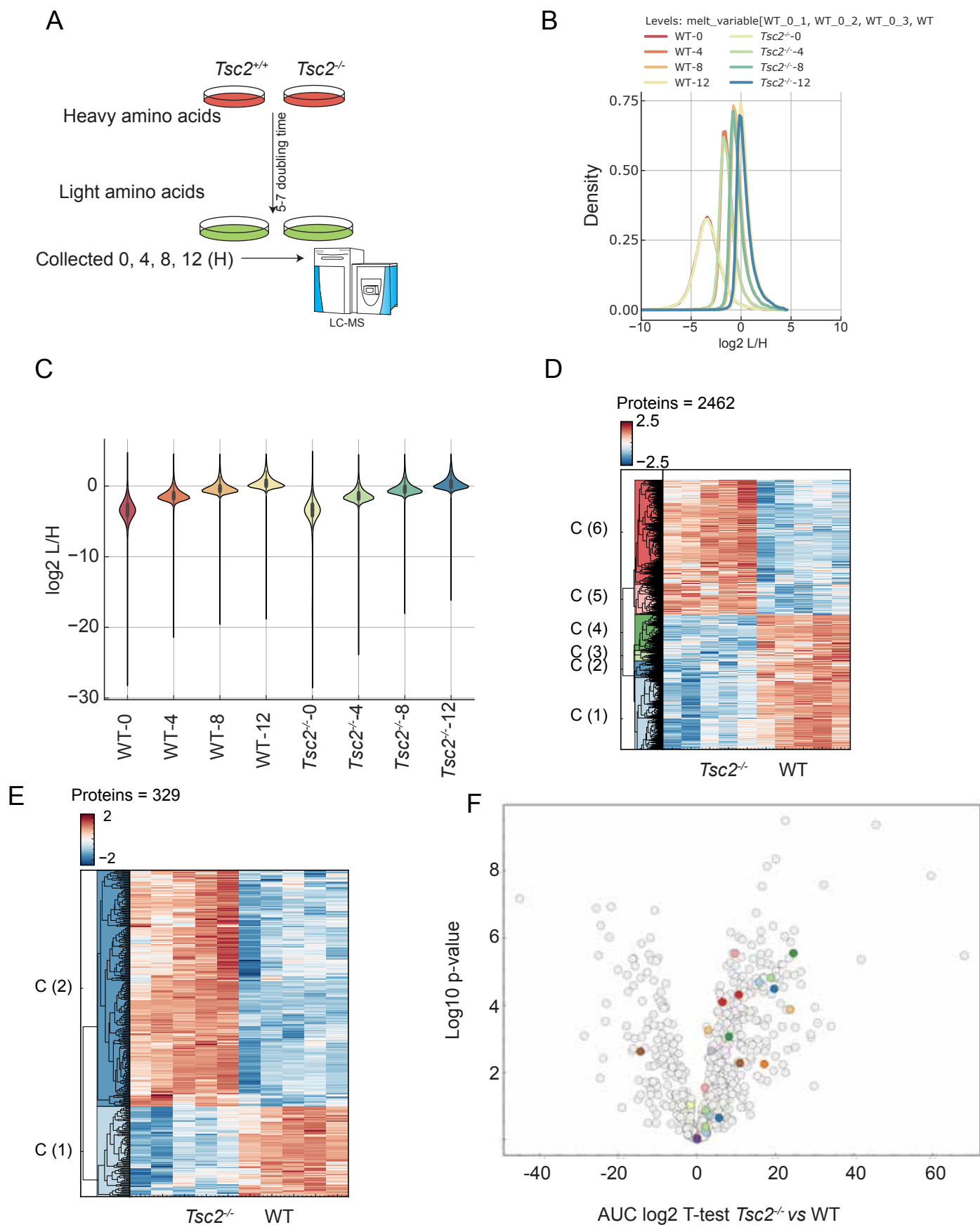
5.8. mTORC1 inhibits AFG3L2 dependent proteolysis

A. Schematic depiction of workflow for Dynamic SILAC for WT and TSC2^{-/-}. (n=5) B. Incorporation of Light to heavy intenties of WT and TSC2^{-/-}. C. The time dependent light amino acids incorporation D. Heatmap of Z- scores transformed heavy intensites area under curve (AUC) of significantly changed proteins. E. Heatmap of Z- scores calculated for heavy intensites area under curve (AUC) of significantly changed mitochondrial proteins. F. Volcano plot representing Log2 fold changes of heavy intensites calculated AUC for both WT and TSC2[-/-, c]olour dots represents AFG3L2 substrates.

substrates were significantly stable in TSC2 KO compared to the wild type (Fig 5.8F).These results further confirmed that mTORC1 inhibits AFG3L2-dependent proteolysis.

5.7 Regulatory mechanism of AFG3L2 dependent proteolysis:

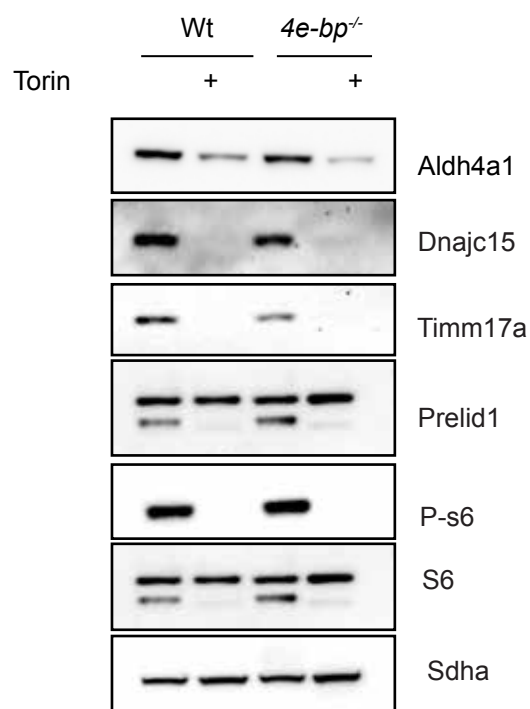AFG3L2 dependent proteolysis is independent of mTORC1 mediated translation:
mTORC1 promotes protein synthesis by phosphorylating a plethora of substrates. The two well-established substrates of mTORC1 signaling on protein synthesis are the eukaryotic translation initiation factor 4E (eIF4E) -binding protein and ribosomal protein S6 kinases (S6K) (60). Recent reports showed that mTROC1 promotes the translation of several nuclear-encoded mitochondrial transcripts in 4E-BP dependent manner (92). We reasoned whether mTORC1-mediated translation regulation plays any role in the reduced protein levels of AFG3L2 substrates. We have 4E-BP deficient cells cultured in hypoxia and normoxia for 16 hours. Both wild-type and 4E-BP deficient cells showed reduced levels of AFG3L2 substrates (Fig 5.9 A). Similar to hypoxia, cells were treated with torin, showed reduced levels of AFG3L2 substrates in both wildtype and 4E-BP KO cells (Fig 5.9B). These results indicate reduced levels of AFG3L2 substrates in hypoxia and mTORC1 inhibition is independent of4E-BP-dependent translation.

mTORC1 promotes anabolism and inhibits catabolism. One such catabolic process is autophagy, it is a central process in the clearance of damaged cellular components (60). mTORC1 regulates autophagy at several levels by phosphorylating key components of autophagic machinery (97,98) We investigated whether the reduced level of AFG3L2 substates in mTORC1 inhibition is dependent on autophagy. ATG (autophagy-related proteins) proteins play a key role in the autophagy process. So, we used autophagy-deficient cells, ATG5 knock out. Upon inhibition of mTORC1 with torin, AFG3L2 substrates were reduced in both wildtype and autophagy-deficient (ATG5 knockout) cells. This result indicates reduced levels of AFG3L2 substrates in mTORC1 inhibition is independent of autophagy but rather dependent in proteolysis (Fig 5.9C). These results again support our finding, that only a subset of mitochondrial proteome undergoes a faster turnover in hypoxia and nutrient stress.
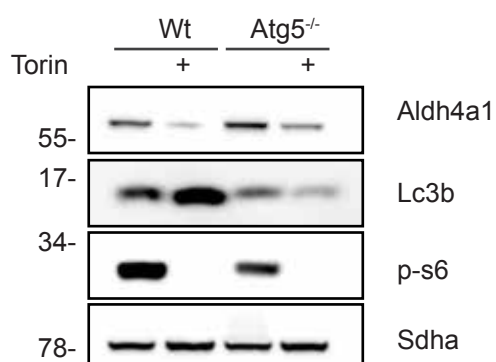
A
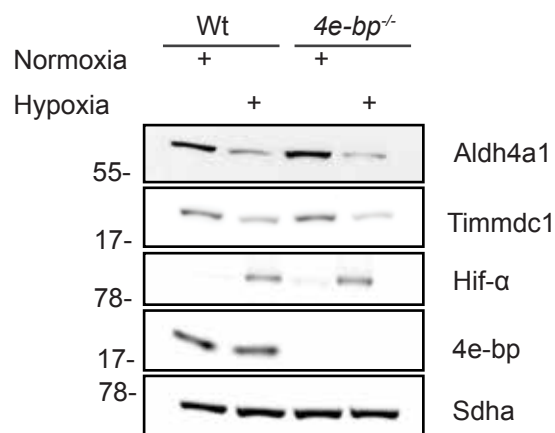
B

C

**5.9 AFG3L2 dependent proteolysis independent of Autophgy**
A. Immunoblot analysis for WT and 4E-BP^{-/-} in the pressence of normoxia and hypoxia for
16 hours (n=3) B. Immunoblot analysis for WT and 4E-BP^{-/-} , treated with Torin for 8 hours (n=3).
C. Immunoblot analysis for WT and ATG^{-/-}, treated with Torin for 8 hours (n=3).

**5.8 NCLX regulates AFG3L2 dependent proteolysis**

mTORC1 regulates lipid metabolism to support membrane biogenesis. Recently it has been shown that mTORC1- LIPIN1 axis regulates mitochondrial lipid composition, especially mitochondrial phosphatidylethanolamine (PE) levels. Reduced PE levels in the mitochondria under hypoxia and mTORC1 inhibition, stimulate i-AAA protease YME1L-dependent proteolysis (94). Since AFG3L2 is an m-AAA protease stationed in the inner mitochondrial membrane (IMM), there could be a potential possibility that alerted PE levels may regulate AFG3L2-dependent proteolysis. To check the role of mitochondrial PE in AFG3L2-dependent proteolysis, we have used PRELID3B (also known as SLOM2) deficient cells, PRELID3B is a lipid transfer protein shuttles phosphatidylserine (PS) to the inner membrane (IMM) for its conversion to PE by PISD. PRELID3B deficient cells showed no change in the levels of AFG3L2 substrates but YME1L substrates were reduced (Fig 5.10A). To confirm further our findings cells were treated with lyso-phosphatidyl ethanolamine (Lyso -PE) in the presence of mTORC1 inhibition. AFG3L2 substrates were reduced in both ethanol as well as Lyso -PE treatment and we could observe accumulation of YME1L substate in Lyso-PE treatment. These results indicate that altered mitochondrial PE doesn't affect AFG3L2-dependent proteolysis.

NCLX is a Na+/Ca2+ exchanger that maintains ion homeostasis in the mitochondria by importing Na+ and exporting Ca2+. A recent report suggested hypoxia activates NCLX and stimulates Na+ entry to the mitochondrial matrix, regulating mitochondrial inner membrane fluidity (REF). Since it has greater importance in ischemia-reperfusion injury and also now in hypoxia signaling, we investigated its role in AFG3L2-dependent proteolysis. We depleted NCLX with small interfering RNA (esiRNA), and observed reduced levels of AFG3L2 substrates in normoxia (Fig 5.10C). These results indicate loss of NCLX or altering the ion homeostasis in the mitochondria regulates AFG3L2 activity.

A
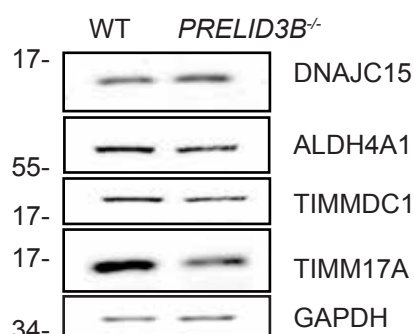
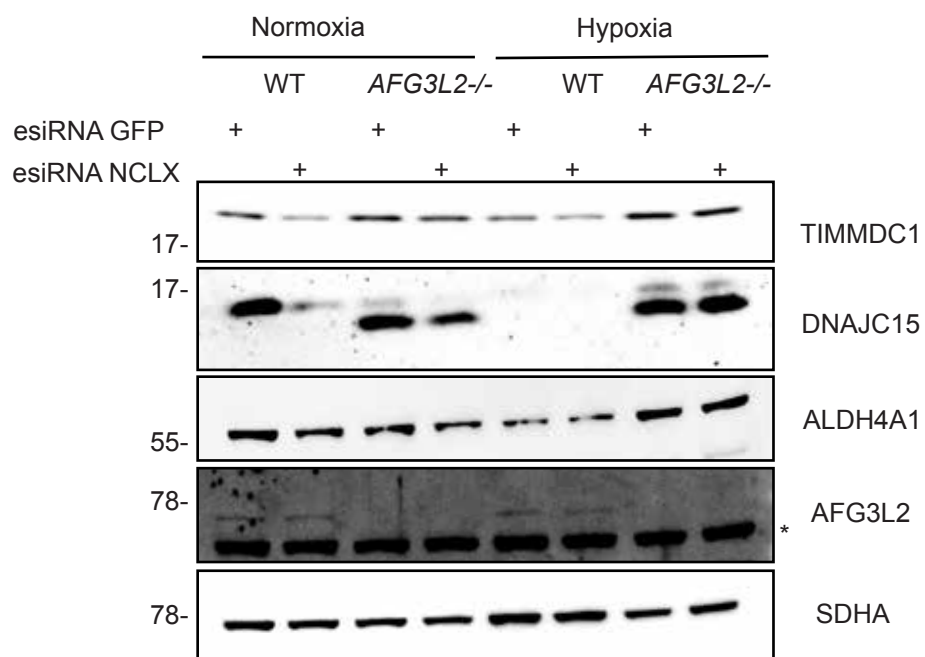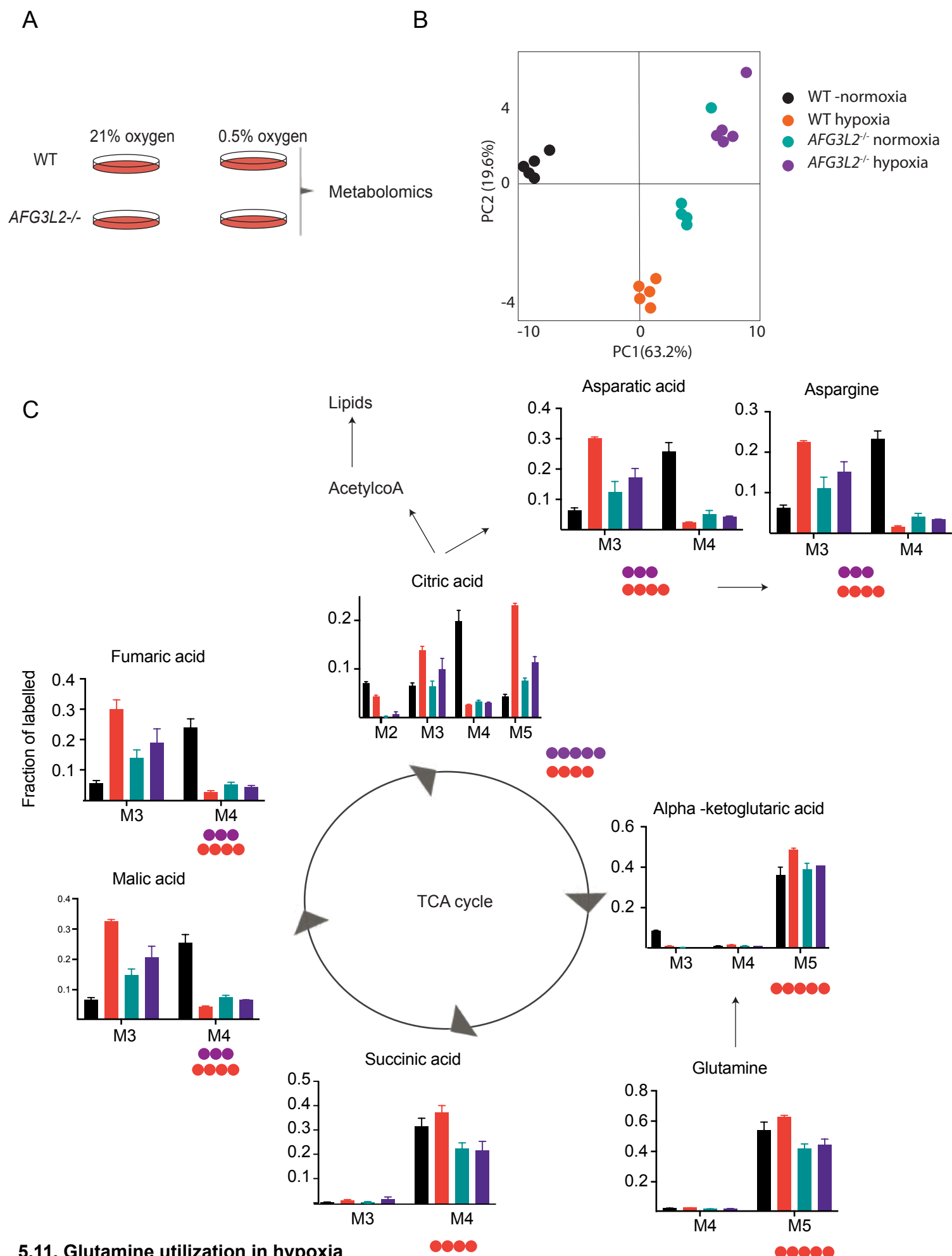B
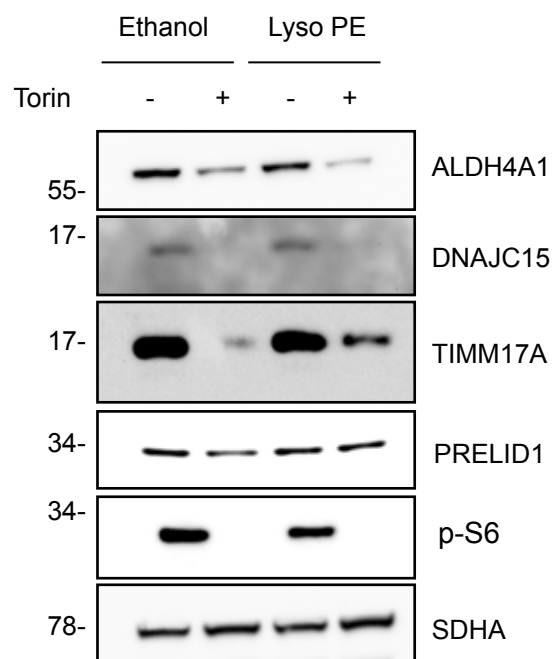
C

5.10. NCLX regulates AFG3L2 function

A. Immunoblot analysis for AFG3L2 substrates in WT and PRELID3B-/-. (n=3) B. Immunoblot analysis of AFG3L2 and YME1L substates in the presence of Lyso PE for 12 hours and treated with Torin (200nM) for 8 hours. C. Immunoblot analysis for esiRNA knockdown of NCLX in WT and AFG3L2$^{-/-}$ in the pressence of normoxia and hypoxia (16 hours) (N=3).

5.9 Glutamine utilization in hypoxia:

In hypoxia, most of the glucose is converted to lactate, which leads to the overuse of glutamine. This enhanced usage of glutamine in hypoxia preferentially provides carbon for fatty acid biosynthesis through reductive carboxylation (43,44,45). Glutamine derived α- ketoglutarate is reduced to citric acid by IDH2 (isocitrate dehydrogenase 2) with NADPH oxidation (45). To monitor glutamine utilization in hypoxia, cells were supplemented with $^{13}C_5$ glutamine: $^{12}C_5$ glutamine (1:1 ratio) for 10 hours (Fig 5.11A). In principal component analysis (PCA), there is a marked difference in hypoxia and normoxia glutamine utilization. When comes to cells lacking AFG3L2, PCA clustered more towards wildtype hypoxia (Fig 5.11B). The uptake of labeled glutamine in AFG3L2 knockout is lower compared to wildtype but there is no difference in the levels of α- ketoglutarate (Fig 5.11C). In normoxia labeled glutamine (M5) entered into the TCA cycle through α- ketoglutarate (M5) and it is further converted mainly to succinic acid (M4). This is succinic acid further converted to malic acid (M4), Fumaric acid (M4), and citric acid (M4). One of the essential metabolites derived from the TCA cycle is aspartate is also M4. Observing a large portion of labeled glutamine-formed M4 TCA cycle metabolites indicates that in normoxia cells utilizing glutamine through oxidative TCA cycle.

Whereas in hypoxia TCA cycle metabolites such as malic acid, fumaric acid, aspartic acid and asparagine generated M5 citric acid. α- ketoglutarate (M5) converted citric acid (M5) by IDH2 and it undergoes lysis by citrate lyase generating oxaloacetate (M3) and acetyl-CoA. This oxaloacetate (M3) being used to generate aspartate (M3), asparagine (M3), Malic acid (M3) and fumaric acid (M3). This large fraction of TCA metabolites generated from M3, indicates wildtype cells following the reductive TCA cycle in hypoxia (Fig 5.11C).

The cells lacking AFG3L2 either in normoxia or hypoxia produced M5 citric acid and the remaining metabolites are M3 (malic acid, fumaric acid, aspartate and asparagine). This indicates that cells lacking AFG3L2 followed the reductive TCA cycle irrespective of oxygen availability (Fig 5.11C). It has been known that dysfunctional mitochondria or defective ETC follow the reductive TCA cycle to support fatty acid biosynthesis(43, 44,45) Since the pleiotropic nature of AFG3L2, a wide variety of substrates and OXPHOS defect in cells lacking AFG3L2 explains very well glutamine utilization in a reductive manner.

A. 21% oxygen, 0.5% oxygen — WT, AFG3L2-/- → Metabolomics

B. PC2 (19.6%) vs PC1 (63.2%)
- WT -normoxia
- WT hypoxia
- AFG3L2-/- normoxia
- AFG3L2-/- hypoxia

C. Lipids ← AcetylcoA ← Citric acid; TCA cycle with Asparatic acid, Aspargine, Alpha-ketoglutaric acid, Glutamine, Succinic acid, Malic acid, Fumaric acid

5.11. Glutamine utilization in hypoxia

A. schematic depiction of experimental work flow for $^{13}C_5$-glutamine tracing in hypoxia and normoxia. B. Principal component analysis of metabolites measured in glutamine tacing in hypoxia and normoxia (WT & AFG3L2 -/-) C. $^{13}C_5$Glutamine tracing of TCA metabolites measured in mass spectrometry in hypoxia and normoxia for both WT and AFG3L2-/-.

6. Discussion:

Oxygen is an essential element in the metabolic functioning of a cell. Reduced oxygen concentration (hypoxia) is a major stressor induced during various pathological states such as bacterial infections, wounds, inflammation, cancer, and cardiovascular defects resulting in a dysregulated cellular homeostasis (205). Molecular oxygen is essential for mitochondrial ATP generation, the cellular energy currency. A healthy adult consumes approximately 380 liters of oxygen every day and around 90% of this oxygen is utilized in the electron transport chain (ETC) and subsequent synthesis of ATP (58). Mitochondria is a hub for many metabolic reactions and metabolites and hence it is pivotal to understand how oxygen levels influence mitochondrial functioning and how mitochondria and the cells in turn adapt to the changes in oxygen tension.

6.1 Hypoxia activates AFG3L2-dependent proteolysis:

Despite the fundamental importance of oxygen in human physiology and disease, we currently lack a complete understanding of how the mitochondrial proteome adapts fluctuations in oxygen tensions (58). Mitochondria harbors 20 resident proteases, that broadly affect mitochondrial functions, such as lipid homeostasis, protein import, mitochondrial gene expression, calcium signaling, and oxidative phosphorylation (OXPHOS) complex assembly to mitochondrial dynamics, mitophagy, and cell death (207). It is known that hypoxia alters mitochondrial proteome but the involved mechanisms are unknown. In this study, we adapted the dynamic SILAC (**Stable Isotope Labeling with Amino acids in Cell culture**) approach to monitor protein turnover rates in hypoxia and determined the protein half-lives during varied oxygen tensions. As previously described, we could observe a faster turnover of HIF1a target proteins in hypoxia compared to normoxia (Fig 5.1). Following a Reactome analysis for faster turnover proteins, we observed an increase in the turnover rate of genes involved in glucose homeostasis pathways are one of the highly affected pathways (Fig 5.1C). In hypoxia, cells consume more glucose and prefer glycolysis over oxidative phosphorylation. This switch which is governed by pyruvate dehydrogenase kinases (PDK) has a faster turnover in hypoxia (36,37). This study documented protein turnover rates in hypoxia (Fig 5.1B). A major limitation in protein turnover studies is that the dynamic changes in protein turnover rate constants are calculated using linear rate assumptions, which does not accurately represent the true physiological behavior of dynamically adjusting proteomes. Achieving an accurate model of dynamic turnover rate changes is still an open question in the field of proteome turnover. (6)

A recent finding suggests that hypoxia proteolytically rewires mitochondrial inner membrane space (IMS) and Inner membrane (IMM) proteome by *i*-AAA protease YME1L (93). In this study, we could successfully recapitulate the previous finding of YME1L-dependent proteolysis. The identified YME1L substrates have faster turnover in hypoxia. Hypoxia promotes mitophagy by expressing BNIP3L and dephosphorylating FUNC1(57). These proteins are localized to the mitochondrial outer membrane and serve as a receptor for mitophagy machinery. Mitophagy is a catabolic process involving lysosomal degradation of dysfunctional and superfluous mitochondria. In hypoxia, only 10% of mitochondrial proteome has a faster turnover and which suggests that the faster turnover of mitochondrial proteins is not due to the mitophagy. To check whether hypoxia induced mitophagy plays a role in AFG3L2-dependent proteolysis, we have used ATG5 deficient cells. Upon hypoxia, both wildtype and ATG5 knockout shows an AFG3L2 dependent proteolysis which confirms that AFG3L2 dependent proteolysis independent of lysosomal degradation.

The human brain is constantly exposed to a lower oxygen tension compared to other organs such as the heart and kidney (35). AFG3L2 is activated in brain hypoxia suggesting a critical role in the normal functioning of brain. Mutation in genes encoding the AFG3L2 protease subunit causes spinocerebellar ataxia type 28 (SCA28), an autosomal dominant disorder and rare ataxia with an early onset, wherein cerebellar dysfunction occurs due to a deterioration of Purkinje cells resulting in progressive gait and limb ataxia with eye movement abnormalities (219). The mechanisms describing SCA28 progression and the substrates responsible for it are yet unknown. In this study, we could conclusively show that the AFG3L2 is activated in hypoxia, and enhances the turnover of nearly 72 mitochondrial proteins (Fig 5.4 D, E, F). These proteins could be putative substrates of AFG3L2 and verified that these proteins with immunoblot (Fig 5.3D). We could also recapitulate previously identified substrates of AFG3L2and generated a comprehensive list of the AFG3L2 substrates, which are involved in ETC maintenance, gene expression, protein import, ferroptosis, and metabolism. which will help in further understanding the disease mechanisms causing spinocerebellar ataxia type 28 (SCA28).

6.2 mTORC1 inhibits AFG3L2 – dependent proteolysis:

Hypoxia is one of the major stressors for mTORC1 signaling. mTORC1 is a master regulator of nutrient sensing and mitochondria are the hub for metabolizing nutrients. Hence, mTORC1 regulates mitochondria at different levels (91, 92). Active mTORC1 promotes mitochondrial biogenesis via PGC1α (PPARγ coactivator 1α) and 4E-BP. mTORC1 enhances the expression of mitochondrial genes by yin–yang 1 (YY1) –PPARγ coactivator 1α (PGC1α) transcriptional complex (91). mTORC1 selectively translates nucleus-encoded mitochondria-related mRNAs in 4E-BP dependent manner (92). Collectively, mTORC1 promotes mitochondrial biogenesis. Upon nutrient starvation, mTORC1 is inactive and activates mitochondrial i-AAA protease YME1L and reshapes mitochondrial proteome, especially in IMS and IMM (93). In this study, we could observe an enhanced AFG3L2-dependent proteolysis upon mTORC1 inhibition (Fig 5.6A). Nutrient starvation (Amino acid & Glutamine) also increased AFG3L2-dependent proteolysis (Fig 5.6 B, C). mTORC1 regulates some of the nuclear-encoded mitochondrial genes translation in 4E-BP dependent manner, so we tested whether reduced levels of AFG3L2 substrates in mTORC1 inhibition are due to reduced translation (92). To verify this, we used 4E-BP deficient cells and treated them with Torin. Upon mTORC1 inhibition, we could see proteolysis in both wildtype and 4E-BP knockout (Fig 5.9B). This indicates that AFG3L2-dependent proteolysis is independent of mTORC1-mediated mitochondrial translational regulation.

mTORC1 controls autophagy at several stages via the phosphorylation of key components of the autophagic machinery. mTORC1 inhibits autophagy at the stage of initiation by phosphorylating ULK1 and ATG13 (96, 97, 98). mTORC1 also inhibits autophagosome maturation and the conversion of endosomes into lysosomes. In starvation, autophagy breakdown proteins and macromolecules in the lysosome. To test autophagy's role in AFG3L2-dependent proteolysis, we have used autophagy-deficient cells (ATG5 Knockout). The cells lacking ATG5 didn't affect the AFG3L2-dependent proteolysis upon mTORC1 inhibition (Fig 5.9C). This suggests that AFG3L2-mediated proteolysis in nutrient starvation and mTORC1 inhibition is independent of autophagy.

Abundant nutrient availability activates mTORC1. Active mTORC1 promotes mitochondrial biogenesis by enhancing the transcription and translation of nuclear-encoded mitochondrial genes (91, 92). Cells that lack TSC2 are constitutively active for mTORC1 signaling (114).

TSC2 knockout cells showed inhibition of AFG3L2 dependent proteolysis when cells treated with Torin promote AFG3L2 mediated proteolysis (Fig 5.7B). These results were further confirmed with quantitative proteomics from isolated mitochondria from Wildtype and TSC2 knockout (Fig 5.7D). To confirm further it is proteolysis not any other means of regulation, we have employed a dynamic SILAC approach for wildtype and TSC2 knockout. Monitoring protein degradation with heavy intensities revealed active mTORC1 inhibits AFG3L2-dependent proteolysis (Fig 5.10F). These findings suggest that nutrients and oxygen regulate AFG3L2-dependent proteolysis.

6.3 Regulation of AFG3L2 dependent proteolysis:

The inner mitochondrial membrane (IM) harbors *m*-AAA and the *i*-AAA, two ATP- dependent proteases, which serve as quality control enzymes in the inner mitochondria and regulates membrane-associated processes (207). The i-AAA protease is composed of YME1L subunits and rewires mitochondrial proteome in IMM and IMS upon nutrient starvation and hypoxia. The PA phosphatase LIPIN1 converts phosphatidic acid (PA) to diacylglycerol (DAG) and thereby regulates the synthesis of glycerophospholipids and triacylglycerides (TAG). The LIPIN1 is a direct target of the mTORC1 kinase complex and upon inhibition of mTORC1 activates LIPIN1 and modulates lipid metabolism. The LIPIN1 activation reduces the conversion of phosphatidylcholine (PC) to phosphatidylserine (PS), which is required for the generation of Phosphatidylethanolamine (PE) in the mitochondria. Inhibition of mTORC1 in hypoxia or upon nutrient starvation reduces mitochondrial PE levels and activates YME1L (93). Since AFG3L2 is an ATP-dependent *m*-AAA protease, we sought mitochondrial PE level's role in the activation of AFG3L2. PRELID3B transfers mitochondrial PS, and ablation of PRELID3B reduces mitochondrial PE levels in the mitochondria. The cells lacking PRELIDB showed no role in AFG3L2 - dependent proteolysis (Fig 5.10A). Cells supplemented with Lyso PE in the presence of mTORC1 inhibition reduced YME1L-mediated proteolysis but does not affect AFG3L2-mediated proteolysis Fig 5.10B). These findings suggest that though AFG3L2 is an ATP-dependent m-AAA protease differs in its regulation from *i*-AAA protease YME1L.

Mitochondria are a major hub for calcium signaling. Mitochondrial calcium homeostasis is mediated by mainly three proteins MCU (Mitochondrial Calcium Uniporter), NCLX (Na$^+$/Ca2$^+$ exchanger) and TMBIM5 (224). The MCU is involved in the uptake of calcium into the

mitochondria whereas NCLX and TMBIM5 efflux calcium. Disruption of calcium homeostasis leads to various pathological conditions such as senescence and neurodegeneration (15, 16). NCLX is a $Na^+/Ca2^+$ exchanger, which effluxes $Ca2^+$ from the matrix in exchange for Na^+ from the intermembrane space. In acute hypoxia, mitochondrial complex I undergo conformational changes that drives acidification of the matrix and release calcium from calcium precipitates (CaP) in exchange with Na+. The NCLX imported Na^+ affects membrane fluidity of mitochondria intermembrane and superoxide production at complex III (229). We tested the role of NCLX in the AFG3L2-dependent proteolysis. Genetic ablation NCLX using esiRNA enhanced AFG3L2 dependent proteolysis in normoxia (Fig 5.10C). The mechanism behind AFG3L2 activation upon loss of NCLX is not yet known. A recent report suggests that TMBIM5 ($Ca2^+/H^+$ antiporter) regulates AFG3L2 activity (230). Future studies should address how ion homeostasis ($Na^+/Ca^{2+)}$ regulates AFG3L2 activity.

Glutamine utilization in hypoxia:

Glutamine is the one of most abundant amino acids in the body. In hypoxia, glucose-derived citrate is reduced and glutamine becomes a major source of citrate. Mitochondrial isocitrate dehydrogenase (IDH2) reductively carboxylates glutamine-derived α-ketoglutarate to citrate. This reductive TCA cycle-generated citrate provides both the acetyl-coenzyme A for lipid synthesis and the four-carbon intermediates needed to produce the remaining TCA cycle metabolites and related macromolecular precursors. Hypoxia and ETC dysfunction operate a reductive TCA cycle and glutamine anaplerosis can therefore maintain lipid homeostasis (43, 44, 45). To determine the glutamine utilization in hypoxia we have used $^{13}C_5$ glutamine tracing. In normoxia, glutamine is used in an oxidative manner, whereas in hypoxia it is used reductive manner. The cells lacking AFG3L2 utilize glutamine in a reductive manner and operate a reductive TCA cycle irrespective of the availability of oxygen (Fig 5.11C). This is mainly due to defective OXPHOS or mitochondrial dysfunction in AFG3L2 knockout.

In this study, we have monitored protein turnover rates in hypoxia and found a new target for hypoxia signaling. AFG3L2 is activated in hypoxia and rewires mitochondrial proteomes. Here we could provide a comprehensive list of AFG3L2 putative substrates, which are involved in mitochondrial protein import, ferroptosis, ETC maintenance, lipid metabolism and metabolism. This study added a new arm to the mTORC1-mediated regulation of mitochondria. Our results will help in further understanding in mechanism of spinocerebellar ataxia (SCA28).

7. Summary

In this study we documented protein turnover rates in hypoxia and found a new target for hypoxia signaling. AFG3L2 is activated in hypoxia and rewires mitochondrial proteome. Upon nutrient starvation and low oxygen mTORC1 inhibited and activates AFG3L2 dependent proteolysis in the mitochondria. The two mitochondrial AAA-proteases, YME1L and AFG3L2 togethers rewires mitochondrial proteome in low nutrients and oxygen.
This proteolytic rewiring enables cells to adapt to hypoxia and nutrient stress.
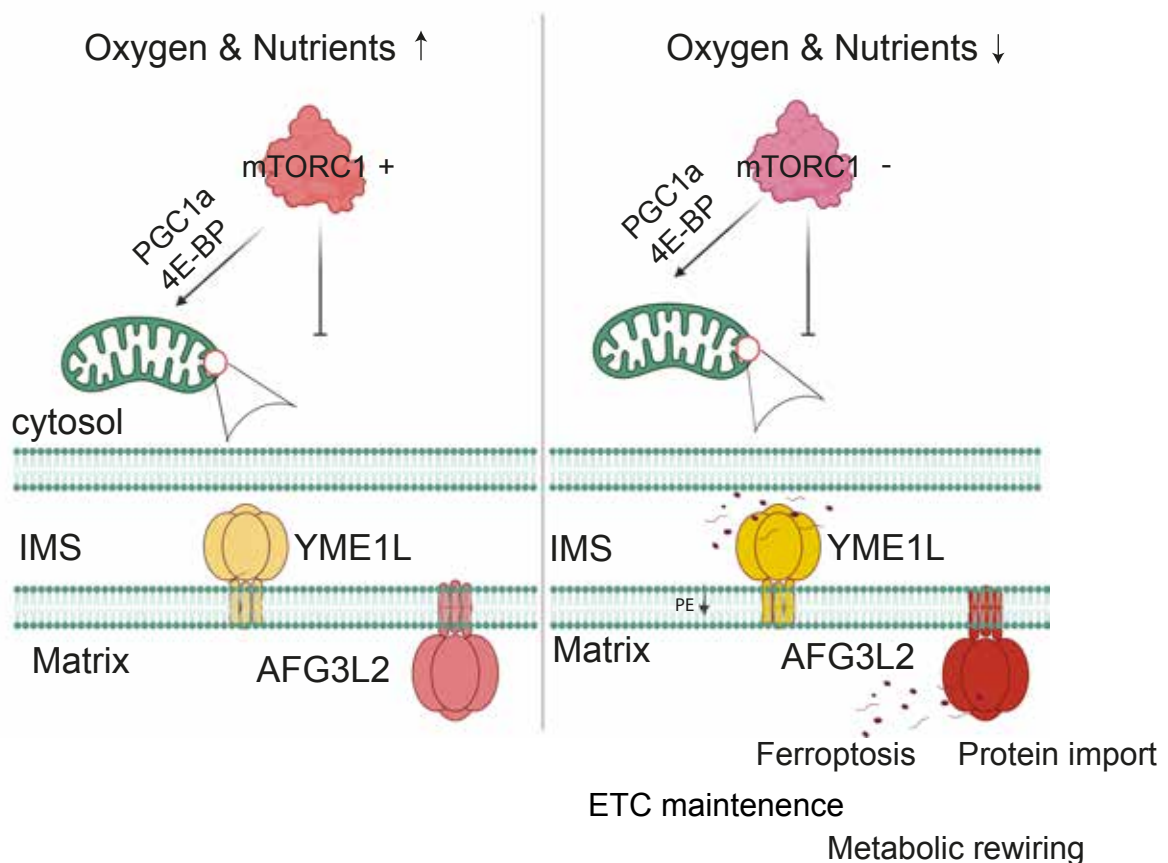
8. References

1. Rich P. Chemiosmotic coupling: The cost of living. Nature. 2003 Feb 6;421(6923):583. doi: 10.1038/421583a. PMID: 12571574.

2. Raymond J, Segrè D. The effect of oxygen on biochemical networks and the evolution of complex life. Science. 2006 Mar 24;311(5768):1764-7. doi: 10.1126/science.1118439. PMID: 16556842.

3. Taylor CT, Doherty G, Fallon PG, Cummins EP. Hypoxia-dependent regulation of inflammatory pathways in immune cells. J Clin Invest. 2016 Oct 3;126(10):3716-3724. doi: 10.1172/JCI84433. Epub 2016 Jul 25. PMID: 27454299; PMCID: PMC5096820.

4. Semenza GL, Wang GL. A nuclear factor induced by hypoxia via de novo protein synthesis binds to the human erythropoietin gene enhancer at a site required for transcriptional activation. Mol Cell Biol. 1992 Dec;12(12):5447-54. doi: 10.1128/mcb.12.12.5447-5454.1992. PMID: 1448077; PMCID: PMC360482

5. Wang GL, Semenza GL. Purification and characterization of hypoxia-inducible factor 1. J Biol Chem. 1995 Jan 20;270(3):1230-7. doi: 10.1074/jbc.270.3.1230. PMID: 7836384.

6. Ema M, Taya S, Yokotani N, Sogawa K, Matsuda Y, Fujii-Kuriyama Y. A novel bHLH-PAS factor with close sequence similarity to hypoxia-inducible factor 1alpha regulates the VEGF expression and is potentially involved in lung and vascular development. Proc Natl Acad Sci U S A. 1997 Apr 29;94(9):4273-8. doi: 10.1073/pnas.94.9.4273. PMID: 9113979; PMCID: PMC20712.

7. Tian H, McKnight SL, Russell DW. Endothelial PAS domain protein 1 (EPAS1), a transcription factor selectively expressed in endothelial cells. Genes Dev. 1997 Jan 1;11(1):72-82. doi: 10.1101/gad.11.1.72. PMID: 9000051.

8. Ivan M, Kondo K, Yang H, Kim W, Valiando J, Ohh M, Salic A, Asara JM, Lane WS, Kaelin WG Jr. HIFalpha targeted for VHL-mediated destruction by proline hydroxylation: implications for O2 sensing. Science. 2001 Apr 20;292(5516):464-8. doi: 10.1126/science.1059817. Epub 2001 Apr 5. PMID: 11292862.

9. Jaakkola P, Mole DR, Tian YM, Wilson MI, Gielbert J, Gaskell SJ, von Kriegsheim A, Hebestreit HF, Mukherji M, Schofield CJ, Maxwell PH, Pugh CW, Ratcliffe PJ. Targeting of HIF-alpha to the von Hippel-Lindau ubiquitylation complex by O2-regulated prolyl hydroxylation. Science. 2001 Apr

10. Dalgard CL, Lu H, Mohyeldin A, Verma A. Endogenous 2-oxoacids differentially regulate expression of oxygen sensors. Biochem J. 2004 Jun 1;380(Pt 2):419-24. doi: 10.1042/BJ20031647. PMID: 14984367; PMCID: PMC1224179.

11. Selak MA, Armour SM, MacKenzie ED, Boulahbel H, Watson DG, Mansfield KD, Pan Y, Simon MC, Thompson CB, Gottlieb E. Succinate links TCA cycle dysfunction to oncogenesis by inhibiting HIF-alpha prolyl hydroxylase. Cancer Cell. 2005 Jan;7(1):77-85. doi: 10.1016/j.ccr.2004.11.022. PMID: 15652751.

12. Maxwell PH, Wiesener MS, Chang GW, Clifford SC, Vaux EC, Cockman ME, Wykoff CC, Pugh CW, Maher ER, Ratcliffe PJ. The tumour suppressor protein VHL targets hypoxia-inducible factors for oxygen-dependent proteolysis. Nature. 1999 May 20;399(6733):271-5. doi: 10.1038/20459. PMID: 10353251.

13. Lando D, Peet DJ, Whelan DA, Gorman JJ, Whitelaw ML. Asparagine hydroxylation of the HIF transactivation domain a hypoxic switch. Science. 2002 Feb 1;295(5556):858-61. doi: 10.1126/science.1068592. PMID: 11823643.

14. Lando D, Peet DJ, Whelan DA, Gorman JJ, Whitelaw ML. Asparagine hydroxylation of the HIF transactivation domain a hypoxic switch. Science. 2002 Feb 1;295(5556):858-61. doi: 10.1126/science.1068592. PMID: 11823643.

15. Hewitson KS, McNeill LA, Riordan MV, Tian YM, Bullock AN, Welford RW, Elkins JM, Oldham NJ, Bhattacharya S, Gleadle JM, Ratcliffe PJ, Pugh CW, Schofield CJ. Hypoxia-inducible factor (HIF) asparagine hydroxylase is identical to factor inhibiting HIF (FIH) and is related to the cupin structural family. J Biol Chem. 2002 Jul 19;277(29):26351-5. doi: 10.1074/jbc.C200273200. Epub 2002 May 31. PMID: 12042299.

16. Lando D, Peet DJ, Gorman JJ, Whelan DA, Whitelaw ML, Bruick RK. FIH-1 is an asparaginyl hydroxylase enzyme that regulates the transcriptional activity of hypoxia-inducible factor. Genes Dev. 2002 Jun 15;16(12):1466-71. doi: 10.1101/gad.991402. PMID: 12080085; PMCID: PMC186346.

17. Dayan F, Roux D, Brahimi-Horn MC, Pouyssegur J, Mazure NM. The oxygen sensor factor-inhibiting hypoxia-inducible factor-1 controls expression of distinct genes through the bifunctional transcriptional character of hypoxia-inducible factor-1alpha. Cancer Res. 2006 Apr 1;66(7):3688-98. doi: 10.1158/0008-5472.CAN-05-4564. PMID: 16585195.

18. Koivunen P, Hirsilä M, Günzler V, Kivirikko KI, Myllyharju J. Catalytic properties of the asparaginyl hydroxylase (FIH) in the oxygen sensing pathway are distinct from those

of its prolyl 4-hydroxylases. J Biol Chem. 2004 Mar 12;279(11):9899-904. doi: 10.1074/jbc.M312254200. Epub 2003 Dec 29. PMID: 14701857.

19. Melvin A, Rocha S. Chromatin as an oxygen sensor and active player in the hypoxia response. Cell Signal. 2012 Jan;24(1):35-43. doi: 10.1016/j.cellsig.2011.08.019. Epub 2011 Sep 8. PMID: 21924352; PMCID: PMC3476533.

20. Batie M, Frost J, Frost M, Wilson JW, Schofield P, Rocha S. Hypoxia induces rapid changes to histone methylation and reprograms chromatin. Science. 2019 Mar 15;363(6432):1222-1226. doi: 10.1126/science.aau5870. Epub 2019 Mar 14. PMID: 30872526.

21. Chakraborty AA, Laukka T, Myllykoski M, Ringel AE, Booker MA, Tolstorukov MY, Meng YJ, Meier SR, Jennings RB, Creech AL, Herbert ZT, McBrayer SK, Olenchock BA, Jaffe JD, Haigis MC, Beroukhim R, Signoretti S, Koivunen P, Kaelin WG Jr. Histone demethylase KDM6A directly senses oxygen to control chromatin and cell fate. Science. 2019 Mar 15;363(6432):1217-1222. doi: 10.1126/science.aaw1026. Epub 2019 Mar 14. PMID: 30872525; PMCID: PMC7336390.

22. Tsukihara T, Aoyama H, Yamashita E, Tomizaki T, Yamaguchi H, Shinzawa-Itoh K, Nakashima R, Yaono R, Yoshikawa S. The whole structure of the 13-subunit oxidized cytochrome c oxidase at 2.8 A. Science. 1996 May 24;272(5265):1136-44. doi: 10.1126/science.272.5265.1136. PMID: 8638158.

23. Fukuda R, Zhang H, Kim JW, Shimoda L, Dang CV, Semenza GL. HIF-1 regulates cytochrome oxidase subunits to optimize efficiency of respiration in hypoxic cells. Cell. 2007 Apr 6;129(1):111-22. doi: 10.1016/j.cell.2007.01.047. PMID: 17418790.

24. Hayashi T, Asano Y, Shintani Y, Aoyama H, Kioka H, Tsukamoto O, Hikita M, Shinzawa-Itoh K, Takafuji K, Higo S, Kato H, Yamazaki S, Matsuoka K, Nakano A, Asanuma H, Asakura M, Minamino T, Goto Y, Ogura T, Kitakaze M, Komuro I, Sakata Y, Tsukihara T, Yoshikawa S, Takashima S. Higd1a is a positive regulator of cytochrome c oxidase. Proc Natl Acad Sci U S A. 2015 Feb 3;112(5):1553-8. doi: 10.1073/pnas.1419767112. Epub 2015 Jan 20. PMID: 25605899; PMCID: PMC4321285.

25. Tello D, Balsa E, Acosta-Iborra B, Fuertes-Yebra E, Elorza A, Ordóñez Á, Corral-Escariz M, Soro I, López-Bernardo E, Perales-Clemente E, Martínez-Ruiz A, Enríquez JA, Aragonés J, Cadenas S, Landázuri MO. Induction of the mitochondrial NDUFA4L2 protein by HIF-1α decreases oxygen consumption by inhibiting Complex I activity. Cell

Metab. 2011 Dec 7;14(6):768-79. doi: 10.1016/j.cmet.2011.10.008. Epub 2011 Nov 17. PMID: 22100406.

26. Chan SY, Zhang YY, Hemann C, Mahoney CE, Zweier JL, Loscalzo J. MicroRNA-210 controls mitochondrial metabolism during hypoxia by repressing the iron-sulfur cluster assembly proteins ISCU1/2. Cell Metab. 2009 Oct;10(4):273-84. doi: 10.1016/j.cmet.2009.08.015. PMID: 19808020; PMCID: PMC2759401.

27. Rouault TA, Tong WH. Iron-sulfur cluster biogenesis and human disease. Trends Genet. 2008 Aug;24(8):398-407. doi: 10.1016/j.tig.2008.05.008. Epub 2008 Jul 5. PMID: 18606475; PMCID: PMC2574672.

28. Chen Z, Li Y, Zhang H, Huang P, Luthra R. Hypoxia-regulated microRNA-210 modulates mitochondrial function and decreases ISCU and COX10 expression. Oncogene. 2010 Jul 29;29(30):4362-8. doi: 10.1038/onc.2010.193. Epub 2010 May 24. PMID: 20498629.

29. Puisségur MP, Mazure NM, Bertero T, Pradelli L, Grosso S, Robbe-Sermesant K, Maurin T, Lebrigand K, Cardinaud B, Hofman V, Fourre S, Magnone V, Ricci JE, Pouysségur J, Gounon P, Hofman P, Barbry P, Mari B. miR-210 is overexpressed in late stages of lung cancer and mediates mitochondrial alterations associated with modulation of HIF-1 activity. Cell Death Differ. 2011 Mar;18(3):465-78. doi: 10.1038/cdd.2010.119. Epub 2010 Oct 1. PMID: 20885442; PMCID: PMC3131992.

30. Jain IH, Zazzeron L, Goli R, Alexa K, Schatzman-Bone S, Dhillon H, Goldberger O, Peng J, Shalem O, Sanjana NE, Zhang F, Goessling W, Zapol WM, Mootha VK. Hypoxia as a therapy for mitochondrial disease. Science. 2016 Apr 1;352(6281):54-61. doi: 10.1126/science.aad9642. Epub 2016 Feb 25. PMID: 26917594; PMCID: PMC4860742.

31. Lake NJ, Bird MJ, Isohanni P, Paetau A. Leigh syndrome: neuropathology and pathogenesis. J Neuropathol Exp Neurol. 2015 Jun;74(6):482-92. doi: 10.1097/NEN.0000000000000195. PMID: 25978847.

32. Kruse SE, Watt WC, Marcinek DJ, Kapur RP, Schenkman KA, Palmiter RD. Mice with mitochondrial complex I deficiency develop a fatal encephalomyopathy. Cell Metab. 2008 Apr;7(4):312-20. doi: 10.1016/j.cmet.2008.02.004. PMID: 18396137; PMCID: PMC2593686.

33. Jain IH, Zazzeron L, Goldberger O, Marutani E, Wojtkiewicz GR, Ast T, Wang H, Schleifer G, Stepanova A, Brepoels K, Schoonjans L, Carmeliet P, Galkin A, Ichinose F, Zapol WM, Mootha VK. Leigh Syndrome Mouse Model Can Be Rescued by

Interventions that Normalize Brain Hyperoxia, but Not HIF Activation. Cell Metab. 2019 Oct 1;30(4):824-832.e3. doi: 10.1016/j.cmet.2019.07.006. Epub 2019 Aug 8. PMID: 31402314; PMCID: PMC6903907.

34. Ferrari M, Jain IH, Goldberger O, Rezoagli E, Thoonen R, Cheng KH, Sosnovik DE, Scherrer-Crosbie M, Mootha VK, Zapol WM. Hypoxia treatment reverses neurodegenerative disease in a mouse model of Leigh syndrome. Proc Natl Acad Sci USA. 2017 May 23;114(21):E4241-E4250. doi: 10.1073/pnas.1621511114. Epub 2017 May 8. Erratum in: Proc Natl Acad Sci U S A. 2017 Jun 13;114(24):E4894-E4896. Erratum in: Proc Natl Acad Sci U S A. 2018 Jan 30;: PMID: 28483998; PMCID: PMC5448167.

35. Jain IH, Calvo SE, Markhard AL, Skinner OS, To TL, Ast T, Mootha VK. Genetic Screen for Cell Fitness in High or Low Oxygen Highlights Mitochondrial and Lipid Metabolism. Cell. 2020 Apr 30;181(3):716-727.e11. doi: 10.1016/j.cell.2020.03.029. Epub 2020 Apr 6. PMID: 32259488; PMCID: PMC7293541.

36. Papandreou I, Cairns RA, Fontana L, Lim AL, Denko NC. HIF-1 mediates adaptation to hypoxia by actively downregulating mitochondrial oxygen consumption. Cell Metab. 2006 Mar;3(3):187-97. doi: 10.1016/j.cmet.2006.01.012. PMID: 16517406.

37. Kim JW, Tchernyshyov I, Semenza GL, Dang CV. HIF-1-mediated expression of pyruvate dehydrogenase kinase: a metabolic switch required for cellular adaptation to hypoxia. Cell Metab. 2006 Mar;3(3):177-85. doi: 10.1016/j.cmet.2006.02.002. PMID: 16517405.

38. Iyer NV, Kotch LE, Agani F, Leung SW, Laughner E, Wenger RH, Gassmann M, Gearhart JD, Lawler AM, Yu AY, Semenza GL. Cellular and developmental control of O2 homeostasis by hypoxia-inducible factor 1 alpha. Genes Dev. 1998 Jan 15;12(2):149-62. doi: 10.1101/gad.12.2.149. PMID: 9436976; PMCID: PMC316445.

39. Birsoy K, Wang T, Chen WW, Freinkman E, Abu-Remaileh M, Sabatini DM. An Essential Role of the Mitochondrial Electron Transport Chain in Cell Proliferation Is to Enable Aspartate Synthesis. Cell. 2015 Jul 30;162(3):540-51. doi: 10.1016/j.cell.2015.07.016. PMID: 26232224; PMCID: PMC4522279.

40. Sullivan LB, Gui DY, Hosios AM, Bush LN, Freinkman E, Vander Heiden MG. Supporting Aspartate Biosynthesis Is an Essential Function of Respiration in Proliferating Cells. Cell. 2015 Jul 30;162(3):552-63. doi: 10.1016/j.cell.2015.07.017. PMID: 26232225; PMCID: PMC4522278.

41. Garcia-Bermudez J, Baudrier L, La K, Zhu XG, Fidelin J, Sviderskiy VO, Papagiannakopoulos T, Molina H, Snuderl M, Lewis CA, Possemato RL, Birsoy K. Aspartate is a limiting metabolite for cancer cell proliferation under hypoxia and in tumours. Nat Cell Biol. 2018 Jul;20(7):775-781. doi: 10.1038/s41556-018-0118-z. Epub 2018 Jun 25. Erratum in: Nat Cell Biol. 2018 Oct;20(10):1228. PMID: 29941933; PMCID: PMC6030478.

42. Sullivan LB, Luengo A, Danai LV, Bush LN, Diehl FF, Hosios AM, Lau AN, Elmiligy S, Malstrom S, Lewis CA, Vander Heiden MG. Aspartate is an endogenous metabolic limitation for tumour growth. Nat Cell Biol. 2018 Jul;20(7):782-788. doi: 10.1038/s41556-018-0125-0. Epub 2018 Jun 25. PMID: 29941931; PMCID: PMC6051729.

43. Wise DR, Ward PS, Shay JE, Cross JR, Gruber JJ, Sachdeva UM, Platt JM, DeMatteo RG, Simon MC, Thompson CB. Hypoxia promotes isocitrate dehydrogenase-dependent carboxylation of α-ketoglutarate to citrate to support cell growth and viability. Proc Natl Acad Sci U S A. 2011 Dec 6;108(49):19611-6. doi: 10.1073/pnas.1117773108. Epub 2011 Nov 21. PMID: 22106302; PMCID: PMC3241793.

44. Metallo CM, Gameiro PA, Bell EL, Mattaini KR, Yang J, Hiller K, Jewell CM, Johnson ZR, Irvine DJ, Guarente L, Kelleher JK, Vander Heiden MG, Iliopoulos O, Stephanopoulos G. Reductive glutamine metabolism by IDH1 mediates lipogenesis under hypoxia. Nature. 2011 Nov 20;481(7381):380-4. doi: 10.1038/nature10602. PMID: 22101433; PMCID: PMC3710581.

45. Mullen AR, Wheaton WW, Jin ES, Chen PH, Sullivan LB, Cheng T, Yang Y, Linehan WM, Chandel NS, DeBerardinis RJ. Reductive carboxylation supports growth in tumour cells with defective mitochondria. Nature. 2011 Nov 20;481(7381):385-8. doi: 10.1038/nature10642. PMID: 22101431; PMCID: PMC3262117.

46. Hochachka PW, Storey KB. Metabolic consequences of diving in animals and man. Science. 1975 Feb 21;187(4177):613-21. doi: 10.1126/science.163485. PMID: 163485.

47. Chouchani ET, Pell VR, James AM, Work LM, Saeb-Parsy K, Frezza C, Krieg T, Murphy MP. A Unifying Mechanism for Mitochondrial Superoxide Production during Ischemia-Reperfusion Injury. Cell Metab. 2016 Feb 9;23(2):254-63. doi: 10.1016/j.cmet.2015.12.009. Epub 2016 Jan 14. PMID: 26777689.

48. Chouchani ET, Pell VR, Gaude E, Aksentijević D, Sundier SY, Robb EL, Logan A, Nadtochiy SM, Ord ENJ, Smith AC, Eyassu F, Shirley R, Hu CH, Dare AJ, James AM,

Rogatti S, Hartley RC, Eaton S, Costa ASH, Brookes PS, Davidson SM, Duchen MR, Saeb-Parsy K, Shattock MJ, Robinson AJ, Work LM, Frezza C, Krieg T, Murphy MP. Ischaemic accumulation of succinate controls reperfusion injury through mitochondrial ROS. Nature. 2014 Nov 20;515(7527):431-435. doi: 10.1038/nature13909. Epub 2014 Nov 5. PMID: 25383517; PMCID: PMC4255242.

49. Spinelli JB, Rosen PC, Sprenger HG, Puszynska AM, Mann JL, Roessler JM, Cangelosi AL, Henne A, Condon KJ, Zhang T, Kunchok T, Lewis CA, Chandel NS, Sabatini DM. Fumarate is a terminal electron acceptor in the mammalian electron transport chain. Science. 2021 Dec 3;374(6572):1227-1237. doi: 10.1126/science.abi7495. Epub 2021 Dec 2. PMID: 34855504; PMCID: PMC8803114.

50. Robb EL, Hall AR, Prime TA, Eaton S, Szibor M, Viscomi C, James AM, Murphy MP. Control of mitochondrial superoxide production by reverse electron transport at complex I. J Biol Chem. 2018 Jun 22;293(25):9869-9879. doi: 10.1074/jbc.RA118.003647. Epub 2018 May 9. Erratum in: J Biol Chem. 2019 May 10;294(19):7966. PMID: 29743240; PMCID: PMC6016480.

51. Faubert B, Li KY, Cai L, Hensley CT, Kim J, Zacharias LG, Yang C, Do QN, Doucette S, Burguete D, Li H, Huet G, Yuan Q, Wigal T, Butt Y, Ni M, Torrealba J, Oliver D, Lenkinski RE, Malloy CR, Wachsmann JW, Young JD, Kernstine K, DeBerardinis RJ. Lactate Metabolism in Human Lung Tumors. Cell. 2017 Oct 5;171(2):358-371.e9. doi: 10.1016/j.cell.2017.09.019. PMID: 28985563; PMCID: PMC5684706.

52. Fuhrmann DC, Brüne B. Mitochondrial composition and function under the control of hypoxia. Redox Biol. 2017 Aug;12:208-215. doi: 10.1016/j.redox.2017.02.012. Epub 2017 Feb 24. PMID: 28259101; PMCID: PMC5333533.

53. Ong SB, Subrayan S, Lim SY, Yellon DM, Davidson SM, Hausenloy DJ. Inhibiting mitochondrial fission protects the heart against ischemia/reperfusion injury. Circulation. 2010 May 11;121(18):2012-22. doi: 10.1161/CIRCULATIONAHA.109.906610. Epub 2010 Apr 26. PMID: 20421521.

54. Wang JX, Jiao JQ, Li Q, Long B, Wang K, Liu JP, Li YR, Li PF. miR-499 regulates mitochondrial dynamics by targeting calcineurin and dynamin-related protein-1. Nat Med. 2011 Jan;17(1):71-8. doi: 10.1038/nm.2282. Epub 2010 Dec 26. PMID: 21186368.

55. Kim H, Scimia MC, Wilkinson D, Trelles RD, Wood MR, Bowtell D, Dillin A, Mercola M, Ronai ZA. Fine-tuning of Drp1/Fis1 availability by AKAP121/Siah2 regulates

mitochondrial adaptation to hypoxia. Mol Cell. 2011 Nov 18;44(4):532-44. doi: 10.1016/j.molcel.2011.08.045. PMID: 22099302; PMCID: PMC3360955.

56. Zhou R, Yazdi AS, Menu P, Tschopp J. A role for mitochondria in NLRP3 inflammasome activation. Nature. 2011 Jan 13;469(7329):221-5. doi: 10.1038/nature09663. Epub 2010 Dec 1. Erratum in: Nature. 2011 Jul 7;475(7354):122. PMID: 21124315.

57. Liu L, Feng D, Chen G, Chen M, Zheng Q, Song P, Ma Q, Zhu C, Wang R, Qi W, Huang L, Xue P, Li B, Wang X, Jin H, Wang J, Yang F, Liu P, Zhu Y, Sui S, Chen Q. Mitochondrial outer-membrane protein FUNDC1 mediates hypoxia-induced in mammalian cells. Nat Cell Biol. 2012 Jan 22;14(2):177-85. doi: 10.1038/ncb2422. PMID: 22267086.

58. Lee P, Chandel NS, Simon MC. Cellular adaptation to hypoxia through hypoxia inducible factors and beyond. Nat Rev Mol Cell Biol. 2020 May;21(5):268-283. doi: 10.1038/s41580-020-0227-y. Epub 2020 Mar 6. PMID: 32144406; PMCID: PMC7222024.

59. Keith CT, Schreiber SL. PIK-related kinases: DNA repair, recombination, and cell cycle checkpoints. Science. 1995 Oct 6;270(5233):50-1. doi: 10.1126/science.270.5233.50. PMID: 7569949.

60. Saxton RA, Sabatini DM. mTOR Signaling in Growth, Metabolism, and Disease. Cell. 2017 Mar 9;168(6):960-976. doi: 10.1016/j.cell.2017.02.004. Erratum in: Cell. 2017 Apr 6;169(2):361-371. PMID: 28283069; PMCID: PMC5394987.

61. Kim DH, Sarbassov DD, Ali SM, Latek RR, Guntur KV, Erdjument-Bromage H, Tempst P, Sabatini DM. GbetaL, a positive regulator of the rapamycin-sensitive pathway required for the nutrient-sensitive interaction between raptor and mTOR. Mol Cell. 2003 Apr;11(4):895-904. doi: 10.1016/s1097-2765(03)00114-x. PMID: 12718876.

62. Hara K, Maruki Y, Long X, Yoshino K, Oshiro N, Hidayat S, Tokunaga C, Avruch J, Yonezawa K. Raptor, a binding partner of target of rapamycin (TOR), mediates TOR action. Cell. 2002 Jul 26;110(2):177-89. doi: 10.1016/s0092-8674(02)00833-4. PMID: 12150926.

63. Kim DH, Sarbassov DD, Ali SM, King JE, Latek RR, Erdjument-Bromage H, Tempst P, Sabatini DM. mTOR interacts with raptor to form a nutrient-sensitive complex that signals to the cell growth machinery. Cell. 2002 Jul 26;110(2):163-75. doi: 10.1016/s0092-8674(02)00808-5. PMID: 12150925.

64. Yang H, Rudge DG, Koos JD, Vaidialingam B, Yang HJ, Pavletich NP. mTOR kinase structure, mechanism and regulation. Nature. 2013 May 9;497(7448):217-23. doi: 10.1038/nature12122. Epub 2013 May 1. PMID: 23636326; PMCID: PMC4512754.

65. Guertin DA, Stevens DM, Thoreen CC, Burds AA, Kalaany NY, Moffat J, Brown M, Fitzgerald KJ, Sabatini DM. Ablation in mice of the mTORC components raptor, rictor, or mLST8 reveals that mTORC2 is required for signaling to Akt-FOXO and PKCalpha, but not S6K1. Dev Cell. 2006 Dec;11(6):859-71. doi: 10.1016/j.devcel.2006.10.007. PMID: 17141160.

66. Vander Haar E, Lee SI, Bandhakavi S, Griffin TJ, Kim DH. Insulin signalling to mTOR mediated by the Akt/PKB substrate PRAS40. Nat Cell Biol. 2007 Mar;9(3):316-23. doi: 10.1038/ncb1547. Epub 2007 Feb 4. PMID: 17277771.

67. Sancak Y, Thoreen CC, Peterson TR, Lindquist RA, Kang SA, Spooner E, Carr SA, Sabatini DM. PRAS40 is an insulin-regulated inhibitor of the mTORC1 protein kinase. Mol Cell. 2007 Mar 23;25(6):903-15. doi: 10.1016/j.molcel.2007.03.003. PMID: 17386266.

68. Peterson TR, Laplante M, Thoreen CC, Sancak Y, Kang SA, Kuehl WM, Gray NS, Sabatini DM. DEPTOR is an mTOR inhibitor frequently overexpressed in multiple myeloma cells and required for their survival. Cell. 2009 May 29;137(5):873-86. doi: 10.1016/j.cell.2009.03.046. Epub 2009 May 14. PMID: 19446321; PMCID: PMC2758791.

69. Buttgereit F, Brand MD. A hierarchy of ATP-consuming processes in mammalian cells. Biochem J. 1995 Nov 15;312 (Pt 1)(Pt 1):163-7. doi: 10.1042/bj3120163. PMID: 7492307; PMCID: PMC1136240.

70. Brunn GJ, Hudson CC, Sekulić A, Williams JM, Hosoi H, Houghton PJ, Lawrence JC Jr, Abraham RT. Phosphorylation of the translational repressor PHAS-I by the mammalian target of rapamycin. Science. 1997 Jul 4;277(5322):99-101. doi: 10.1126/science.277.5322.99. PMID: 9204908.

71. Gingras AC, Gygi SP, Raught B, Polakiewicz RD, Abraham RT, Hoekstra MF, Aebersold R, Sonenberg N. Regulation of 4E-BP1 phosphorylation: a novel two-step mechanism. Genes Dev. 1999 Jun 1;13(11):1422-37. doi: 10.1101/gad.13.11.1422. PMID: 10364159; PMCID: PMC316780.

72. Hara K, Yonezawa K, Kozlowski MT, Sugimoto T, Andrabi K, Weng QP, Kasuga M, Nishimoto I, Avruch J. Regulation of eIF-4E BP1 phosphorylation by mTOR. J Biol Chem. 1997 Oct 17;272(42):26457-63. doi: 10.1074/jbc.272.42.26457. PMID: 9334222.

73. Pullen N, Dennis PB, Andjelkovic M, Dufner A, Kozma SC, Hemmings BA, Thomas G. Phosphorylation and activation of p70s6k by PDK1. Science. 1998 Jan 30;279(5351):707-10. doi: 10.1126/science.279.5351.707. PMID: 9445476.

74. Burnett PE, Barrow RK, Cohen NA, Snyder SH, Sabatini DM. RAFT1 phosphorylation of the translational regulators p70 S6 kinase and 4E-BP1. Proc Natl Acad Sci U S A. 1998 Feb 17;95(4):1432-7. doi: 10.1073/pnas.95.4.1432. PMID: 9465032; PMCID: PMC19032.

75. Ruvinsky I, Sharon N, Lerer T, Cohen H, Stolovich-Rain M, Nir T, Dor Y, Zisman P, Meyuhas O. Ribosomal protein S6 phosphorylation is a determinant of cell size and glucose homeostasis. Genes Dev. 2005 Sep 15;19(18):2199-211. doi: 10.1101/gad.351605. PMID: 16166381; PMCID: PMC1221890.

76. Jia JJ, Lahr RM, Solgaard MT, Moraes BJ, Pointet R, Yang AD, Celucci G, Graber TE, Hoang HD, Niklaus MR, Pena IA, Hollensen AK, Smith EM, Chaker-Margot M, Anton L, Dajadian C, Livingstone M, Hearnden J, Wang XD, Yu Y, Maier T, Damgaard CK, Berman AJ, Alain T, Fonseca BD. mTORC1 promotes TOP mRNA translation through site-specific phosphorylation of LARP1. Nucleic Acids Res. 2021 Apr 6;49(6):3461-3489. doi: 10.1093/nar/gkaa1239. PMID: 33398329; PMCID: PMC8034618.

77. Mayer C, Zhao J, Yuan X, Grummt I. mTOR-dependent activation of the transcription factor TIF-IA links rRNA synthesis to nutrient availability. Genes Dev. 2004 Feb 15;18(4):423-34. doi: 10.1101/gad.285504. PMID: 15004009; PMCID: PMC359396.

78. Shor B, Wu J, Shakey Q, Toral-Barza L, Shi C, Follettie M, Yu K. Requirement of the mTOR kinase for the regulation of Maf1 phosphorylation and control of RNA polymerase III-dependent transcription in cancer cells. J Biol Chem. 2010 May 14;285(20):15380-15392. doi: 10.1074/jbc.M109.071639. Epub 2010 Mar 16. PMID: 20233713; PMCID: PMC2865278.

79. Hannan KM, Brandenburger Y, Jenkins A, Sharkey K, Cavanaugh A, Rothblum L, Moss T, Poortinga G, McArthur GA, Pearson RB, Hannan RD. mTOR-dependent regulation of ribosomal gene transcription requires S6K1 and is mediated by phosphorylation of the carboxy-terminal activation domain of the nucleolar transcription factor UBF. Mol Cell

Biol. 2003 Dec;23(23):8862-77. doi: 10.1128/MCB.23.23.8862-8877.2003. PMID: 14612424; PMCID: PMC262650.

80. Holz MK, Ballif BA, Gygi SP, Blenis J. mTOR and S6K1 mediate assembly of the translation preinitiation complex through dynamic protein interchange and ordered phosphorylation events. Cell. 2005 Nov 18;123(4):569-80. doi: 10.1016/j.cell.2005.10.024. PMID: 16286006.

81. Ma XM, Yoon SO, Richardson CJ, Jülich K, Blenis J. SKAR links pre-mRNA splicing to mTOR/S6K1-mediated enhanced translation efficiency of spliced mRNAs. Cell. 2008 Apr 18;133(2):303-13. doi: 10.1016/j.cell.2008.02.031. PMID: 18423201.

82. Pende M, Um SH, Mieulet V, Sticker M, Goss VL, Mestan J, Mueller M, Fumagalli S, Kozma SC, Thomas G. S6K1(-/-)/S6K2(-/-) mice exhibit perinatal lethality and rapamycin-sensitive 5'-terminal oligopyrimidine mRNA translation and reveal a mitogen-activated protein kinase-dependent S6 kinase pathway. Mol Cell Biol. 2004 Apr;24(8):3112-24. doi: 10.1128/MCB.24.8.3112-3124.2004. PMID: 15060135; PMCID: PMC381608.

83. Mieulet V, Roceri M, Espeillac C, Sotiropoulos A, Ohanna M, Oorschot V, Klumperman J, Sandri M, Pende M. S6 kinase inactivation impairs growth and translational target phosphorylation in muscle cells maintaining proper regulation of protein turnover. Am J Physiol Cell Physiol. 2007 Aug;293(2):C712-22. doi: 10.1152/ajpcell.00499.2006. Epub 2007 May 9. PMID: 17494629.

84. Ben-Sahra I, Hoxhaj G, Ricoult SJH, Asara JM, Manning BD. mTORC1 induces purine synthesis through control of the mitochondrial tetrahydrofolate cycle. Science. 2016 Feb 12;351(6274):728-733. doi: 10.1126/science.aad0489. PMID: 26912861; PMCID: PMC4786372.

85. Ben-Sahra I, Howell JJ, Asara JM, Manning BD. Stimulation of de novo pyrimidine synthesis by growth signaling through mTOR and S6K1. Science. 2013 Mar 15;339(6125):1323-8. doi: 10.1126/science.1228792. Epub 2013 Feb 21. PMID: 23429703; PMCID: PMC3753690.

86. Düvel K, Yecies JL, Menon S, Raman P, Lipovsky AI, Souza AL, Triantafellow E, Ma Q, Gorski R, Cleaver S, Vander Heiden MG, MacKeigan JP, Finan PM, Clish CB, Murphy LO, Manning BD. Activation of a metabolic gene regulatory network downstream of mTOR complex 1. Mol Cell. 2010 Jul 30;39(2):171-83. doi: 10.1016/j.molcel.2010.06.022. PMID: 20670887; PMCID: PMC2946786.

87. Peterson TR, Sengupta SS, Harris TE, Carmack AE, Kang SA, Balderas E, Guertin DA, Madden KL, Carpenter AE, Finck BN, Sabatini DM. mTOR complex 1 regulates lipin 1 localization to control the SREBP pathway. Cell. 2011 Aug 5;146(3):408-20. doi: 10.1016/j.cell.2011.06.034. PMID: 21816276; PMCID: PMC3336367.

88. Peterson TR, Sengupta SS, Harris TE, Carmack AE, Kang SA, Balderas E, Guertin DA, Madden KL, Carpenter AE, Finck BN, Sabatini DM. mTOR complex 1 regulates lipin 1 localization to control the SREBP pathway. Cell. 2011 Aug 5;146(3):408-20. doi: 10.1016/j.cell.2011.06.034. PMID: 21816276; PMCID: PMC3336367.

89. Kim JE, Chen J. regulation of peroxisome proliferator-activated receptor-gamma activity by mammalian target of rapamycin and amino acids in adipogenesis. Diabetes. 2004 Nov;53(11):2748-56. doi: 10.2337/diabetes.53.11.2748. PMID: 15504954.

90. Lu XY, Shi XJ, Hu A, Wang JQ, Ding Y, Jiang W, Sun M, Zhao X, Luo J, Qi W, Song BL. Feeding induces cholesterol biosynthesis via the mTORC1-USP20-HMGCR axis. Nature. 2020 Dec;588(7838):479-484. doi: 10.1038/s41586-020-2928-y. Epub 2020 Nov 11. PMID: 33177714.

91. Cunningham JT, Rodgers JT, Arlow DH, Vazquez F, Mootha VK, Puigserver P. mTOR controls mitochondrial oxidative function through a YY1-PGC-1alpha transcriptional complex. Nature. 2007 Nov 29;450(7170):736-40. doi: 10.1038/nature06322. PMID: 18046414.

92. Morita M, Gravel SP, Chénard V, Sikström K, Zheng L, Alain T, Gandin V, Avizonis D, Arguello M, Zakaria C, McLaughlan S, Nouet Y, Pause A, Pollak M, Gottlieb E, Larsson O, St-Pierre J, Topisirovic I, Sonenberg N. mTORC1 controls mitochondrial activity and biogenesis through 4E-BP-dependent translational regulation. Cell Metab. 2013 Nov 5;18(5):698-711. doi: 10.1016/j.cmet.2013.10.001. PMID: 24206664.

93. MacVicar T, Ohba Y, Nolte H, Mayer FC, Tatsuta T, Sprenger HG, Lindner B, Zhao Y, Li J, Bruns C, Krüger M, Habich M, Riemer J, Schwarzer R, Pasparakis M, Henschke S, Brüning JC, Zamboni N, Langer T. Lipid signalling drives proteolytic rewiring of mitochondria by YME1L. Nature. 2019 Nov;575(7782):361-365. doi: 10.1038/s41586-019-1738-6. Epub 2019 Nov 6. PMID: 31695197.

94. He L, Gomes AP, Wang X, Yoon SO, Lee G, Nagiec MJ, Cho S, Chavez A, Islam T, Yu Y, Asara JM, Kim BY, Blenis J. mTORC1 Promotes Metabolic Reprogramming by the Suppression of GSK3-Dependent Foxk1 Phosphorylation. Mol Cell. 2018 Jun

7;70(5):949-960.e4. doi: 10.1016/j.molcel.2018.04.024. Epub 2018 May 31. PMID: 29861159; PMCID: PMC6591025.

95. Zhong H, Chiles K, Feldser D, Laughner E, Hanrahan C, Georgescu MM, Simons JW, Semenza GL. Modulation of hypoxia-inducible factor 1alpha expression by the epidermal growth factor/phosphatidylinositol 3-kinase/PTEN/AKT/FRAP pathway in human prostate cancer cells: implications for tumor angiogenesis and therapeutics. Cancer Res. 2000 Mar 15;60(6):1541-5. PMID: 1074

96. Zid BM, Rogers AN, Katewa SD, Vargas MA, Kolipinski MC, Lu TA, Benzer S, Kapahi P. 4E-BP extends lifespan upon dietary restriction by enhancing mitochondrial activity in Drosophila. Cell. 2009 Oct 2;139(1):149-60. doi: 10.1016/j.cell.2009.07.034. PMID: 19804760; PMCID: PMC2759400. 9120.

97. Kim J, Kundu M, Viollet B, Guan KL. AMPK and mTOR regulate autophagy through direct phosphorylation of Ulk1. Nat Cell Biol. 2011 Feb;13(2):132-41. doi: 10.1038/ncb2152. Epub 2011 Jan 23. PMID: 21258367; PMCID: PMC3987946.

98. Ganley IG, Lam du H, Wang J, Ding X, Chen S, Jiang X. ULK1.ATG13.FIP200 complex mediates mTOR signaling and is essential for autophagy. J Biol Chem. 2009 May 1;284(18):12297-305. doi: 10.1074/jbc.M900573200. Epub 2009 Mar 3. PMID: 19258318; PMCID: PMC2673298.

99. Nazio F, Strappazzon F, Antonioli M, Bielli P, Cianfanelli V, Bordi M, Gretzmeier C, Dengjel J, Piacentini M, Fimia GM, Cecconi F. mTOR inhibits autophagy by controlling ULK1 ubiquitylation, self-association and function through AMBRA1 and TRAF6. Nat Cell Biol. 2013 Apr;15(4):406-16. doi: 10.1038/ncb2708. Epub 2013 Mar 24. PMID: 23524951.

100. Yuan HX, Russell RC, Guan KL. Regulation of PIK3C3/VPS34 complexes by MTOR in nutrient stress-induced autophagy. Autophagy. 2013 Dec;9(12):1983-95. doi: 10.4161/auto.26058. PMID: 24013218; PMCID: PMC4028342.

101. Kim YM, Jung CH, Seo M, Kim EK, Park JM, Bae SS, Kim DH. mTORC1 phosphorylates UVRAG to negatively regulate autophagosome and endosome maturation. Mol Cell. 2015 Jan 22;57(2):207-18. doi: 10.1016/j.molcel.2014.11.013. Epub 2014 Dec 18. PMID: 25533187;

102. Settembre C, Zoncu R, Medina DL, Vetrini F, Erdin S, Erdin S, Huynh T, Ferron M, Karsenty G, Vellard MC, Facchinetti V, Sabatini DM, Ballabio A. A lysosome-to-nucleus signalling mechanism senses and regulates the lysosome via mTOR and TFEB. EMBO J.

2012 Mar 7;31(5):1095-108. doi: 10.1038/emboj.2012.32. Epub 2012 Feb 17. PMID: 22343943; PMCID: PMC3298007.

103. Martina JA, Chen Y, Gucek M, Puertollano R. MTORC1 functions as a transcriptional regulator of autophagy by preventing nuclear transport of TFEB. Autophagy. 2012 Jun;8(6):903-14. doi: 10.4161/auto.19653. Epub 2012 May 11. PMID: 22576015; PMCID: PMC3427256.

104. Roczniak-Ferguson A, Petit CS, Froehlich F, Qian S, Ky J, Angarola B, Walther TC, Ferguson SM. The transcription factor TFEB links mTORC1 signaling to transcriptional control of lysosome homeostasis. Sci Signal. 2012 Jun 12;5(228):ra42. doi: 10.1126/scisignal.2002790. PMID: 22692423; PMCID: PMC3437338.

105. Yu L, McPhee CK, Zheng L, Mardones GA, Rong Y, Peng J, Mi N, Zhao Y, Liu Z, Wan F, Hailey DW, Oorschot V, Klumperman J, Baehrecke EH, Lenardo MJ. Termination of autophagy and reformation of lysosomes regulated by mTOR. Nature. 2010 Jun 17;465(7300):942-6. doi: 10.1038/nature09076. Epub 2010 Jun 6. PMID: 20526321; PMCID: PMC2920749.

106. Wyant GA, Abu-Remaileh M, Frenkel EM, Laqtom NN, Dharamdasani V, Lewis CA, Chan SH, Heinze I, Ori A, Sabatini DM. NUFIP1 is a ribosome receptor for starvation-induced ribophagy. Science. 2018 May 18;360(6390):751-758. doi: 10.1126/science.aar2663. Epub 2018 Apr 26. PMID: 29700228; PMCID: PMC6020066.

107. Tee AR, Fingar DC, Manning BD, Kwiatkowski DJ, Cantley LC, Blenis J. Tuberous sclerosis complex-1 and -2 gene products function together to inhibit mammalian target of rapamycin (mTOR)-mediated downstream signaling. Proc Natl Acad Sci U S A. 2002 Oct 15;99(21):13571-6. doi: 10.1073/pnas.202476899. Epub 2002 Sep 23. Erratum in: Proc Natl Acad Sci U S A. 2021 Aug 17;118(33): PMID: 12271141; PMCID: PMC129715.

108. Dibble CC, Elis W, Menon S, Qin W, Klekota J, Asara JM, Finan PM, Kwiatkowski DJ, Murphy LO, Manning BD. TBC1D7 is a third subunit of the TSC1-TSC2 complex upstream of mTORC1. Mol Cell. 2012 Aug 24;47(4):535-46. doi: 10.1016/j.molcel.2012.06.009. Epub 2012 Jul 12. PMID: 22795129; PMCID: PMC3693578.

109. Inoki K, Li Y, Xu T, Guan KL. Rheb GTPase is a direct target of TSC2 GAP activity and regulates mTOR signaling. Genes Dev. 2003 Aug 1;17(15):1829-34. doi: 10.1101/gad.1110003. Epub 2003 Jul 17. PMID: 12869586; PMCID: PMC196227.

110. Tee AR, Manning BD, Roux PP, Cantley LC, Blenis J. Tuberous sclerosis complex gene products, Tuberin and Hamartin, control mTOR signaling by acting as a GTPase-activating protein complex toward Rheb. Curr Biol. 2003 Aug 5;13(15):1259-68. doi: 10.1016/s0960-9822(03)00506-2. Erratum in: Curr Biol. 2022 Feb 7;32(3):733-734. PMID: 12906785.

111. Garami A, Zwartkruis FJ, Nobukuni T, Joaquin M, Roccio M, Stocker H, Kozma SC, Hafen E, Bos JL, Thomas G. Insulin activation of Rheb, a mediator of mTOR/S6K/4E-BP signaling, is inhibited by TSC1 and 2. Mol Cell. 2003 Jun;11(6):1457-66. doi: 10.1016/s1097-2765(03)00220-x. PMID: 12820960.

112. Manning BD, Tee AR, Logsdon MN, Blenis J, Cantley LC. Identification of the tuberous sclerosis complex-2 tumor suppressor gene product tuberin as a target of the phosphoinositide 3-kinase/akt pathway. Mol Cell. 2002 Jul;10(1):151-62. doi: 10.1016/s1097-2765(02)00568-3. PMID: 12150915.

113. Menon S, Dibble CC, Talbott G, Hoxhaj G, Valvezan AJ, Takahashi H, Cantley LC, Manning BD. Spatial control of the TSC complex integrates insulin and nutrient regulation of mTORC1 at the lysosome. Cell. 2014 Feb 13;156(4):771-85. doi: 10.1016/j.cell.2013.11.049. PMID: 24529379; PMCID: PMC4030681.

114. Demetriades C, Doumpas N, Teleman AA. Regulation of TORC1 in response to amino acid starvation via lysosomal recruitment of TSC2. Cell. 2014 Feb 13;156(4):786-99. doi: 10.1016/j.cell.2014.01.024. PMID: 24529380; PMCID: PMC4346203.

115. Harrington LS, Findlay GM, Gray A, Tolkacheva T, Wigfield S, Rebholz H, Barnett J, Leslie NR, Cheng S, Shepherd PR, Gout I, Downes CP, Lamb RF. The TSC1-2 tumor suppressor controls insulin-PI3K signaling via regulation of IRS proteins. J Cell Biol. 2004 Jul 19;166(2):213-23. doi: 10.1083/jcb.200403069. Epub 2004 Jul 12. PMID: 15249583; PMCID: PMC2172316.

116. Shah OJ, Wang Z, Hunter T. Inappropriate activation of the TSC/Rheb/mTOR/S6K cassette induces IRS1/2 depletion, insulin resistance, and cell survival deficiencies. Curr Biol. 2004 Sep 21;14(18):1650-6. doi: 10.1016/j.cub.2004.08.026. PMID: 15380067.

117. Sarbassov DD, Guertin DA, Ali SM, Sabatini DM. Phosphorylation and regulation of Akt/PKB by the rictor-mTOR complex. Science. 2005 Feb 18;307(5712):1098-101. doi: 10.1126/science.1106148. PMID: 15718470.

118. Roux PP, Ballif BA, Anjum R, Gygi SP, Blenis J. Tumor-promoting phorbol esters and activated Ras inactivate the tuberous sclerosis tumor suppressor complex via p90

ribosomal S6 kinase. Proc Natl Acad Sci U S A. 2004 Sep 14;101(37):13489-94. doi: 10.1073/pnas.0405659101. Epub 2004 Sep 1. PMID: 15342917; PMCID: PMC518784.

119. Inoki K, Ouyang H, Zhu T, Lindvall C, Wang Y, Zhang X, Yang Q, Bennett C, Harada Y, Stankunas K, Wang CY, He X, MacDougald OA, You M, Williams BO, Guan KL. TSC2 integrates Wnt and energy signals via a coordinated phosphorylation by AMPK and GSK3 to regulate cell growth. Cell. 2006 Sep 8;126(5):955-68. doi: 10.1016/j.cell.2006.06.055. PMID: 16959574.

120. Lee DF, Kuo HP, Chen CT, Hsu JM, Chou CK, Wei Y, Sun HL, Li LY, Ping B, Huang WC, He X, Hung JY, Lai CC, Ding Q, Su JL, Yang JY, Sahin AA, Hortobagyi GN, Tsai FJ, Tsai CH, Hung MC. IKK beta suppression of TSC1 links inflammation and tumor angiogenesis via the mTOR pathway. Cell. 2007 Aug 10;130(3):440-55. doi: 10.1016/j.cell.2007.05.058. PMID: 17693255.

121. Emmanuel N, Ragunathan S, Shan Q, Wang F, Giannakou A, Huser N, Jin G, Myers J, Abraham RT, Unsal-Kacmaz K. Purine Nucleotide Availability Regulates mTORC1 Activity through the Rheb GTPase. Cell Rep. 2017 Jun 27;19(13):2665-2680. doi: 10.1016/j.celrep.2017.05.043. PMID: 28658616.

122. Hoxhaj G, Hughes-Hallett J, Timson RC, Ilagan E, Yuan M, Asara JM, Ben-Sahra I, Manning BD. The mTORC1 Signaling Network Senses Changes in Cellular Purine Nucleotide Levels. Cell Rep. 2017 Oct 31;21(5):1331-1346. doi: 10.1016/j.celrep.2017.10.029. PMID: 29091770; PMCID: PMC5689476.

123. Frias MA, Mukhopadhyay S, Lehman E, Walasek A, Utter M, Menon D, Foster DA. Phosphatidic acid drives mTORC1 lysosomal translocation in the absence of amino acids. J Biol Chem. 2020 Jan 3;295(1):263-274. doi: 10.1074/jbc.RA119.010892. Epub 2019 Nov 24. PMID: 31767684; PMCID: PMC6952608.

124. Davis OB, Shin HR, Lim CY, Wu EY, Kukurugya M, Maher CF, Perera RM, Ordonez MP, Zoncu R. NPC1-mTORC1 Signaling Couples Cholesterol Sensing to Organelle Homeostasis and Is a Targetable Pathway in Niemann-Pick Type C. Dev Cell. 2021 Feb 8;56(3):260-276.e7. doi: 10.1016/j.devcel.2020.11.016. Epub 2020 Dec 11. PMID: 33308480; PMCID: PMC8919971.

125. Lim CY, Davis OB, Shin HR, Zhang J, Berdan CA, Jiang X, Counihan JL, Ory DS, Nomura DK, Zoncu R. ER-lysosome contacts enable cholesterol sensing by mTORC1 and drive aberrant growth signalling in Niemann-Pick type C. Nat Cell Biol. 2019

Oct;21(10):1206-1218. doi: 10.1038/s41556-019-0391-5. Epub 2019 Sep 23. PMID: 31548609; PMCID: PMC6936960.

126. Castellano BM, Thelen AM, Moldavski O, Feltes M, van der Welle RE, Mydock-McGrane L, Jiang X, van Eijkeren RJ, Davis OB, Louie SM, Perera RM, Covey DF, Nomura DK, Ory DS, Zoncu R. Lysosomal cholesterol activates mTORC1 via an SLC38A9-Niemann-Pick C1 signaling complex. Science. 2017 Mar 24;355(6331):1306-1311. doi: 10.1126/science.aag1417. PMID: 28336668; PMCID: PMC5823611.

127. Shaw RJ, Bardeesy N, Manning BD, Lopez L, Kosmatka M, DePinho RA, Cantley LC. The LKB1 tumor suppressor negatively regulates mTOR signaling. Cancer Cell. 2004 Jul;6(1):91-9. doi: 10.1016/j.ccr.2004.06.007. PMID: 15261145.

128. Gwinn DM, Shackelford DB, Egan DF, Mihaylova MM, Mery A, Vasquez DS, Turk BE, Shaw RJ. AMPK phosphorylation of raptor mediates a metabolic checkpoint. Mol Cell. 2008 Apr 25;30(2):214-26. doi: 10.1016/j.molcel.2008.03.003. PMID: 18439900; PMCID: PMC2674027.

129. Orozco JM, Krawczyk PA, Scaria SM, Cangelosi AL, Chan SH, Kunchok T, Lewis CA, Sabatini DM. Dihydroxyacetone phosphate signals glucose availability to mTORC1. Nat Metab. 2020 Sep;2(9):893-901. doi: 10.1038/s42255-020-0250-5. Epub 2020 Jul 27. PMID: 32719541; PMCID: PMC7995735.

130. Brugarolas J, Lei K, Hurley RL, Manning BD, Reiling JH, Hafen E, Witters LA, Ellisen LW, Kaelin WG Jr. Regulation of mTOR function in response to hypoxia by REDD1 and the TSC1/TSC2 tumor suppressor complex. Genes Dev. 2004 Dec 1;18(23):2893-904. doi: 10.1101/gad.1256804. Epub 2004 Nov 15. PMID: 15545625; PMCID: PMC534650.

131. DeYoung MP, Horak P, Sofer A, Sgroi D, Ellisen LW. Hypoxia regulates TSC1/2-mTOR signaling and tumor suppression through REDD1-mediated 14-3-3 shuttling. Genes Dev. 2008 Jan 15;22(2):239-51. doi: 10.1101/gad.1617608. PMID: 18198340; PMCID: PMC2192757.

132. Sancak Y, Peterson TR, Shaul YD, Lindquist RA, Thoreen CC, Bar-Peled L, Sabatini DM. The Rag GTPases bind raptor and mediate amino acid signaling to mTORC1. Science. 2008 Jun 13;320(5882):1496-501. doi: 10.1126/science.1157535. Epub 2008 May 22. PMID: 18497260; PMCID: PMC2475333.

133. Kim E, Goraksha-Hicks P, Li L, Neufeld TP, Guan KL. Regulation of TORC1 by Rag GTPases in nutrient response. Nat Cell Biol. 2008 Aug;10(8):935-45. doi: 10.1038/ncb1753. Epub 2008 Jul 6. PMID: 18604198; PMCID: PMC2711503.

134. Shen K, Choe A, Sabatini DM. Intersubunit Crosstalk in the Rag GTPase Heterodimer Enables mTORC1 to Respond Rapidly to Amino Acid Availability. Mol Cell. 2017 Nov 16;68(4):821. doi: 10.1016/j.molcel.2017.10.031. Erratum for: Mol Cell. 2017 Nov 2;68(3):552-565.e8. PMID: 29149601; PMCID: PMC5746184.

135. Bar-Peled L, Chantranupong L, Cherniack AD, Chen WW, Ottina KA, Grabiner BC, Spear ED, Carter SL, Meyerson M, Sabatini DM. A Tumor suppressor complex with GAP activity for the Rag GTPases that signal amino acid sufficiency to mTORC1. Science. 2013 May 31;340(6136):1100-6. doi: 10.1126/science.1232044. PMID: 23723238; PMCID: PMC3728654.

136. Shen K, Valenstein ML, Gu X, Sabatini DM. Arg-78 of Nprl2 catalyzes GATOR1-stimulated GTP hydrolysis by the Rag GTPases. J Biol Chem. 2019 Feb 22;294(8):2970-2975. doi: 10.1074/jbc.AC119.007382. Epub 2019 Jan 16. PMID: 30651352; PMCID: PMC6393612.

137. Shen K, Huang RK, Brignole EJ, Condon KJ, Valenstein ML, Chantranupong L, Bomaliyamu A, Choe A, Hong C, Yu Z, Sabatini DM. Architecture of the human GATOR1 and GATOR1-Rag GTPases complexes. Nature. 2018 Apr 5;556(7699):64-69. doi: 10.1038/nature26158. Epub 2018 Mar 28. PMID: 29590090; PMCID: PMC5975964.

138. Tsun ZY, Bar-Peled L, Chantranupong L, Zoncu R, Wang T, Kim C, Spooner E, Sabatini DM. The folliculin tumor suppressor is a GAP for the RagC/D GTPases that signal amino acid levels to mTORC1. Mol Cell. 2013 Nov 21;52(4):495-505. doi: 10.1016/j.molcel.2013.09.016. Epub 2013 Oct 3. PMID: 24095279; PMCID: PMC3867817.

139. Petit CS, Roczniak-Ferguson A, Ferguson SM. Recruitment of folliculin to lysosomes supports the amino acid-dependent activation of Rag GTPases. J Cell Biol. 2013 Sep 30;202(7):1107-22. doi: 10.1083/jcb.201307084. PMID: 24081491; PMCID: PMC3787382.

140. Zoncu R, Bar-Peled L, Efeyan A, Wang S, Sancak Y, Sabatini DM. mTORC1 senses lysosomal amino acids through an inside-out mechanism that requires the vacuolar H(+)-ATPase. Science. 2011 Nov 4;334(6056):678-83. doi: 10.1126/science.1207056. PMID: 22053050; PMCID: PMC3211112.

141. Saxton RA, Knockenhauer KE, Wolfson RL, Chantranupong L, Pacold ME, Wang T, Schwartz TU, Sabatini DM. Structural basis for leucine sensing by the Sestrin2-mTORC1

pathway. Science. 2016 Jan 1;351(6268):53-8. doi: 10.1126/science.aad2087. Epub 2015 Nov 19. PMID: 26586190; PMCID: PMC4698039.

142. Wolfson RL, Chantranupong L, Saxton RA, Shen K, Scaria SM, Cantor JR, Sabatini DM. Sestrin2 is a leucine sensor for the mTORC1 pathway. Science. 2016 Jan 1;351(6268):43-8. doi: 10.1126/science.aab2674. Epub 2015 Oct 8. PMID: 26449471; PMCID: PMC4698017.

143. Han JM, Jeong SJ, Park MC, Kim G, Kwon NH, Kim HK, Ha SH, Ryu SH, Kim S. Leucyl-tRNA synthetase is an intracellular leucine sensor for the mTORC1-signaling pathway. Cell. 2012 Apr 13;149(2):410-24. doi: 10.1016/j.cell.2012.02.044. Epub 2012 Mar 15. PMID: 22424946.

144. Son SM, Park SJ, Lee H, Siddiqi F, Lee JE, Menzies FM, Rubinsztein DC. Leucine Signals to mTORC1 via Its Metabolite Acetyl-Coenzyme A. Cell Metab. 2019 Jan 8;29(1):192-201.e7. doi: 10.1016/j.cmet.2018.08.013. Epub 2018 Sep 6. PMID: 30197302; PMCID: PMC6331339.

145. Chantranupong L, Scaria SM, Saxton RA, Gygi MP, Shen K, Wyant GA, Wang T, Harper JW, Gygi SP, Sabatini DM. The CASTOR Proteins Are Arginine Sensors for the mTORC1 Pathway. Cell. 2016 Mar 24;165(1):153-164. doi: 10.1016/j.cell.2016.02.035. Epub 2016 Mar 10. PMID: 26972053; PMCID: PMC4808398.

146. Saxton RA, Chantranupong L, Knockenhauer KE, Schwartz TU, Sabatini DM. Mechanism of arginine sensing by CASTOR1 upstream of mTORC1. Nature. 2016 Aug 11;536(7615):229-33. doi: 10.1038/nature19079. Epub 2016 Aug 3. PMID: 27487210; PMCID: PMC4988899.

147. Rebsamen M, Pochini L, Stasyk T, de Araújo ME, Galluccio M, Kandasamy RK, Snijder B, Fauster A, Rudashevskaya EL, Bruckner M, Scorzoni S, Filipek PA, Huber KV, Bigenzahn JW, Heinz LX, Kraft C, Bennett KL, Indiveri C, Huber LA, Superti-Furga G. SLC38A9 is a component of the lysosomal amino acid sensing machinery that controls mTORC1. Nature. 2015 Mar 26;519(7544):477-81. doi: 10.1038/nature14107. Epub 2015 Jan 7. PMID: 25561175; PMCID: PMC4376665.

148. Wang S, Tsun ZY, Wolfson RL, Shen K, Wyant GA, Plovanich ME, Yuan ED, Jones TD, Chantranupong L, Comb W, Wang T, Bar-Peled L, Zoncu R, Straub C, Kim C, Park J, Sabatini BL, Sabatini DM. Metabolism. Lysosomal amino acid transporter SLC38A9 signals arginine sufficiency to mTORC1. Science. 2015 Jan 9;347(6218):188-94. doi: 10.1126/science.1257132. Epub 2015 Jan 7. PMID: 25567906; PMCID: PMC4295826.

149. Gu X, Orozco JM, Saxton RA, Condon KJ, Liu GY, Krawczyk PA, Scaria SM, Harper JW, Gygi SP, Sabatini DM. SAMTOR is an *S*-adenosylmethionine sensor for the mTORC1 pathway. Science. 2017 Nov 10;358(6364):813-818. doi: 10.1126/science.aao3265. PMID: 29123071; PMCID: PMC5747364.

150. Kim SH, Choi JH, Wang P, Go CD, Hesketh GG, Gingras AC, Jafarnejad SM, Sonenberg N. Mitochondrial Threonyl-tRNA Synthetase TARS2 Is Required for Threonine-Sensitive mTORC1 Activation. Mol Cell. 2021 Jan 21;81(2):398-407.e4. doi: 10.1016/j.molcel.2020.11.036. Epub 2020 Dec 18. PMID: 33340489.

151. Saxton RA, Sabatini DM. mTOR Signaling in Growth, Metabolism, and Disease. Cell. 2017 Mar 9;168(6):960-976. doi: 10.1016/j.cell.2017.02.004. Erratum in: Cell. 2017 Apr 6;169(2):361-371. PMID: 28283069; PMCID: PMC5394987.

152. Sengupta S, Peterson TR, Laplante M, Oh S, Sabatini DM. mTORC1 controls fasting-induced ketogenesis and its modulation by ageing. Nature. 2010 Dec 23;468(7327):1100-4. doi: 10.1038/nature09584. PMID: 21179166.

153. Komatsu M, Waguri S, Ueno T, Iwata J, Murata S, Tanida I, Ezaki J, Mizushima N, Ohsumi Y, Uchiyama Y, Kominami E, Tanaka K, Chiba T. Impairment of starvation-induced and constitutive autophagy in Atg7-deficient mice. J Cell Biol. 2005 May 9;169(3):425-34. doi: 10.1083/jcb.200412022. Epub 2005 May 2. PMID: 15866887; PMCID: PMC2171928.

154. Mori H, Inoki K, Opland D, Münzberg H, Villanueva EC, Faouzi M, Ikenoue T, Kwiatkowski DJ, Macdougald OA, Myers MG Jr, Guan KL. Critical roles for the TSC-mTOR pathway in β-cell function. Am J Physiol Endocrinol Metab. 2009 Nov;297(5):E1013-22. doi: 10.1152/ajpendo.00262.2009. Epub 2009 Aug 18. PMID: 19690069; PMCID: PMC2781354.

155. Shigeyama Y, Kobayashi T, Kido Y, Hashimoto N, Asahara S, Matsuda T, Takeda A, Inoue T, Shibutani Y, Koyanagi M, Uchida T, Inoue M, Hino O, Kasuga M, Noda T. Biphasic response of pancreatic beta-cell mass to ablation of tuberous sclerosis complex 2 in mice. Mol Cell Biol. 2008 May;28(9):2971-9. doi: 10.1128/MCB.01695-07. Epub 2008 Mar 3. PMID: 18316403; PMCID: PMC2293082.

156. Lamming DW, Ye L, Katajisto P, Goncalves MD, Saitoh M, Stevens DM, Davis JG, Salmon AB, Richardson A, Ahima RS, Guertin DA, Sabatini DM, Baur JA. Rapamycin-induced insulin resistance is mediated by mTORC2 loss and uncoupled from longevity.

Science. 2012 Mar 30;335(6076):1638-43. doi: 10.1126/science.1215135. PMID: 22461615; PMCID: PMC3324089.

157. Um SH, Frigerio F, Watanabe M, Picard F, Joaquin M, Sticker M, Fumagalli S, Allegrini PR, Kozma SC, Auwerx J, Thomas G. Absence of S6K1 protects against age- and diet-induced obesity while enhancing insulin sensitivity. Nature. 2004 Sep 9;431(7005):200-5. doi: 10.1038/nature02866. Epub 2004 Aug 11. Erratum in: Nature. 2004 Sep 23;431(7007):485. PMID: 15306821.

158. Polak P, Cybulski N, Feige JN, Auwerx J, Rüegg MA, Hall MN. Adipose-specific knockout of raptor results in lean mice with enhanced mitochondrial respiration. Cell Metab. 2008 Nov;8(5):399-410. doi: 10.1016/j.cmet.2008.09.003. PMID: 19046571.

159. Lee PL, Tang Y, Li H, Guertin DA. Raptor/mTORC1 loss in adipocytes causes progressive lipodystrophy and fatty liver disease. Mol Metab. 2016 Apr 11;5(6):422-432. doi: 10.1016/j.molmet.2016.04.001. PMID: 27257602; PMCID: PMC4877665.

160. Menon S, Manning BD. Common corruption of the mTOR signaling network in human tumors. Oncogene. 2008 Dec;27 Suppl 2(0 2):S43-51. doi: 10.1038/onc.2009.352. PMID: 19956179; PMCID: PMC3752670.

161. Rodrik-Outmezguine VS, Okaniwa M, Yao Z, Novotny CJ, McWhirter C, Banaji A, Won H, Wong W, Berger M, de Stanchina E, Barratt DG, Cosulich S, Klinowska T, Rosen N, Shokat KM. Overcoming mTOR resistance mutations with a new-generation mTOR inhibitor. Nature. 2016 Jun 9;534(7606):272-6. doi: 10.1038/nature17963. Epub 2016 May 18. PMID: 27279227; PMCID: PMC4902179.

162. Partridge L, Deelen J, Slagboom PE. Facing up to the global challenges of ageing. Nature. 2018 Sep;561(7721):45-56. doi: 10.1038/s41586-018-0457-8. Epub 2018 Sep 5. PMID: 30185958.

163. Kaeberlein M, Powers RW 3rd, Steffen KK, Westman EA, Hu D, Dang N, Kerr EO, Kirkland KT, Fields S, Kennedy BK. Regulation of yeast replicative life span by TOR and Sch9 in response to nutrients. Science. 2005 Nov 18;310(5751):1193-6. doi: 10.1126/science.1115535. PMID: 16293764.

164. Vellai T, Takacs-Vellai K, Zhang Y, Kovacs AL, Orosz L, Müller F. Genetics: influence of TOR kinase on lifespan in C. elegans. Nature. 2003 Dec 11;426(6967):620. doi: 10.1038/426620a. PMID: 14668850.

165. Kapahi P, Zid BM, Harper T, Koslover D, Sapin V, Benzer S. Regulation of lifespan in Drosophila by modulation of genes in the TOR signaling pathway. Curr Biol. 2004 May

25;14(10):885-90. doi: 10.1016/j.cub.2004.03.059. PMID: 15186745; PMCID: PMC2754830.

166. Wu JJ, Liu J, Chen EB, Wang JJ, Cao L, Narayan N, Fergusson MM, Rovira II, Allen M, Springer DA, Lago CU, Zhang S, DuBois W, Ward T, deCabo R, Gavrilova O, Mock B, Finkel T. Increased mammalian lifespan and a segmental and tissue-specific slowing of aging after genetic reduction of mTOR expression. Cell Rep. 2013 Sep 12;4(5):913-20. doi: 10.1016/j.celrep.2013.07.030. Epub 2013 Aug 29. PMID: 23994476; PMCID: PMC3784301.

167. Bitto A, Ito TK, Pineda VV, LeTexier NJ, Huang HZ, Sutlief E, Tung H, Vizzini N, Chen B, Smith K, Meza D, Yajima M, Beyer RP, Kerr KF, Davis DJ, Gillespie CH, Snyder JM, Treuting PM, Kaeberlein M. Transient rapamycin treatment can increase lifespan and healthspan in middle-aged mice. Elife. 2016 Aug 23;5:e16351. doi: 10.7554/eLife.16351. PMID: 27549339; PMCID: PMC4996648.

168. Hansen M, Taubert S, Crawford D, Libina N, Lee SJ, Kenyon C. Lifespan extension by conditions that inhibit translation in Caenorhabditis elegans. Aging Cell. 2007 Feb;6(1):95-110. doi: 10.1111/j.1474-9726.2006.00267.x. PMID: 17266679.

169. Chen J, Ou Y, Luo R, Wang J, Wang D, Guan J, Li Y, Xia P, Chen PR, Liu Y. SAR1B senses leucine levels to regulate mTORC1 signalling. Nature. 2021 Aug;596(7871):281-284. doi: 10.1038/s41586-021-03768-w. Epub 2021 Jul 21. PMID: 34290409.

170. Hinkson IV, Elias JE. The dynamic state of protein turnover: It's about time. Trends Cell Biol. 2011 May;21(5):293-303. doi: 10.1016/j.tcb.2011.02.002. Epub 2011 Apr 7. PMID: 21474317.

171. Labbadia J, Morimoto RI. The biology of proteostasis in aging and disease. Annu Rev Biochem. 2015;84:435-64. doi: 10.1146/annurev-biochem-060614-033955. Epub 2015 Mar 12. PMID: 25784053; PMCID: PMC4539002.

172. Pohl C, Dikic I. Cellular quality control by the ubiquitin-proteasome system and autophagy. Science. 2019 Nov 15;366(6467):818-822. doi: 10.1126/science.aax3769. Epub 2019 Nov 14. PMID: 31727826.

173. Harshbarger W, Miller C, Diedrich C, Sacchettini J. Crystal structure of the human 20S proteasome in complex with carfilzomib. Structure. 2015 Feb 3;23(2):418-24. doi: 10.1016/j.str.2014.11.017. Epub 2015 Jan 15. PMID: 25599644.

174. Huang X, Luan B, Wu J, Shi Y. An atomic structure of the human 26S proteasome. Nat Struct Mol Biol. 2016 Sep;23(9):778-85. doi: 10.1038/nsmb.3273. Epub 2016 Jul 18. PMID: 27428775.

175. Groll M, Ditzel L, Löwe J, Stock D, Bochtler M, Bartunik HD, Huber R. Structure of 20S proteasome from yeast at 2.4 A resolution. Nature. 1997 Apr 3;386(6624):463-71. doi: 10.1038/386463a0. PMID: 9087403.

176. Groll M, Bajorek M, Köhler A, Moroder L, Rubin DM, Huber R, Glickman MH, Finley D. A gated channel into the proteasome core particle. Nat Struct Biol. 2000 Nov;7(11):1062-7. doi: 10.1038/80992. PMID: 11062564.

177. Bajorek M, Finley D, Glickman MH. Proteasome disassembly and downregulation is correlated with viability during stationary phase. Curr Biol. 2003 Jul 1;13(13):1140-4. doi: 10.1016/s0960-9822(03)00417-2. PMID: 12842014.

178. Dong Y, Zhang S, Wu Z, Li X, Wang WL, Zhu Y, Stoilova-McPhie S, Lu Y, Finley D, Mao Y. Cryo-EM structures and dynamics of substrate-engaged human 26S proteasome. Nature. 2019 Jan;565(7737):49-55. doi: 10.1038/s41586-018-0736-4. Epub 2018 Nov 12. PMID: 30479383; PMCID: PMC6370054.

179. Collins GA, Goldberg AL. The Logic of the 26S Proteasome. Cell. 2017 May 18;169(5):792-806. doi: 10.1016/j.cell.2017.04.023. PMID: 28525752; PMCID: PMC5609836.

180. Bard JAM, Goodall EA, Greene ER, Jonsson E, Dong KC, Martin A. Structure and Function of the 26S Proteasome. Annu Rev Biochem. 2018 Jun 20;87:697-724. doi: 10.1146/annurev-biochem-062917-011931. Epub 2018 Apr 13. PMID: 29652515; PMCID: PMC6422034.

181. Schubert U, Antón LC, Gibbs J, Norbury CC, Yewdell JW, Bennink JR. Rapid degradation of a large fraction of newly synthesized proteins by proteasomes. Nature. 2000 Apr 13;404(6779):770-4. doi: 10.1038/35008096. PMID: 10783891.

182. Craiu A, Gaczynska M, Akopian T, Gramm CF, Fenteany G, Goldberg AL, Rock KL. Lactacystin and clasto-lactacystin beta-lactone modify multiple proteasome beta-subunits and inhibit intracellular protein degradation and major histocompatibility complex class I antigen presentation. J Biol Chem. 1997 May 16;272(20):13437-45. doi: 10.1074/jbc.272.20.13437. PMID: 9148969.

183. Scheffner M, Nuber U, Huibregtse JM. Protein ubiquitination involving an E1-E2-E3 enzyme ubiquitin thioester cascade. Nature. 1995 Jan 5;373(6509):81-3. doi: 10.1038/373081a0. PMID: 7800044.

184. Wang Y, Argiles-Castillo D, Kane EI, Zhou A, Spratt DE. HECT E3 ubiquitin ligases - emerging insights into their biological roles and disease relevance. J Cell Sci. 2020 Apr 7;133(7):jcs228072. doi: 10.1242/jcs.228072. Erratum in: J Cell Sci. 2020 Dec 21;133(24): PMID: 32265230; PMCID: PMC7157599.

185. Jacobson AD, Zhang NY, Xu P, Han KJ, Noone S, Peng J, Liu CW. The lysine 48 and lysine 63 ubiquitin conjugates are processed differently by the 26 s proteasome. J Biol Chem. 2009 Dec 18;284(51):35485-94. doi: 10.1074/jbc.M109.052928. PMID: 19858201; PMCID: PMC2790978.

186. Xu P, Duong DM, Seyfried NT, Cheng D, Xie Y, Robert J, Rush J, Hochstrasser M, Finley D, Peng J. Quantitative proteomics reveals the function of unconventional ubiquitin chains in proteasomal degradation. Cell. 2009 Apr 3;137(1):133-45. doi: 10.1016/j.cell.2009.01.041. PMID: 19345192; PMCID: PMC2668214.

187. Abada A, Elazar Z. Getting ready for building: signaling and autophagosome biogenesis. EMBO Rep. 2014 Aug;15(8):839-52. doi: 10.15252/embr.201439076. Epub 2014 Jul 15. PMID: 25027988; PMCID: PMC4197041.

188. Lamb CA, Yoshimori T, Tooze SA. The autophagosome: origins unknown, biogenesis complex. Nat Rev Mol Cell Biol. 2013 Dec;14(12):759-74. doi: 10.1038/nrm3696. Epub 2013 Nov 8. PMID: 24201109.

189. Mizushima N, Komatsu M. Autophagy: renovation of cells and tissues. Cell. 2011 Nov 11;147(4):728-41. doi: 10.1016/j.cell.2011.10.026. PMID: 22078875.

190. Singh R, Kaushik S, Wang Y, Xiang Y, Novak I, Komatsu M, Tanaka K, Cuervo AM, Czaja MJ. Autophagy regulates lipid metabolism. Nature. 2009 Apr 30;458(7242):1131-5. doi: 10.1038/nature07976. Epub 2009 Apr 1. PMID: 19339967; PMCID: PMC2676208.

191. Kaushik S, Cuervo AM. Degradation of lipid droplet-associated proteins by chaperone-mediated autophagy facilitates lipolysis. Nat Cell Biol. 2015 Jun;17(6):759-70. doi: 10.1038/ncb3166. Epub 2015 May 11. PMID: 25961502; PMCID: PMC4449813.

192. Leidal AM, Levine B, Debnath J. Autophagy and the cell biology of age-related disease. Nat Cell Biol. 2018 Dec;20(12):1338-1348. doi: 10.1038/s41556-018-0235-8. Epub 2018 Nov 26. PMID: 30482941.

193. Pickles S, Vigié P, Youle RJ. Mitophagy and Quality Control Mechanisms in Mitochondrial Maintenance. Curr Biol. 2018 Feb 19;28(4):R170-R185. doi: 10.1016/j.cub.2018.01.004. PMID: 29462587; PMCID: PMC7255410.

194. Deas E, Plun-Favreau H, Gandhi S, Desmond H, Kjaer S, Loh SH, Renton AE, Harvey RJ, Whitworth AJ, Martins LM, Abramov AY, Wood NW. PINK1 cleavage at position A103 by the mitochondrial protease PARL. Hum Mol Genet. 2011 Mar 1;20(5):867-79. doi: 10.1093/hmg/ddq526. Epub 2010 Dec 6. PMID: 21138942; PMCID: PMC3033179.

195. Harper JW, Ordureau A, Heo JM. Building and decoding ubiquitin chains for mitophagy. Nat Rev Mol Cell Biol. 2018 Jan 23;19(2):93-108. doi: 10.1038/nrm.2017.129. PMID: 29358684.

196. Fu M, St-Pierre P, Shankar J, Wang PT, Joshi B, Nabi IR. Regulation of mitophagy by the Gp78 E3 ubiquitin ligase. Mol Biol Cell. 2013 Apr;24(8):1153-62. doi: 10.1091/mbc.E12-08-0607. Epub 2013 Feb 20. PMID: 23427266; PMCID: PMC3623636.

197. Orvedahl A, Sumpter R Jr, Xiao G, Ng A, Zou Z, Tang Y, Narimatsu M, Gilpin C, Sun Q, Roth M, Forst CV, Wrana JL, Zhang YE, Luby-Phelps K, Xavier RJ, Xie Y, Levine B. Image-based genome-wide siRNA screen identifies selective autophagy factors. Nature. 2011 Dec 1;480(7375):113-7. doi: 10.1038/nature10546. PMID: 22020285; PMCID: PMC3229641.

198. Szargel R, Shani V, Abd Elghani F, Mekies LN, Liani E, Rott R, Engelender S. The PINK1, synphilin-1 and SIAH-1 complex constitutes a novel mitophagy pathway. Hum Mol Genet. 2016 Aug 15;25(16):3476-3490. doi: 10.1093/hmg/ddw189. Epub 2016 Jun 22. PMID: 27334109.

199. Villa E, Proïcs E, Rubio-Patiño C, Obba S, Zunino B, Bossowski JP, Rozier RM, Chiche J, Mondragón L, Riley JS, Marchetti S, Verhoeyen E, Tait SWG, Ricci JE. Parkin-Independent Mitophagy Controls Chemotherapeutic Response in Cancer Cells. Cell Rep. 2017 Sep 19;20(12):2846-2859. doi: 10.1016/j.celrep.2017.08.087. PMID: 28930681.

200. Kanki T, Wang K, Cao Y, Baba M, Klionsky DJ. Atg32 is a mitochondrial protein that confers selectivity during mitophagy. Dev Cell. 2009 Jul;17(1):98-109. doi: 10.1016/j.devcel.2009.06.014. PMID: 19619495; PMCID: PMC2746076.

201. Sandoval H, Thiagarajan P, Dasgupta SK, Schumacher A, Prchal JT, Chen M, Wang J. Essential role for Nix in autophagic maturation of erythroid cells. Nature. 2008 Jul

10;454(7201):232-5. doi: 10.1038/nature07006. Epub 2008 May 4. PMID: 18454133; PMCID: PMC2570948.

202. Wei Y, Chiang WC, Sumpter R Jr, Mishra P, Levine B. Prohibitin 2 Is an Inner Mitochondrial Membrane Mitophagy Receptor. Cell. 2017 Jan 12;168(1-2):224-238.e10. doi: 10.1016/j.cell.2016.11.042. Epub 2016 Dec 22. PMID: 28017329; PMCID: PMC5235968.

203. Chu CT, Ji J, Dagda RK, Jiang JF, Tyurina YY, Kapralov AA, Tyurin VA, Yanamala N, Shrivastava IH, Mohammadyani D, Wang KZQ, Zhu J, Klein-Seetharaman J, Balasubramanian K, Amoscato AA, Borisenko G, Huang Z, Gusdon AM, Cheikhi A, Steer EK, Wang R, Baty C, Watkins S, Bahar I, Bayir H, Kagan VE. Cardiolipin externalization to the outer mitochondrial membrane acts as an elimination signal for mitophagy in neuronal cells. Nat Cell Biol. 2013 Oct;15(10):1197-1205. doi: 10.1038/ncb2837. Epub 2013 Sep 15. PMID: 24036476; PMCID: PMC3806088.

204. Palikaras K, Lionaki E, Tavernarakis N. Mechanisms of mitophagy in cellular homeostasis, physiology and pathology. Nat Cell Biol. 2018 Sep;20(9):1013-1022. doi: 10.1038/s41556-018-0176-2. Epub 2018 Aug 28. PMID: 30154567.

205. Semenza GL. Oxygen sensing, hypoxia-inducible factors, and disease pathophysiology. Annu Rev Pathol. 2014;9:47-71. doi: 10.1146/annurev-pathol-012513-104720. Epub 2013 Aug 7. PMID: 23937437.

206. Huo M, Wang L, Chen Y, Shi J. Oxygen pathology and oxygen-functional materials for therapeutics. Matter. 2020 May 6;2(5):1115-47

207. Deshwal S, Fiedler KU, Langer T. Mitochondrial Proteases: Multifaceted Regulators of Mitochondrial Plasticity. Annu Rev Biochem. 2020 Jun 20;89:501-528. doi: 10.1146/annurev-biochem-062917-012739. Epub 2020 Feb 19. PMID: 32075415.

208. Lu B, Lee J, Nie X, Li M, Morozov YI, Venkatesh S, Bogenhagen DF, Temiakov D, Suzuki CK. Phosphorylation of human TFAM in mitochondria impairs DNA binding and promotes degradation by the AAA+ Lon protease. Mol Cell. 2013 Jan 10;49(1):121-32. doi: 10.1016/j.molcel.2012.10.023. Epub 2012 Nov 29. PMID: 23201127; PMCID: PMC3586414.

209. Szczepanowska K, Senft K, Heidler J, Herholz M, Kukat A, Höhne MN, Hofsetz E, Becker C, Kaspar S, Giese H, Zwicker K, Guerrero-Castillo S, Baumann L, Kauppila J, Rumyantseva A, Müller S, Frese CK, Brandt U, Riemer J, Wittig I, Trifunovic A. A salvage pathway maintains highly functional respiratory complex I. Nat Commun. 2020

Apr 2;11(1):1643. doi: 10.1038/s41467-020-15467-7. PMID: 32242014; PMCID: PMC7118099.

210. Pryde KR, Taanman JW, Schapira AH. A LON-ClpP Proteolytic Axis Degrades Complex I to Extinguish ROS Production in Depolarized Mitochondria. Cell Rep. 2016 Dec 6;17(10):2522-2531. doi: 10.1016/j.celrep.2016.11.027. PMID: 27926857; PMCID: PMC5177631.

211. Szczepanowska K, Maiti P, Kukat A, Hofsetz E, Nolte H, Senft K, Becker C, Ruzzenente B, Hornig-Do HT, Wibom R, Wiesner RJ, Krüger M, Trifunovic A. CLPP coordinates mitoribosomal assembly through the regulation of ERAL1 levels. EMBO J. 2016 Dec 1;35(23):2566-2583. doi: 10.15252/embj.201694253. Epub 2016 Oct 20. PMID: 27797820; PMCID: PMC5283601.

212. Wai T, Saita S, Nolte H, Müller S, König T, Richter-Dennerlein R, Sprenger HG, Madrenas J, Mühlmeister M, Brandt U, Krüger M, Langer T. The membrane scaffold SLP2 anchors a proteolytic hub in mitochondria containing PARL and the i-AAA protease YME1L. EMBO Rep. 2016 Dec;17(12):1844-1856. doi: 10.15252/embr.201642698. Epub 2016 Oct 13. PMID: 27737933; PMCID: PMC5283581.

213. Anand R, Wai T, Baker MJ, Kladt N, Schauss AC, Rugarli E, Langer T. The i-AAA protease YME1L and OMA1 cleave OPA1 to balance mitochondrial fusion and fission. J Cell Biol. 2014 Mar 17;204(6):919-29. doi: 10.1083/jcb.201308006. Epub 2014 Mar 10. PMID: 24616225; PMCID: PMC3998800.

214. Wai T, García-Prieto J, Baker MJ, Merkwirth C, Benit P, Rustin P, Rupérez FJ, Barbas C, Ibañez B, Langer T. Imbalanced OPA1 processing and mitochondrial fragmentation cause heart failure in mice. Science. 2015 Dec 4;350(6265):aad0116. doi: 10.1126/science.aad0116. PMID: 26785494.

215. Sprenger HG, Wani G, Hesseling A, König T, Patron M, MacVicar T, Ahola S, Wai T, Barth E, Rugarli EI, Bergami M, Langer T. Loss of the mitochondrial i-AAA protease YME1L leads to ocular dysfunction and spinal axonopathy. EMBO Mol Med. 2019 Jan;11(1):e9288. doi: 10.15252/emmm.201809288. PMID: 30389680; PMCID: PMC6328943.

216. Sprenger HG, MacVicar T, Bahat A, Fiedler KU, Hermans S, Ehrentraut D, Ried K, Milenkovic D, Bonekamp N, Larsson NG, Nolte H, Giavalisco P, Langer T. Cellular pyrimidine imbalance triggers mitochondrial DNA-dependent innate immunity. Nat

Metab. 2021 May;3(5):636-650. doi: 10.1038/s42255-021-00385-9. Epub 2021 Apr 26. PMID: 33903774; PMCID: PMC8144018.

217. Koppen M, Metodiev MD, Casari G, Rugarli EI, Langer T. Variable and tissue-specific subunit composition of mitochondrial m-AAA protease complexes linked to hereditary spastic paraplegia. Mol Cell Biol. 2007 Jan;27(2):758-67. doi: 10.1128/MCB.01470-06. Epub 2006 Nov 13. PMID: 17101804; PMCID: PMC1800790.

218. Casari G, De Fusco M, Ciarmatori S, Zeviani M, Mora M, Fernandez P, De Michele G, Filla A, Cocozza S, Marconi R, Dürr A, Fontaine B, Ballabio A. Spastic paraplegia and OXPHOS impairment caused by mutations in paraplegin, a nuclear-encoded mitochondrial metalloprotease. Cell. 1998 Jun 12;93(6):973-83. doi: 10.1016/s0092-8674(00)81203-9. PMID: 9635427.

219. Di Bella D, Lazzaro F, Brusco A, Plumari M, Battaglia G, Pastore A, Finardi A, Cagnoli C, Tempia F, Frontali M, Veneziano L, Sacco T, Boda E, Brussino A, Bonn F, Castellotti B, Baratta S, Mariotti C, Gellera C, Fracasso V, Magri S, Langer T, Plevani P, Di Donato S, Muzi-Falconi M, Taroni F. Mutations in the mitochondrial protease gene AFG3L2 cause dominant hereditary ataxia SCA28. Nat Genet. 2010 Apr;42(4):313-21. doi: 10.1038/ng.544. Epub 2010 Mar 7. PMID: 20208537.

220. Nolden M, Ehses S, Koppen M, Bernacchia A, Rugarli EI, Langer T. The m-AAA protease defective in hereditary spastic paraplegia controls ribosome assembly in mitochondria. Cell. 2005 Oct 21;123(2):277-89. doi: 10.1016/j.cell.2005.08.003. PMID: 16239145.

221. Ehses S, Raschke I, Mancuso G, Bernacchia A, Geimer S, Tondera D, Martinou JC, Westermann B, Rugarli EI, Langer T. Regulation of OPA1 processing and mitochondrial fusion by m-AAA protease isoenzymes and OMA1. J Cell Biol. 2009 Dec 28;187(7):1023-36. doi: 10.1083/jcb.200906084. PMID: 20038678; PMCID: PMC2806285.

222. Shanmughapriya S, Rajan S, Hoffman NE, Higgins AM, Tomar D, Nemani N, Hines KJ, Smith DJ, Eguchi A, Vallem S, Shaikh F, Cheung M, Leonard NJ, Stolakis RS, Wolfers MP, Ibetti J, Chuprun JK, Jog NR, Houser SR, Koch WJ, Elrod JW, Madesh M. SPG7 Is an Essential and Conserved Component of the Mitochondrial Permeability Transition Pore. Mol Cell. 2015 Oct 1;60(1):47-62. doi: 10.1016/j.molcel.2015.08.009. Epub 2015 Sep 17. PMID: 26387735; PMCID: PMC4592475.

223. König T, Tröder SE, Bakka K, Korwitz A, Richter-Dennerlein R, Lampe PA, Patron M, Mühlmeister M, Guerrero-Castillo S, Brandt U, Decker T, Lauria I, Paggio A, Rizzuto R, Rugarli EI, De Stefani D, Langer T. The m-AAA Protease Associated with Neurodegeneration Limits MCU Activity in Mitochondria. Mol Cell. 2016 Oct 6;64(1):148-162. doi: 10.1016/j.molcel.2016.08.020. Epub 2016 Sep 15. PMID: 27642048.

224. Patron M, Sprenger HG, Langer T. m-AAA proteases, mitochondrial calcium homeostasis and neurodegeneration. Cell Res. 2018 Mar;28(3):296-306. doi: 10.1038/cr.2018.17. Epub 2018 Feb 16. PMID: 29451229; PMCID: PMC5835776.

225. Bonekamp NA, Peter B, Hillen HS, Felser A, Bergbrede T, Choidas A, Horn M, Unger A, Di Lucrezia R, Atanassov I, Li X, Koch U, Menninger S, Boros J, Habenberger P, Giavalisco P, Cramer P, Denzel MS, Nussbaumer P, Klebl B, Falkenberg M, Gustafsson CM, Larsson NG. Small-molecule inhibitors of human mitochondrial DNA transcription. Nature. 2020 Dec;588(7839):712-716. doi: 10.1038/s41586-020-03048-z. Epub 2020 Dec 16. PMID: 33328633.

226. Schwaiger M, Rampler E, Hermann G, Miklos W, Berger W, Koellensperger G. Anion-Exchange Chromatography Coupled to High-Resolution Mass Spectrometry: A Powerful Tool for Merging Targeted and Non-targeted Metabolomics. Anal Chem. 2017 Jul 18;89(14):7667-7674. doi: 10.1021/acs.analchem.7b01624. Epub 2017 Jun 27. PMID: 28581703.

227. Fecher C, Trovò L, Müller SA, Snaidero N, Wettmarshausen J, Heink S, Ortiz O, Wagner I, Kühn R, Hartmann J, Karl RM, Konnerth A, Korn T, Wurst W, Merkler D, Lichtenthaler SF, Perocchi F, Misgeld T. Cell-type-specific profiling of brain mitochondria reveals functional and molecular diversity. Nat Neurosci. 2019 Oct;22(10):1731-1742. doi: 10.1038/s41593-019-0479-z. Epub 2019 Sep 9. PMID: 31501572.

228. Ross AB, Langer JD, Jovanovic M. Proteome Turnover in the Spotlight: Approaches, Applications, and Perspectives. Mol Cell Proteomics. 2021;20:100016. doi: 10.1074/mcp.R120.002190. Epub 2020 Dec 7. PMID: 33556866; PMCID: PMC7950106.

229. Hernansanz-Agustín P, Choya-Foces C, Carregal-Romero S, Ramos E, Oliva T, Villa-Piña T, Moreno L, Izquierdo-Álvarez A, Cabrera-García JD, Cortés A, Lechuga-Vieco AV, Jadiya P, Navarro E, Parada E, Palomino-Antolín A, Tello D, Acín-Pérez R, Rodríguez-Aguilera JC, Navas P, Cogolludo Á, López-Montero I, Martínez-Del-Pozo Á,

Egea J, López MG, Elrod JW, Ruíz-Cabello J, Bogdanova A, Enríquez JA, Martínez-Ruiz A. Na$^+$ controls hypoxic signalling by the mitochondrial respiratory chain. Nature. 2020 Oct;586(7828):287-291. doi: 10.1038/s41586-020-2551-y. Epub 2020 Jul 29. PMID: 32728214; PMCID: PMC7992277.

230. Patron M, Tarasenko D, Nolte H, Kroczek L, Ghosh M, Ohba Y, Lasarzewski Y, Ahmadi ZA, Cabrera-Orefice A, Eyiama A, Kellermann T, Rugarli EI, Brandt U, Meinecke M, Langer T. Regulation of mitochondrial proteostasis by the proton gradient. EMBO J. 2022 Aug 16;41(16):e110476. doi: 10.15252/embj.2021110476. Epub 2022 Aug 1. PMID: 35912435; PMCID: PMC9379554.

Curriculum vitae

<div align="center">

Srikanth Chandragiri

Max Planck Institute for Biology of Ageing
Cologne, Germany

</div>

Education:

Kakatiya University, Warangal, Telangana, India 5.2003 -5.2005
Bachelor of science in Biotechnology

Osmania university, Hyderabad, Telangana, India 5.2005 – 5. 2007
Masters in Genetics

National Center for Biological Science, Bangalore, India 12. 2008 – 12. 2010
Junior research fellow

University of Fribourg, Fribourg, Switzerland 1. 2011- 2. 2013
PhD program

University of Cologne, Cologne, Germany 2. 2018 – 1. 2023 (expected)
PhD student

Erklärung zur Dissertation
gemäß der Promotionsordnung vom 12. März 2020

Diese Erklärung muss in der Dissertation enthalten sein.
(***This version must be included in the doctoral thesis***)

„Hiermit versichere ich an Eides statt, dass ich die vorliegende Dissertation selbstständig und ohne die Benutzung anderer als der angegebenen Hilfsmittel und Literatur angefertigt habe. Alle Stellen, die wörtlich oder sinngemäß aus veröffentlichten und nicht veröffentlichten Werken dem Wortlaut oder dem Sinn nach entnommen wurden, sind als solche kenntlich gemacht. Ich versichere an Eides statt, dass diese Dissertation noch keiner anderen Fakultät oder Universität zur Prüfung vorgelegen hat; dass sie - abgesehen von unten angegebenen Teilpublikationen und eingebundenen Artikeln und Manuskripten - noch nicht veröffentlicht worden ist sowie, dass ich eine Veröffentlichung der Dissertation vor Abschluss der Promotion nicht ohne Genehmigung des Promotionsausschusses vornehmen werde. Die Bestimmungen dieser Ordnung sind mir bekannt. Darüber hinaus erkläre ich hiermit, dass ich die Ordnung zur Sicherung guter wissenschaftlicher Praxis und zum Umgang mit wissenschaftlichem Fehlverhalten der Universität zu Köln gelesen und sie bei der Durchführung der Dissertation zugrundeliegenden Arbeiten und der schriftlich verfassten Dissertation beachtet habe und verpflichte mich hiermit, die dort genannten Vorgaben bei allen wissenschaftlichen Tätigkeiten zu beachten und umzusetzen. Ich versichere, dass die eingereichte elektronische Fassung der eingereichten Druckfassung vollständig entspricht."

Teilpublikationen:

Datum, Name und Unterschrift

Chandragiri Srikanth
6.November.2022

Mathematisch-Naturwissenschaftliche Fakultät der Universität zu Köln
Zustimmung zur Veröffentlichung der Dissertation

Faculty of Mathematics and Natural Sciences - University of Cologne
Approval of publication of the doctoral thesis

Name last name	Chandragiri
Vorname first name	Srikanth
Betreuerin / Betreuer Supervisor	Thomas Langer
Erste/r Gutachter/in first reviewer	Thomas Langer

Titel der zur Promotion eingereichten Dissertation / title of the submitted doctoral thesis

Proteolytic Rewiring of the Mitochondria in Hypoxia

Hiermit bestätige ich, dass mir die oben genannte Dissertation vorgelegen hat und dass ich gegen deren Veröffentlichung nichts einzuwenden habe. An der Dissertation wurden keine oder nur unwesentliche Änderungen (z.B. Rechtschreibung, Formatierung) vorgenommen. / I herewith confirm that the above-mentioned dissertation has been presented to me and that I have no objection to its publication. No or only minor changes (e.g. spelling, formatting) have been made to the doctoral thesis.

Die Dissertation kann veröffentlicht werden / The thesis can be published

- ☒ in elektronischer Form auf dem Hochschulserver KUPS / in electronic form on the university server KUPS .

- ◯ durch privaten Druck und Abgabe von 9 gebundenen Exemplaren bei der USB sowie der Veröffentlichung der Zusammenfassung der Dissertation in deutscher und in englischer Sprache auf dem Hochschulserver KUPS / by private printing and submission of 9 bound copies to the USB and additional publication of the summary of the doctoral thesis in German and English on the university server KUPS.

- ◯ als Einzelpublikation in einem Verlag mit ISBN oder ISSN und Abgabe von fünf gebundenen Exemplaren bei der USB sowie der Veröffentlichung der Zusammenfassung der Dissertation in deutscher und in englischer Sprache auf dem Hochschulserver KUPS / as a single publication in a publishing house with ISBN or ISSN and submission of five bound copies to the to the USB and additional publication of the summary of the doctoral thesis in German and English on the university server KUPS.

Hinweis: Die Veröffentlichung muss auf dem Titelblatt oder auf der Rückseite des Titelblatts einen Hinweis enthalten, aus der oder dem hervorgeht, dass es sich um eine von der Mathematisch-Naturwissen-schaftlichen Fakultät der Universität zu Köln angenommene Dissertation handelt; dabei ist das Jahr der Disputation zu nennen. Von der veröffentlichten Fassung der Dissertation ist eine elektronische Version (PDF-Datei) der veröffentlichten Fassung der Dissertation in Docfile zu hinterlegen.
Note: The publication must include a statement on the title page or on the back of the title page declaring that the dissertation has been accepted by the Faculty of Mathematics and Natural Sciences of the University of Cologne; the year of the disputation must be stated. In addition, the electronic version (PDF-file) of the published version of the doctoral thesis must be uploaded in Docfile.

11.5.23

Datum / date Unterschrift Betreuer/in
supervisor's signature

Datum / date Unterschrift Erstgutachter/in (sofern nicht Betreuende/r)
first reviewer's signature (if different than supervisor)

Institut bzw. Forschungseinrichtung mit Anschrift research institution and address